TECHNISCHE UNIVERSITÄT MÜNCHEN

TUM School of Computation, Information and Technology

Information Disclosure and Pricing in On-Demand Service Platforms

Donghao Zhu

Vollständiger Abdruck der von der TUM School of Computation, Information and Technology der Technischen Universität München zur Erlangung eines

Doktors der Naturwissenschaften (Dr. rer. nat.)

genehmigten Dissertation.

Vorsitz:	Prof. Dr. Stefanie Rinderle-Ma
Prüfende der Dissertation:	1. Prof. Dr. Martin Bichler 2. Prof. Dr. Stefan Minner

Die Dissertation wurde am 28.06.2023 bei der Technischen Universität München eingereicht und durch die TUM School of Computation, Information and Technology am 20.11.2023 angenommen.

Abstract

The rapid growth of the sharing economy has spurred an increase in research on on-demand service platforms, including a wide range of topics such as optimization and fairness. However, providing prescriptive design guidelines based on empirical studies proves to be challenging due to the complex interplay of multiple design factors. Economic research has increasingly focused on developing novel modeling analysis, particularly for platforms with dynamic supply and demand, enabling a comprehensive understanding of market dynamics while maintaining tractability and extensibility. This thesis addresses design issues within on-demand service platforms and provides managerial implications.

Regarding the information disclosure policy about service delays, specifically the availability of current queue-length information in a two-sided marketplace, we illuminate how this disclosure influences user behavior, thereby impacting platform revenues. Utilizing queueing theory, we investigate the preferred information policy to maximize the expected revenue. In a model of multiple platforms, we incorporate an endogenous user arrival rate to capture the increased correlation between service quality and user arrivals. Our findings indicate that while the recommendation for selecting information policies remains qualitatively the same, the revenue difference between these policies increases.

We investigate the joint effect of pricing and service delay information disclosure policies on the platform's expected profit. The pricing policy may be dynamic or static, depending on the current queue length state in the market. Optimal prices under both dynamic and static pricing policies are derived by applying uniformization to the underlying Semi-Markov decision processes. By comparing optimal prices under different pricing and information policies, we propose a strategy to maximize the expected profit. Our results demonstrate that implementing a dynamic pricing policy and disclosing service delay information result in a higher expected profit, whereas a static pricing policy and concealing service delay information increase throughput.

Finally, this thesis discusses the background of the research question, conducts a comprehensive literature survey, outlines the modeling approach, analyzes results, and offers managerial insights regarding platform pricing and information disclosure policies. These studies are poised to deepen our understanding of the mechanisms governing on-demand service platforms and inspire further research in the field of economics.

Zusammenfassung

Das rasante Wachstum der Sharing Economy hat zu einer Zunahme von Forschung zu On-Demand-Serviceplattformen geführt, die eine Vielzahl von Themen wie Optimierung und Fairness abdeckt. Die Bereitstellung präskriptiver Designempfehlungen aufgrund empirischer Studien erweist sich jedoch aufgrund des komplexen Zusammenspiels mehrerer Designfaktoren als herausfordernd. Die Wirtschaftsforschung konzentriert sich zunehmend auf die Entwicklung innovativer Modellanalysen, insbesondere für Plattformen mit dynamischem Angebot und Nachfrage, um ein umfassendes Verständnis der Marktdynamik zu ermöglichen und gleichzeitig Handhabbarkeit und Erweiterbarkeit zu gewährleisten. Diese Dissertation behandelt Designfragen innerhalb von On-Demand-Serviceplattformen und liefert damit verbundene managementbezogene Implikationen.

Hinsichtlich der Informationsweitergabepolitik bezüglich Serviceverzögerungen, insbesondere der Verfügbarkeit von aktuellen Warteschlangeninformationen in einem zweiseitigen Markt, beleuchten wir, wie die Offenlegung das Nutzerverhalten beeinflusst und die Einnahmen der Plattform beeinflusst. Unter Verwendung der Warteschlangentheorie untersuchen wir die bevorzugte Informationspolitik zur Maximierung der erwarteten Einnahmen. In einem Modell mehrerer Plattformen integrieren wir eine endogene Benutzerankunftsrate, um die gesteigerte Korrelation zwischen Servicequalität und Benutzerankünften zu erfassen. Unsere Ergebnisse deuten darauf hin, dass, obwohl die qualitative Empfehlung für die Auswahl von Informationsrichtlinien gleich bleibt, die Einnahmenunterschiede zwischen diesen Richtlinien zunehmen.

Wir untersuchen den gemeinsamen Effekt von Preis- und Informationsrichtlinien zur Offenlegung von Serviceverzögerungen auf den erwarteten Gewinn der Plattform. Die Preispolitik kann dynamisch oder statisch sein, abhängig vom aktuellen Zustand der Warteschlangenlänge auf dem Markt. Optimale Preise unter sowohl dynamischen als auch statischen Preisrichtlinien werden durch Anwendung der Uniformisierung auf die zugrunde liegenden Semi-Markov-Entscheidungsprozesse abgeleitet. Durch den Vergleich optimaler Preise unter verschiedenen Preis- und Informationsrichtlinien schlagen wir eine Strategie vor, um den erwarteten Gewinn zu maximieren. Unsere Ergebnisse zeigen, dass die Implementierung einer dynamischen Preispolitik und die Offenlegung von Serviceverzögerungsinformationen zu einem höheren erwarteten Gewinn führen, während eine statische Preispolitik und die Verheimlichung von Serviceverzögerungsinformationen die Durchsatzrate erhöhen.

Abschließend diskutiert diese Dissertation den Hintergrund der Forschungsfrage, führt eine umfassende Literaturübersicht durch, skizziert den Modellierungsansatz, analysiert Ergebnisse und bietet managementbezogene Einblicke zu Plattformpreisen und Informationsweitergaberichtlinien. Diese Studien sind darauf ausgerichtet, unser Verständnis der Mechanismen von On-Demand-Serviceplattformen zu vertiefen und weitere Forschung im Bereich der Wirtschaftsforschung anzuregen.

Acknowledgements

I would like to express my sincere gratitude to my two supervisors, Martin Bichler and Stefan Minner (listed in alphabetical order), for their invaluable guidance and support throughout my journey as a PhD student. I am grateful for the opportunities you have provided me with, and for sharing your wisdom and expertise in the field. Thank you for your patience, encouragement, and commitment to my success. I would also like to express my gratitude to the chairperson of the doctoral committee, Stefanie Rinderle-Ma.

I am grateful to my cherished friends and colleagues in Germany, including Stefan Kober, Martin Bullinger, Johannes Bäumler, Eleni Batziou, Johannes Knörr, Mete Ahunbay, Matthias Oberlechner (listed in contribution order), and all my colleagues at the Chair of Decision Sciences & Systems. I also want to extend my thanks to Alexandre Forel, Isabel Koch, Maximilian Kolter, Alexandros Tsigonias-Dimitriadis (listed in alphabetical order), and all my colleagues at AdONE (Advanced Optimization in a Networked Economy) PhD training group. Additionally, I would like to thank Yifan Cao, Eunji Lee, Chunting Liu, Yihua Wang, Zhaoguang Xu (listed in alphabetical order), and all my colleagues at the Chair of Logistics and Supply Chain Management for their collaboration and enjoyable working experience. Your support has been invaluable, both in terms of academic work and personal life.

In an era of global pandemics, working during these times is not always easy, especially considering that this period covered the majority of my PhD journey. Nevertheless, I am incredibly grateful to all the people I have met (virtually) during these years, including Dongdong Ge, Hanzhang Qin, Ruobing Shen, Yuan Wang, Jiding Zhang, Xusheng Zhang (listed in alphabetical order), and more. The selfless help I received from the people I met in Japan, including Kenji Fukumizu, Takafumi Kajihara, Naonori Kakimura, Fuhito Kojima, Akira Maeda, Shunya Noda (listed in alphabetical order), and more was also greatly appreciated. Your constant moral encouragement and academic discussions in your spare time helped me to gradually develop my perception of academic life.

Lastly, I extend my deepest gratitude to my parents for their unwavering and invaluable support. Their presence in my life has been a constant source of strength and inspiration. Moving forward, I aspire to continue standing up for what I believe in and to become even braver as I navigate the challenges of the future.

Contents

1. Introduction

On-demand service platforms have experienced significant growth across diverse industries, driven by advancements in information technology and the widespread adoption of smartphones. This transformative phenomenon is often referred as the *platform revolution* (Parker et al. 2016). Some examples include: i), Ride-hailing: Platforms like Uber and Lyft connect passengers with drivers, allowing users to request rides on-demand through a mobile app; ii), Food delivery: Services like DoorDash, Uber Eats, and Grubhub enable users to order food from local restaurants and have it delivered to their doorstep; iii), Freight exchange: platforms such as Timocom, Trans EU, and Uber Freight facilitate the connection between shippers and carriers, enabling them to negotiate and arrange services; iv), Grocery Delivery: Apps like Instacart and Shipt allow users to order groceries online from their favorite stores and have them delivered to their homes; v), Healthcare: Telemedicine platforms like Doctor on Demand and Amwell connect patients with healthcare providers via video consultations, enabling convenient access to medical advice and prescriptions; vi), Professional Services: Platforms such as Upwork and Freelancer connect businesses with freelance professionals across various fields, including graphic design, programming, writing, and marketing; vii), Beauty and Wellness: On-demand beauty services like Glamsquad and StyleBee provide users with professional hairstyling, makeup, and other beauty services at their desired location; among others. These examples represent just a few of the many industries that have embraced on-demand service platforms to meet the evolving needs and expectations of customers.

Typically, these platforms follow a similar service process: attracting both customers and suppliers, facilitating matchmaking between heterogeneous requests and services to form a market segment, and generating profits through commission collection. This business model presents many interesting and challenging questions about design factors. The analysis of these factors is constrained by the specificity of application scenarios in empirical studies, thus limiting the understanding of market mechanisms. For instance, user behavior is influenced by multiple factors concurrently, making it challenging to comprehend the impact of a single factor based solely on posteriori observations, with the underlying process proving not easily explicable. Consequently, economic research has increasingly emphasized innovative modeling analyses, particularly within platforms with dynamic supply and demand.

Stochastic modeling is a promising approach for capturing market features in analysis. Firstly, it can accommodate uncertain behaviors in markets, exemplified by user arrival rates through random processes. Secondly, the methodology of stochastic modeling enhances the approach to analyzing research questions, as seen in techniques like Markov decision processes. Lastly, the conclusions and theorems derived from this approach are extensible, making them applicable to a broader range of scenarios and algorithm designs. Stochastic modeling relies on the intersection of informatics, computer science, management, and economics, with the aim of designing reliable models that facilitate the practical and robust analysis of real-world problems.

This thesis adopts a queueing theoretical approach to address design issues in on-demand service platforms and offer relevant managerial implications. In our modeling framework, we account for uncertainty in user behaviors, encompassing not only the user's arrival and platform selection but also their feedback on the implemented policies. Our findings offer prescriptive design guidelines for platform development. We anticipate validating and expanding upon these models and results to address additional challenges in the field of platform design.

1.1. Contributions of this thesis

This thesis addresses fundamental design challenges for on-demand platforms, specifically focusing on information disclosure policies about service delays and the determination of pricing policies, whether static or dynamic. To accomplish this, we explore these issues within a model framework for a two-sided marketplace using queueing theory. Chapter 3 focuses on the impact of information disclosure policies on the market and identifies the preferred policy among the proposed ones that maximizes expected revenue. Chapter 4 delves into the joint effect of pricing policy and information policy on the platform's expected profit. In the following, we offer detailed explanations of our contributions and present the key results we have obtained.

Information disclosure policy about queue length

The disclosure of queue-length information by a platform can have a significant impact on user behavior, thereby influencing the platform's net revenue through commission collection. The empirical literature identifies two primary types of user abandonment behaviors associated with different information disclosure policies. If the queue length is displayed, arriving users may balk at joining the queue when they see a large queue length, indicating long wait times for service. If the queue length is concealed, arriving users may randomly renege the queue while waiting. These two types of user abandonment behavior differ fundamentally: balking behavior is a rational decision based on informed judgment due to the availability of visible information, whereas reneging behavior is a random action resulting from a lack of visible information. Selecting an appropriate disclosure policy can, on one hand, increase the matching rate of the system, resulting in higher revenue, and on the other hand, increase the matching probability of the system, leading to greater user satisfaction and improving the platform's reputation.

In Chapter 3, we analyze the information disclosure policy in both single- and double-sided queueing models within a market segment, considering that customers and suppliers on both sides have homogeneous requests. For example, on a ride-hailing platform, passengers in the same region are assigned to drivers who can pick them up. This service system is modeled as a single-sided queueing model. Conversely, in a freight exchange platform, shippers and carriers must be matched for a specific origin-destination route, and this service system is modeled as a double-sided queueing model. For both the customer and supply side, we propose two information disclosure policies: visible and invisible. Therefore, in a double-sided queueing model, we analyze four different information policies: both-visible, only-demand-visible, only-supply-visible, and both-invisible. Our goal is to understand the difference among these four information policies by analyzing the underlying Markov chains. Subsequently, we identify the market conditions under which a specific policy is preferred in terms of expected net revenue.

We then expand our model into the non-monopoly case, considering scenarios where multiple platforms are available for selection in a service. Users possess the flexibility to switch between platforms if dissatisfied, with service quality directly influencing user arrival rates. We introduce an endogenous arrival rate in our model, where users' arrival rates and their perceived long-term matching probabilities mutually depend on each other. We find that the selection of the preferred information policy remains qualitatively the same, while the revenue effect of the information policy is increased. Our theoretical findings highlight the significance of information design and provide prescriptive design guidelines.

Joint effect of pricing and information design

Pricing policy is a vital element in platform design, with the option to implement dynamic pricing to attract customers and suppliers based on the level of queue congestion, indicated by the current queue length. While dynamic pricing increases net revenue, it may potentially decrease user loyalty compared to a static price. The dissatisfaction could stem from issues such as price discrimination, incurring extra costs associated with calculating the platform's profit. The disclosure of queue-length information, as another vital element in platform design, significantly influences user behavior, impacting the platform's net revenue. When examining its joint effect with the pricing policy, we consider that customers may exhibit balking behavior when they see long queue-length information, while some of they may hesitate and balk when the queue-length information is concealed. This perspective differs from Chapter 3, where we investigate the influence of information disclosure on users' queueing behavior, now focusing on users' ability to estimate the expected waiting time. We analyze the interplay between pricing and information policies, proposing the preferred strategy to select pricing and information policies for maximizing expected profit.

In Chapter 4, we analyze a market segment wherein customers queue and suppliers serve, using an $M/M/1$ queueing model. The platform can choose between a dynamic price, based on the current queue length, or a static price, to attract customers and suppliers. The platform can also decide whether to display the queue-length information to customers, which can trigger corresponding balking behaviors. We obtain the optimality equations of the underlying Markov decision processes through uniformization and compare the optimal pricing solution under the proposed information policy. We provide unique thresholds to determine the preferred strategy of pricing policy and information policy for maximizing the platform's expected profit.

Our results reveal the complementary and substitute ways in which pricing and information policies interact: Dynamic pricing and visible information policies increase expected profit, while static pricing and invisible information policies increase throughput. Dynamic pricing achieves higher profits by increasing the average transaction price and, consequently, commissions. Under the visible queue-length information policy, a truncation point occurs due to customer balk behavior, negatively impacting net revenue under dynamic pricing. This prompts a strategy of dynamic pricing and visible information attracting fewer customers and suppliers, leading to lower throughput. Concealing queue-length information eliminates this truncation but results in decreased arrival rates and throughput, ultimately lowering expected profit. Additionally, high commission rates diminish the effectiveness of concealing queue-length information in increasing throughput.

1.2. Bibliographic notes

Chapter 3 is based on joint work with Stefan Minner and Martin Bichler. A preliminary version of this work was presented in the Manufacturing and Service Operations Management (MSOM) Conference 2022 (Zhu et al. 2023). Chapter 4 is based on a working paper with Stefan Minner and Martin Bichler.

2. Preliminaries

In this chapter, we provide necessary theoretical background for the modeling, methodology, and other technical aspects throughout this thesis. The symbols used in this chapter are intended for descriptive purposes. Notations specific to business models are defined in their respective chapters. We summarize the notations used in Chapter 3 in Appendix A and those used in Chapter 4 in Appendix B.

2.1. Markov chain

The Markov chain provides a powerful framework for describing the transitions between stochastic states in the market. In this section, we introduce the definitions of Markov chains and fundamental concepts that are essential for understanding their behavior. For a deeper understanding of Markov chain theory, we recommend interested readers to refer to the textbook by Norris (1998).

Stochastic process A stochastic process is a mathematical model that describes the evolution of a system over time, where the system's behavior is subject to randomness or uncertainty. Let X_t be the state of a market at time t, which can be viewed as a random variable. A *discrete-time stochastic process* describes the relationship between a sequence of random variables X_0, X_1, X_2, and so on. Each random variable in the sequence corresponds to the state of the market at a specific discrete time point. A *continuous-time stochastic process* describes the relationship between any pair of random variables X_{t_1} and X_{t_2} at different time points t_1 and t_2. This type of process is particularly useful for modeling markets that evolve continuously over time, without discrete intervals. In both cases, the behavior of the stochastic process is described using probability distributions, which provide insights into the potential outcomes of the random variable X_t at each time point. These distributions help us understand the likelihood of various market states occurring at different times.

Poisson process and exponential distribution A Poisson process $Poi(\cdot)$ is a stochastic process that models the occurrence of discrete events over time, where the average time between events is known, but the exact timing of events is random. The time interval between two adjacent events, denoted by x, in a Poisson process follows an exponential distribution $Exp(\cdot)$. The probability density function of an exponential distribution is given by

$$f(x;\lambda) = \begin{cases} \lambda e^{-\lambda x} & x \geq 0 \\ 0 & x < 0. \end{cases}$$

Here, λ is the parameter of the distribution, often referred as the *rate parameter*. The value of λ represents the average rate of occurrence of discrete events per unit time in the corresponding Poisson process. The cumulative distribution function of an exponential distribution is given by

$$F(x;\lambda) = \begin{cases} 1 - e^{-\lambda x} & x \geq 0 \\ 0 & x < 0. \end{cases}$$

The mean of a random variable X following an exponential distribution is $\frac{1}{\lambda}$, which is the reciprocal of the rate parameter in the corresponding Poisson process.

The memoryless property of the Poisson process is an important feature in the application of economic models. This means that the probability distribution of future events is not influenced by the past events. In other words, the occurrence of events in the future is independent of the occurrence of events in the past. This is indicated by the memorylessness property of an exponential random variable, which is rigorously defined as follows:

$$\begin{aligned} \Pr\left(X > t_1 + t_2 \mid X > t_1\right) &= \frac{\Pr\left(X > t_1 + t_2 \ \cap \ X > t_1\right)}{\Pr\left(X > t_1\right)} \\ &= \frac{\Pr\left(X > t_1 + t_2\right)}{\Pr\left(X > t_1\right)} \\ &= \frac{e^{-\lambda(t_1+t_2)}}{e^{-\lambda t_1}} \end{aligned}$$

$$= e^{-\lambda t_2}$$
$$= \Pr(X > t_2).$$

Continuous-time Markov chain A continuous-time Markov chain is a stochastic process where the system's state transitions from one state to another at random times according to exponential random variables. The transition rates determine the probabilities of transitioning between states. A continuous-time Markov chain X_t is characterized by two components: a jump chain and a set of holding time parameters λ_i. The jump chain consists of a countable set of states, e.g., denoted as $S \subset \{0, 1, 2, \ldots\}$, along with transition probabilities p_{ij}. When the system is in state $X_t = i$, the time until the state changes follows an exponential distribution with rate λ_i, represented as $Exp(\lambda_i)$. The next state it transitions to, denoted as j, occurs with a probability p_{ij}.

Stationary distribution The steady-state behavior of a Markov chain refers to the long-term probabilities of the system being in each state, which are described by a distribution known as the stationary distribution $\{\pi_i \mid i \in S\}$. A Markov chain is considered *irreducible* if it is possible to transition from any state to any other state with a positive probability, without any disjoint subsets of states that are inaccessible to each other. A Markov chain is considered *aperiodic* if it lacks any regular pattern or periodicity in its state transitions, meaning there are no fixed intervals at which the chain returns to specific states or sets of states. In an aperiodic chain, states can be revisited at irregular intervals.

Theorem 1 (Theorem 3.8.1, Ergodic theorem, Norris (1998))**.** *A unique stationary distribution exists for a Markov chain when it is both irreducible and aperiodic.*

In this thesis, all Markov chain models used are both irreducible and aperiodic, guaranteeing the existence of unique steady-state distributions. More specifically, our models are *birth-death processes*, which are known to possess unique stationary distributions. We will introduce the concept of birth-death processes in the next sections.

Balance equations Balance equations in a Markov chain are a set of equations that describe the long-term behavior of the chain. They represent the equilibrium conditions or steady-state conditions of the Markov chain that the chain converges to. *Global* *balance equations* are a set of equations that describe the overall balance of probabilities in a Markov chain, given by

$$\pi_i = \sum_{j \in S} \pi_j p_{ij}$$

for each $i \in S$ and $j \in S$. These equations ensure that the flow of probabilities into a state is equal to the flow out of that state, establishing the equilibrium conditions of the chain.

2.2. Markov decision process

Markov decision process A Markov decision process (MDP) is a mathematical framework used to model decision-making problems in situations where outcomes are uncertain and influenced by both random events and the decisions made by an agent. It is a discrete-time stochastic control process that involves a set of states S, actions $a \in A$, transition probabilities $p_{ij}(a)$, and rewards $R_{ij}(a)$. At each discrete time step t, an agent observes the current state $i \in S$ and selects an action $a \in A$ that transitions the system to another state $j \in S$ (which can be the same as i) based on the probability $p_{ij}(a)$. After each transition, the agent receives a reward $R_{ij}(a)$.

Semi-Markov decision process A semi-Markov decision process (SMDP) is an extension of the Markov decision process framework that incorporates the concept of sojourn time being a general continuous random variable. SMDP is a continuous-time stochastic control process that provides a modeling approach for systems with variable state duration.

Methodical process For the information disclosure and pricing issues addressed in this thesis within the on-demand service platform, we apply the aforementioned methodology to model them separately. This involves defining random behaviors, such as the impact of information disclosure itself on users' balking and reneging behaviors, as well as the influence of pricing levels on users' average arrival rates. Specifically, we treat the number of users in the market waiting in the queue for service as the state of the market, which is uncertain and influenced by user behavior. The information disclosure and pricing policies, conceptualized as transition probabilities, are modeled as influential factors governing transitions in the market state. Consequently, we employ the Markov decision process to analyze the problem. Our model demonstrates a unique steady-state distribution, allowing us to analyze and derive preferred policies.

2.3. Uniformization

Uniformization is a technique used in the analysis of semi-Markov decision processes to transform them into equivalent discrete-time models. The following example illustrates the concept of uniformization and outlines the derivation of its optimality equations.

Example 1. Consider an $M/M/1$ queue where customers arrive by a Poisson process with fixed rate λ. The service time follows an exponential distribution with rate μ, which can be selected from a continuous set $[0, \overline{\mu}]$. The service rate remains constant after being selected; it does not change with the queue state. We assume $\overline{\mu} > \lambda$. This indicates that the maximum service rate exceeds the arrival rate, resulting in a bounded queue length. The service rate can be dynamically adjusted based on the queue length i, changing at the times when a customer arrives or departs. We denote the service rate μ at queue length i by μ_i. There is a service cost $C_s(\mu)$ per unit time for using the service rate μ, and a waiting cost $C_w(i)$ per unit time when the queue length is i. We assume that $C_s(\mu)$ is continuous on $[0, \overline{\mu}]$ and $C_s(0) = 0$. Additionally, we assume that $C_w(i)$ is monotonically non-decreasing and convex with the queue length i. How can the service rate be selected to minimize the expected cost of service and waiting?

The transition rate of the Markov chain at state i is

$$r_{i \to j, \forall j \in S} = \begin{cases} \lambda & \text{if} \quad i = 0 \\ \lambda + \mu & \text{if} \quad i \geq 1. \end{cases}$$

We can uniform the Markov chain by using $\lambda + \overline{\mu}$. The transition probabilities of the Markov chain and the corresponding uniformized version are depicted in Figure 2.1. Derived from Bellman's equations, we get

$$V(0) = \frac{1}{\lambda + \overline{\mu}} \min_{\mu \in [0, \overline{\mu}]} \{C_w(0) + \gamma + \overline{\mu} V(0) + \lambda V(1)\} \tag{2.1}$$

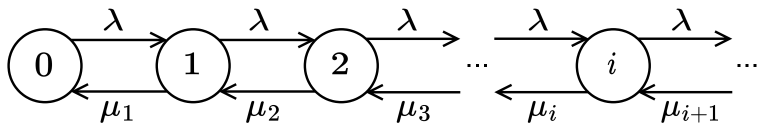

(a)

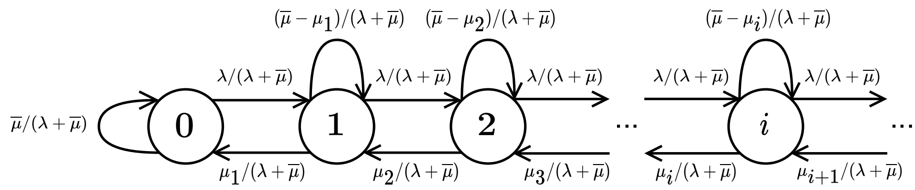

(b)

Figure 2.1.: Top: Markov chain for Example 1. Bottom: Uniformized Markov chain for Example 1.

$$V(i) = \frac{1}{\lambda + \overline{\mu}} \min_{\mu \in [0, \overline{\mu}]} \{C_w(i) + C_s(\mu) + \gamma + \mu V(i-1) + (\overline{\mu} - \mu)\, V(i) + \lambda V(i+1)\} \qquad i = 1, 2, .. \quad (2.2)$$

Here, γ is interpreted as a guess of the maximum average value, which is achievable within the restricted class of policies (Ata and Shneorson 2006). By solving the joint equations of (2.1) and (2.2) for each state i, we can determine the optimal value of μ_i at each queue length i. For detailed proofs, we recommend interested readers refer to the textbook by Bertsekas (2012).

In Chapter 4 of this thesis, we consider a pricing factor as a design element into the queueing system, influencing both the queue arrival rate and service rate. In contrast to the simplicity of Example 1, the model in Chapter 4 involves dynamic changes in the arrival rate and service rate based on the queue state, specifically the current queue length, due to the implementation of a dynamic pricing policy. To address the underlying semi-Markov decision process, we apply the uniformization technique explained in Example 1 and determine optimal prices for the model. Consequently, we analyze the recommended strategy for information disclosure and pricing policies based on the computed solutions.

2.4. Queueing theory

In an on-demand service platform, a user joins a queue to await their turn for service. In this section, we describe the queueing process using mathematical terminology. For a more in-depth understanding of queueing theory, we recommend interested readers to refer to the textbook by Winston (2022).

Arrival and service process The input process of the queue is called the *arrival process*. We call them customers. In all the models discussed in this thesis, we assume that at most one arrival can occur at any given instant, such as in a Poisson process. In queueing theory, when more than one arrival can occur at a given instant, we refer this as the allowance of *bulk arrivals*.

The output process of the queue is known as the service process, which is typically specified by a probability distribution referred as the *service time distribution*. This indicates that the server's work speed does not increase when there are more customers present. In queueing theory, *servers in parallel* refers to the scenario where multiple homogeneous servers work simultaneously to serve the customers in the queue. On the other hand, *servers in series* implies that a customer must go through several servers sequentially before completing the service.

In the models presented in Chapters 3 and 4, we consider a single server, not servers in parallel. Additionally, a single server can complete the service without the need for customers to pass through a series of servers.

Queue discipline The queue discipline defines the method for determining the order in which customers are served. There are four commonly used queue disciplines:

1. First-come-first-served (FCFS) discipline: Customers are served in the order of their arrival.

2. Last-come-first-served (LCFS) discipline: The most recent arrivals are served first. One example is job scheduling, where the most recently submitted jobs are given priority for execution.

3. Serve-in-random-order (SIRO) discipline: Customers waiting in the queue are served in a random order. One example of its application is load balancing in

distributed systems. Tasks or requests are assigned to servers in a random manner to prevent overloading of specific servers.

4. Priority queueing disciplines: A priority discipline categorizes customers and serves them based on their assigned priority. In the field of healthcare, patients are prioritized in emergency rooms based on the severity of their condition.

In this thesis, we use the FCFS principles as the queue disciplines in Chapter 3 and 4. This implies that customers and suppliers on each side of the queueing system are considered homogeneous entities.

The Kendall-Lee notation Kendall (1951) introduced a notation for describing queueing systems based on six characteristics:

$$Arrival/Service/Servers/Discipline/Customers/Population.$$

The first and second characteristics describe the arrival and service process using standard abbreviations: i), M: Intervals between arrivals or service times are independent, identically distributed random variables (iid) and follow an exponential distribution; ii), D: Intervals between arrivals or service times are iid and deterministic; iii), E_k: Intervals between arrivals or service times are iid Erlang random variables with a shape parameter k; iv), G: Intervals between arrivals or service times are iid and follows some general distribution. The third characteristic describes the number of parallel servers. The fourth characteristic describes the queue discipline. The fifth characteristic describes the maximum capacity or limit on the number of customers allowed in the queue at any given time. The sixth characteristic describes the size of the population from which the customers are drawn. In this thesis, we focus on queueing models that adhere to the FCFS principle and assume an infinite population size. We omit the last three characteristics: $Discipline/Customers/Population$.

Birth-death process The birth-death process is a specific case of a continuous-time Markov process in which state transitions occur in only two forms: "births," which increment the state variable by one, and "deaths," which decrement the state by one. A Markov chain is considered *reversible* if, in the steady state, the sequence of states in reverse order is statistically indistinguishable from the sequence in forward order. The birth-death process is reversible and *detailed balance equations* apply, given by

$$\pi_i p_{ij} = \pi_j p_{ji}.$$

for each $i \in S$ and $j \in S$. The queueing models considered in this thesis are based on birth-death processes.

3. Information Disclosure Policy Design

Abstract: Information design in on-demand service platforms matters in applications such as taxi services, ride-hailing platforms, and freight exchanges. Displayed service delay information significantly affects platform revenues, leading users to balk or renege. Information design is crucial for platforms with dynamic supply and demand; however, the effects of various information policies on user behavior are unclear. User arrival rates are not only influenced by the platform's information policy, but also by the perceived long-term matching probability in a model with multiple platforms. We use queueing theory to examine information disclosure policies for maximizing platform revenue in a marketplace featuring single- and double-sided queueing service systems. In a single-sided model, forming the queue on the side with the higher arrival rate generates higher expected revenue. The preferred information policy depends on the arrival rate and system load. In a double-sided model, hiding the queue-length information is preferred for the side with a lower arrival rate, whereas displaying it on both sides proves advantageous when both sides have high arrival rates. Considering the long-term influence of matching probability on user arrival rates, the recommendations for selecting the information policy remain qualitatively the same, but the revenue difference between information policies increases.

3.1. Introduction

Information design is important for facilitating matching for online on-demand service platforms that connect supply and demand. With the rapid rise of service platformization in various fields, competition and promotion among multiple platforms have made information design a critical factor in gaining user reputation and market share. The service systems for these applications can be classified into two categories based on their structure. *1) Markets featuring a single-sided service queue, where customers are assigned services by a centralized center*, encompassing scenarios such as ride-hailing platforms like Uber, DiDi, and Lyft; food delivery services like DoorDash and Uber Eats; and online customer support, including live chat and email support. For these platforms, once a customer arrives, the platform preselects service providers who compete for this customer at that moment. Although there are multiple customers and service providers, to study information design, such platforms are often modeled as single-sided queues (Banerjee et al. 2015; Feng et al. 2021; H. Wang and Yang 2019). For instance, in Lyft and Uber, riders join the system's pool at a certain rate during some period in a specific region. Nearby drivers queue up in the region and wait for dispatched orders. A static pricing policy is considered in each region for the simplicity and fairness of the platform's operation. *2) Markets featuring a double-sided service queue, where both customers and suppliers need to be matched*, including scenarios such as peer-to-peer (P2P) car-sharing platforms like Turo and Getaround; freight exchanges, such as Timocom, Raaltrans, Trans EU, Full Truck Alliance, and Uber Freight; and freelance platforms like Upwork and Fiverr, among others. On these platforms, customers simultaneously interact with multiple service providers, while each provider engages with several customers for service negotiation at a given moment. For instance, on Timocom, carriers near Hamburg may negotiate with multiple shippers for a trip to Cologne, while shippers engage with various carriers listed on the freight exchange. These systems are best represented as double-sided queues.

In recent years, platform designers have increasingly focused on the research question of how to effectively disclose current service delay information in two-sided marketplaces. A good disclosure policy not only attracts more users to the platform but also enhances the platform's reputation and perceived service quality in the long run, while a poor disclosure policy can have adverse effects. In practice, three categories of queue-length information disclosure policies are observed among online service platforms, where users on both sides of the platform are referred to as customers on the demand side and suppliers on the supply side.

1. **Full information**: The platform provides both customers and suppliers with queue-length information. This information can be used to calculate the expected waiting time for incoming users, which may cause them to *balk* at joining the queue and explore alternative options if they perceive the current queue length as too long. In a single-sided queueing service system, we refer as the *visible* information policy. In a double-sided queueing service system, we refer as the *both-visible* (BV) information policy since both customers and suppliers receive the information.

Company	Specialities	Information policy	Daily transactions
Timocom	EU	BV	800,000
Raaltrans	Czech Republic	BV	160,000
Wtransnet	South EU	BV	40,000 (only Iberia)
Trans EU	eastern EU	SV	200,000
Full Truck Alliance	China	SV	200,000
Uber Freight	EU/US	BI (Before 2021)	n.a.

Note. The market size is defined by the number of daily transactions. Data source: Hänel (2021).

Table 3.1.: Comparison of information disclosure policies and daily transactions among European Online Freight Exchange Platforms (Hänel 2021). One such platform, Uber Freight, has been working to enhance the transparency of its displayed information in recent years (Ligon 2021).

2. **No information**: Under this policy, neither customers nor suppliers receive information about the queue length. In a single-sided queueing service system, we refer as the *invisible* information policy. In a double-sided queueing service system, we refer as the *both-invisible* (BI) information policy. Although this approach can help attract more users to the service queue and increase the matching rate between both sides, it may also result in waiting users becoming impatient and *reneging* from the queue.

3. **Differentiated information**: The platform displays the queue-length information to one side while withholding it from the other. This includes two symmetric information policies in a double-sided queueing service system, namely *only-demand-visible* (DV) and *only-supply-visible* (SV). This type of information policy is not considered in a single-sided queueing service system, as suppliers or customers on the server side do not exhibit abandonment behavior in response to queue-length information.

We use freight exchanges as an illustrative example of a double-sided queueing service system. We consider shippers and carriers as customers and suppliers, respectively. Table 3.1 provides an overview of information policies used by some large online freight exchange platforms in Europe. Two noteworthy observations arise in the field of freight exchange in the European region. Firstly, they offer similar services, i.e., deliveries, but implement different queue-length disclosure policies. Secondly, there are numerous platforms offering comparable services, with over one hundred freight exchanges in the European region alone (Hänel 2021).

While the difference between platforms' information policies remain an area that needs further exploration, our study aims to address this gap. Empirical analyses often face challenges due to confounding factors such as pricing and interface design. To overcome these limitations, we propose a theoretical model that isolates the queue-length information disclosure factor. We characterize different user abandonment behaviors under different information policies and determine the preferred policy based on its impact on platform revenue.

3.1.1. Literature review

We first review the relevant empirical literature that illuminates various behaviors of users in the platform. Our model incorporates user behavior responses to information design to understand their impact on platform revenue. We then review the relevant analytical literature, comparing our models with the methodological approaches utilized in previous studies. We highlight that our model both aligns with and distinguishes itself from the literature by addressing assumptions about user behavior in information design and considering the long-term impact of platform service quality in a model with multiple platforms.

Empirical literature Numerous experimental and empirical studies have explored queueing behaviors under various information disclosure policies. For example, Aksin et al. (2019), Pazgal and Radas (2008), and Akşin et al. (2017) demonstrated that user abandonment mainly occurs upon market entry (balking) and while awaiting services (reneging). In queueing systems where users can access real-time service delay information, Batt and Terwiesch (2015) and Akşin et al. (2013) analyzed abandonment data from a hospital emergency department and a call center, respectively. Both studies discovered that the probability of abandonment increases linearly with expected waiting time. Intriguingly, Batt and Terwiesch (2015) found that both queue length and estimated waiting time effectively indicate user abandonment. They investigated the impact of visible queue-length information on the long-term arrival rate, assuming a collinearity between queue length, user waiting time, abandonment rate, and arrival rates at different times of the day. They highlight that the perceived service quality, influenced by different levels of patient acuity, affects the users' long-term arrival rate. In situations with unobservable queues, reneging behavior is highly non-trivial (Hassin 2016). For instance, Maglaras et al. (2014) noted that reneging occurs when customers join the queue without a clear understanding of service speed. Miscalibration is another factor; for example, overly optimistic customers might become impatient and renege, while other customers remain patient and willing to wait. However, empirical studies face challenges in fully understanding the impact of user behavior on platforms solely due to disclosure policies, as user behavior can be influenced by various factors. Consequently, several types of theoretical models have been developed in this field to enhance our understanding of these issues.

Analytical literature Research on information design can be traced back to several seminal studies by Naor (1969), Parkan and Warren Jr (1978), and Martin and Pankoff (1982). Naor (1969) investigated an observable $M/M/1$ queueing system in which users balk at joining the queue based on a self-determined, exogenously given admission level, considering the visibly observed queue length. In an exclusive examination of user balking behavior leading to abandonment, Simhon et al. (2016) concluded that displaying queue-length information when the queue is short and turning off the display when the queue is long is not optimal. B. Kim and J. Kim (2017) further investigated this $M/M/1$ queueing system and identified the optimal threshold for queue length. The queue-length information is displayed when it is below this threshold and hidden when it exceeds it. Their optimization aims to reduce the steady-state probability of the system being an empty queue. Therefore, the key to selecting an information policy is to increase the system load when the queue is short. Amidst the trade-offs in information disclosure policies, Hassin and Koshman (2017) proposed the optimal pricing mechanism for implementing a static pricing policy. Different from previous studies, our model, when the queue length is displayed, does not assume that users' admission levels concerning displayed queue length are exogenously fixed. In our model, the displayed information affects user behaviors in two primary ways: firstly, it instigates balking behavior, prompting users to make informed decisions about joining the queue; secondly, it induces greater user tolerance for longer queue lengths when the service rate is higher.

Parkan and Warren Jr (1978) and Martin and Pankoff (1982) utilized a Bayesian framework to model users' reneging behavior in an unobservable $M/M/1$ queueing system.

They assumed that users, given an a-priori distribution of the market, would decide whether to renege or not after entering the market, based on their individual waiting time and utility functions. Recent game-theoretical literature on invisible service delay information policies examines the ways in which information provision can impact agent behavior (Bergemann and Morris 2019). Assuming such equilibrium behavior, neither a purely display-only nor a hide-only information policy is optimal. The disclosure policy influences the process by which users form their beliefs. Applying this game theory framework, Lingenbrink and Iyer (2019) studied the disclosure of queue-length information in a single-sided queueing service system and designed a binary signaling mechanism, proven to be optimal for maximizing platform revenue. Gur et al. (2023) studied the combined decisions of pricing and information disclosure for a product between sellers and buyers. They broadened the understanding of how information design interacts with other elements in platform development.

Game theory attributes a high level of rationality to users' reneging behavior, assuming that users hold prior beliefs about the market state distribution and update their beliefs as Bayesians (Allon et al. 2019; Jian and Sami 2010). The high level of rationality in decision-making might also be a too strong assumption for this domain (Bisiere et al. 2015). In contrast, our modeling framework, similar to Cui et al. (2022), captures reneging behavior through a Poisson process, indicating a progressive increase in user reneging as waiting time lengthens (Armony et al. 2009). Our model makes fewer assumptions about user rationality and serves as a complement to game-theoretical approaches. We differentiate between balking behavior triggered by displayed information (e.g., long queue length) and reneging within the queue when information is not displayed. By comprehensively considering both types of user behavior in the marketplace, our methodology enables a deeper understanding of the impact of information disclosure on expected revenue while accounting for service quality.

Our work relates to the stream of queueing papers that study the platforms in a competitive environment, where a platform's reputation and quality of service can enhance its attractiveness to potential users over the long term (Parker et al. 2016). Bai et al. (2019) and Ke et al. (2020) found that pricing can influence endogenous user behavior to avoid the Wild Goose Chase (WGC) phenomenon and increase platform revenue. Bai et al. (2019) suggested that if the arrival rates of both sides are high, the platform should apply the same policy on both sides, a finding that aligns with one of our observations in the two-sided queueing model. Bernstein et al. (2021), Jeitschko and Tremblay (2020) and

Bimpikis and Mantegazza (2023) discovered that if all users simultaneously use multiple platforms, social welfare may decrease. Related to information design, Bimpikis et al. (2020) emphasized its role in regulating supply-demand composition and attracting users during early stages. Anunrojwong et al. (2022) explored its effect in congested social service systems. However, all the papers mentioned above only investigate the short-term impact of platform design on user behavior. Our model considers both types of user behaviors influenced by information disclosure. More importantly, it examines the role of information design in a market with multiple platforms, taking into consideration the impact of perceived long-term matching probabilities on user arrival rates. Our findings reveal the impact of endogenous arrival rates on the preferred information policy, specifically the extent of information disclosure by platforms in an environment where users have alternative options, and emphasize the significance of information design in a multi-platform context compared to a monopoly platform.

3.1.2. Results and contributions

We introduce two queueing models for single-sided and double-sided queueing service systems in a segmented market with homogeneous supply and demand requests. For instance, customers with similar needs form a queue to find suppliers capable of performing the work, while homogeneous suppliers on the other side provide the service. To model user abandonment behavior, we analyze two behavioral assumptions that how have been analyzed in previous works (Banerjee et al. 2015; Cui et al. 2022; Taylor 2018). When a user can see queue-length information, she may choose to balk at joining the service queue; while if she cannot see the information, she may renege during the waiting process.

Our study examines the impact of the two user abandonment behaviors on the platform's revenue and offers strategic implications for platform information design. The preferred information policy depends on arrival rate and system load, which is the ratio of demand and supply arrival rates. We show that in the one-sided queueing model, forming the queue on the side with the larger arrival rate and concealing information in an expected longer queue is preferred for higher expected revenue. In the double-sided queueing model, we show that a differentiated information policy is preferred when the arrival rates on both sides are sufficiently different. For a large market, meaning high arrival rates on both sides, the system load determines the preference of displaying information on one side, both sides, or none at all. Our results offer an explanation for the information policies adopted by freight exchanges. For instance, platforms with higher daily transaction rates tend to display the real-time queue length information, as shown in Table 3.1. Conversely, platforms like Trans EU in specialized regions utilize a differentiated information policy. Uber Freight, in its early stage as a relatively new online freight exchange platform, did not disclose queue-length information before 2021 due to its small early market. Our model's predictions are consistent with Uber Freight's apparent consideration of changing its information disclosure policy now that it has gained popularity (Ligon 2021).

An extension of our model incorporates an *endogenous* arrival rate that takes into account the user's perceived long-term matching probability, a feature that captures the increasing sensitivity of users to service quality in the context of multiple platforms, as discussed in previous research (Bernstein et al. 2021; Jeitschko and Tremblay 2020). If users perceive a low matching probability, they may switch to a competing platform. We find that the recommendations regarding the preferred information policy remain qualitatively the same in the endogenous model compared to the exogenously given arrival rate. However, the revenue difference resulting from the right information policy is much larger in the endogenous model. This indicates that higher service quality not only boosts arrival rates but also amplifies the difference between information policies, leading to increased revenue. This underscores the importance of information design in the context of multiple platforms.

3.2. Single-sided queue

3.2.1. Model and notation

We utilize an $M/M/1$ queue to examine a single-sided queueing service system within a segmented market, where customers request homogeneous supplier capacities (e.g., shippers and carriers share the same origin-destination pair in online freight exchanges) and they are matched on a first-come-first-served basis. This is referred to as the single-sided queueing model. The model represents a *demand market* when customers queue and suppliers provide service, and a *supply market* in the opposite scenario. Our analysis in the following section focuses on the demand market, given the structural symmetry between both markets.

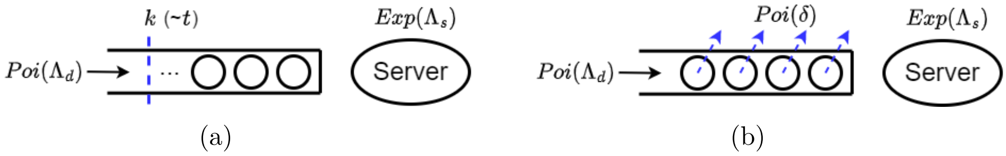

Figure 3.1.: The single-sided queueing model for a demand market. Left: K model. Right: R model.

We assume that customers on the demand side and suppliers on the supply side arrive independently in the market, following Poisson processes with respective arrival rates of Λ_d and Λ_s. In a demand market, customers' service time is an independent and identically distributed exponential random variable with mean $1/\Lambda_s$. The arrival rate of the server side, i.e., Λ_s, is referred to as the *service rate*. We define the system load as $\rho = \Lambda_d/\Lambda_s$. We define the size of the market at steady state as the *market size*, measured by the corresponding user arrival rate. Specifically, the *demand market size* is considered larger when the arrival rate of customers is higher while that of suppliers remains constant; the *supply market size* is larger when the arrival rate of suppliers is higher while that of customers remains constant; the *full market size* is larger when both arrival rates of customers and suppliers are higher while maintaining a fixed system load.

Two information policies named *visible* and *invisible*, defined by whether or not the real-time queue length for customers is displayed, are considered in the demand market. A diagram illustrating the queueing service systems under both information policies can be found in Figure 4.1. Under the visible information policy, a customer balks at entering the system if the indicated waiting time, based on queue length, exceeds the *truncation time* t. In this context, we use an integer $k := \lceil t\Lambda_s \rceil$, representing the corresponding queue length for tolerance, as the *truncation size* for the customer queue. Consequently, the queueing system is an observable $M/M/1/K$ queue, referred to as the K model. Under the invisible information policy, customers renege from the queue during their wait, following an independent Poisson process with a reneging rate δ. The queueing system is an unobservable $M/M/1$ queue with reneging behavior under the invisible information policy, known as the R model. Notably, this rate is smaller than the arrival and service rates, i.e., $\delta < \Lambda_\varpi$ for each $\varpi \in \{d, s\}$, which is a mild assumption in practice. The parameters t and δ represent *user patience*. Thus, if users are more patient, the value of t is larger, or the value of δ is smaller. In the following, we use $\ell \in \{K, R\}$ to represent the information policy.

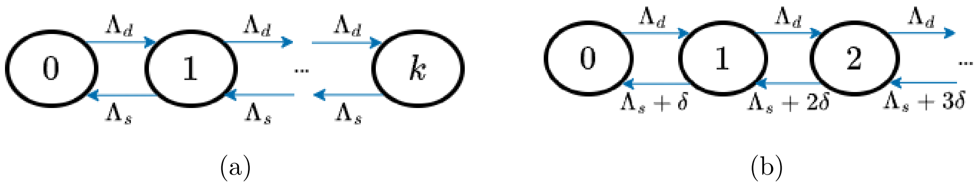

Figure 3.2.: Transitions diagrams of Markov chains for a demand market. Left: K model. Right: R model.

The platform generates net revenue by charging a fixed commission on each matched pair of customers and suppliers, aiming to maximize its expected net revenue. Without causing any ambiguity, the revenue mentioned in Chapter 3 is referring to net revenue. To specifically analyze the impact of information disclosure independently of pricing, we assume the platform implements a static pricing policy. The expected revenue depends on the matching rate, which serves as an indicator of the system's throughput. Accordingly, the platform's expected revenue is denoted as $Rev^{\ell} := \Lambda_{\varpi}\xi_{\varpi}^{\ell}$ for each $\varpi \in d, s$. Here, ξ_{ϖ}^{ℓ} signifies the matching probability of side ϖ under information policy ℓ, representing the long-term ratio of matches to entrants. The matching probability serves as an evaluation of service quality for each side.

3.2.2. Markov chain models

We consider the queue length as the market state, and a uni-chain Markov chain can capture the features of a single-sided queueing service system. The transition diagrams for the Markov chains of both K and R models are provided in Figure 3.2. Formally, the state space for both models are $S_K := \{0, 1, .., k\}$ and $S_R := \mathbb{N}$. The transition rates are

$$r_{ij}^{K} = \begin{cases} \Lambda_d & \text{if } \ j = i+1 \\ \Lambda_s & \text{if } \ j = i-1 \\ 0 & otherwise \end{cases} \qquad \text{and} \qquad r_{ij}^{R} = \begin{cases} \Lambda_d & \text{if } \ j = i+1 \\ \Lambda_s + i\delta & \text{if } \ j = i-1 \\ 0 & otherwise \end{cases}$$

for each $i \in S_{\ell}$ and $j \in S_{\ell}$ where $\ell \in \{K, R\}$.

We solve the steady-state probabilities of Markov chains for K and R models in system load ρ to compare models that have the same arrival rates for customers and suppliers. The steady-state distributions are

$$\pi_0^K = \frac{1-\rho}{1-\rho^{k+1}} \quad \text{and} \quad \pi_i^K = \rho^i \pi_0^K \quad \text{for each} \quad i \in S_K, \tag{3.1}$$

$$\pi_0^R = \frac{1}{1+\sum\limits_{i=1}^{\infty}\prod\limits_{j=1}^{i}\frac{\rho}{1+j\delta/\Lambda_s}} \quad \text{and} \quad \pi_i^R = \prod_{j=1}^{i}\frac{\rho}{1+j\delta/\Lambda_s}\pi_0^R \quad \text{for each} \quad i \in S_R. \tag{3.2}$$

The matching probabilities of customers and suppliers are

$$\xi_d^\ell = (1-\pi_0^\ell)/\rho \quad \text{and} \quad \xi_s^\ell = 1-\pi_0^\ell \tag{3.3}$$

for each $\ell \in \{K, R\}$. The expected revenue is $Rev^\ell = \Lambda_s(1-\pi_0^\ell)$.

3.2.3. Monotonicity of revenue and user patience

The expected revenue is monotonically increasing with user patience.

Proposition 2. *The higher the user patience, the higher the expected revenue. Under the visible information policy, the expected revenue increases with increasing truncation size, i.e.,* $Rev^K(k+1) > Rev^K(k)$. *It increases with increasing truncation time, i.e.,* $\frac{dRev^K}{dt} > 0$. *Under the invisible information policy, it decreases with the reneging rate, i.e.,* $\frac{dRev^R}{d\delta} < 0$.

Proof. K **model.** Since $\pi_0^K = \frac{1-\rho}{1-\rho^{k+1}}$, $\pi_i^K = \rho^i\pi_0^K$ and $Rev^K = \Lambda_s\left(1-\pi_k^K\right) = \Lambda_s\frac{1-\rho^k}{1-\rho^{k+1}}$ where k is an integer, the revenue increment in k is

$$Rev^K(k+1) - Rev^K(k) = \Lambda_s\left(\frac{1-\rho^{k+1}}{1-\rho^{k+2}} - \frac{1-\rho^k}{1-\rho^{k+1}}\right) = \frac{\Lambda_s\rho^k\left(\rho^2-2\rho+1\right)}{\left(1-\rho^{k+1}\right)\left(1-\rho^{k+2}\right)} > 0.$$

We also show that $\frac{dk}{dt} = \frac{d(\Lambda_s t)}{dt} > 0$. As $\frac{dk}{dt} \geq 0$, it implies that the truncation size increases monotonically with the truncation time for fixed arrival rates of customers and suppliers. Therefore, the expected revenue increases monotonically with the truncation time, i.e., $\frac{dRev^K}{dt} \geq 0$.

R model. Since $\pi_i^R = \prod_{j=1}^{i} \frac{\rho}{1+j\delta/\Lambda_s}\pi_0^R$, $\pi_0^R = \frac{1}{1+\zeta}$ and $Rev^R = \left(1-\pi_0^R\right)\Lambda_s$, the first derivative of Rev^R in δ is

$$\frac{dRev^R}{d\delta} = \Lambda_s \frac{1}{(1+\zeta)^2}\cdot\frac{d\zeta}{d\delta} = \frac{\Lambda_s}{(1+\zeta)^2}\sum_{i=1}^{\infty}\prod_{j=1}^{i}\frac{\rho}{1+j\delta/\Lambda_s}\cdot\sum_{j=1}^{i}\frac{-j}{\Lambda_s+j\delta} < 0.$$

■

In our models, user patience parameters are estimated and provided in the market, and the platform planner subsequently determines the preferred information policy. Proposition 2 illustrates that both balking and reneging behaviors result in a decrease in expected revenue, highlighting that maximizing revenue occurs when fewer customers exhibit these behaviors. Specifically, under the visible information policy, when considering the service rate of the system, the truncation size can be interpreted as the truncation time. Proposition 2 establishes the monotonic relationship between expected revenue and user patience parameters (k, t, and δ) under each information policy. This suggests the uniqueness of a threshold for determining the preferred information policy in user patience under the ceteris paribus condition for fixed arrival rates of customers and suppliers.

3.2.4. Queue side for increased revenue

In the single-sided model, we address queueing which side has a higher expected revenue. This analysis adds to the question about comparing customer and supplier markets: which one has a higher expected revenue? We compare the expected revenue of the single-sided queueing model for different sides to queue. For the same arrival rates of customers and suppliers, we denote the expected revenue in a demand market by Rev_d^ℓ and that in a supply market by Rev_s^ℓ.

Proposition 3. *In a single-sided model, queueing the side with a higher arrival rate has a higher expected revenue. Specifically, for each $\ell \in \{K, R\}$, if the system load satisfies $\rho \geq 1$, then the expected revenue in a demand market is higher than or equal to that in a supply market, i.e., $Rev_d^\ell \geq Rev_s^\ell$. Otherwise, if $\rho < 1$, then $Rev_d^\ell < Rev_s^\ell$.*

Proof. We discuss the case where the arrival rate of customers is higher than that of suppliers, i.e., $\Lambda_d \geq \Lambda_s$ and $\rho \geq 1$. We omit the case where $\Lambda_d < \Lambda_s$, as the model setting is symmetric. We compare the expected revenues of single-sided models with different queue sides. Recall that the expected revenue of queueing customers (i.e., a demand market) is denoted by $Rev_d = Rev$, and the expected revenue of queueing suppliers (i.e., a supply market) is denoted by Rev_s.

K **model.** The expected revenue of queueing customers is $Rev_d^K = \Lambda_s(1-\pi_0^K) = \Lambda_s \frac{\rho-\rho^{k+1}}{1-\rho^{k+1}}$, and the expected revenue of queueing suppliers is $Rev_s^K = \Lambda_d \frac{1-\rho^{k^s}}{1-\rho^{k^s+1}}$, where $k^s := t\Lambda_d$ is the truncation size in the supplier market. It holds that

$$Rev_d^K - Rev_s^K = \Lambda_s \rho \frac{1-\rho^{\rho k}}{1-\rho^{\rho k+1}} - \Lambda_d \frac{1-\rho^{k^s}}{1-\rho^{k^s+1}} = \Lambda_d \left(\frac{1-\rho^k}{1-\rho^{k+1}} - \frac{1-\rho^{\lceil k/\rho \rceil}}{1-\rho^{\lceil k/\rho \rceil+1}} \right) \overset{\rho \geq 1}{\geq} 0.$$

R **model.** Denote $\zeta := \sum_{i=1}^{\infty} \prod_{j=1}^{i} \frac{\rho}{1+j\delta/\Lambda_s}$ and $\zeta^s := \sum_{i=1}^{\infty} \prod_{j=1}^{i} \left(\frac{1}{\rho+j\delta/\Lambda_s} \right)$. The expected revenues of queueing different sides are $Rev_d^R = \Lambda_s(1-\pi_0^R) = \Lambda_s \frac{\zeta}{1+\zeta}$ and $Rev_s^R = \Lambda_d \frac{\zeta^s}{1+\zeta^s}$. It holds

$$\begin{aligned} Rev_d^R - Rev_s^R &= \Lambda_s \left(\frac{\zeta}{1+\zeta} - \rho \frac{\zeta^s}{1+\zeta^s} \right) \\ &= \frac{\Lambda_s}{(1+\zeta_x)(1+\zeta^s)} \left(\zeta - \rho\zeta^s - (\rho-1)\zeta\zeta^s \right). \end{aligned} \tag{3.4}$$

Let us denote $f_r = \zeta - \rho\zeta^s - (\rho-1)\zeta\zeta^s$. In the following analysis, we demonstrate that $f_r \geq 0$. To do so, we seek specific different ad-hoc intervals corresponding to different degrees of relaxation for f_r. We first divide the domain of ρ into three segments: (i) $\rho \in [1.8, \infty)$, (ii) $\rho \in [1.06, 1.8)$, and (iii) $\rho \in [1, 1.06)$. We then show that $f_r \geq 0$ in each of the three cases. The magnitude of these values does not impact the generality of our conclusions.

Case (i): $\rho \in [1.8, \infty)$. In this segment, we derive a lower bound equation for f_r (i.e., (3.5)), which is shown to be larger than zero for any $\rho \in [1.8, \infty)$. Denote $z := \delta/\Lambda_s$. We have:

$$\begin{aligned} f_r &\geq \sum_{i=1}^{\infty} \prod_{j=1}^{i} \frac{\rho}{1+jz} - \rho \sum_{i=1}^{\infty} \prod_{j=1}^{i} \frac{1}{\rho+z} - (\rho-1) \sum_{i=1}^{\infty} \prod_{j=1}^{i} \frac{\rho}{1+jz} \sum_{i=1}^{\infty} \prod_{j=1}^{i} \frac{1}{\rho+z} \\ &= \frac{z}{\rho+z-1} \sum_{i=1}^{\infty} \prod_{j=1}^{i} \frac{\rho}{1+jz} - \frac{\rho}{\rho+z-1} = \frac{z}{\rho+z-1} \left(\sum_{i=1}^{\infty} \prod_{j=1}^{i} \frac{\rho}{1+jz} - \frac{\rho}{z} \right) \end{aligned} \tag{3.5}$$

where

$$\frac{d}{d\rho}\left(\sum_{i=1}^{\infty}\prod_{j=1}^{i}\frac{\rho}{1+jz}-\frac{\rho}{z}\right)=\sum_{i=1}^{\infty}\frac{i}{\rho}\prod_{j=1}^{i}\frac{\rho}{1+jz}-\frac{1}{z}\geq\sum_{i=1}^{\infty}i1.8^{i-1}\prod_{j=1}^{i}\frac{1}{1+jz}-\frac{1}{z}>0.$$

This indicates that the term $\sum\limits_{i=1}^{\infty}\prod\limits_{j=1}^{i}\frac{\rho}{1+jz}-\frac{\rho}{z}$ monotonically increases with ρ for any $\rho\in[1.8,\infty)$. As shown by the inequality

$$\begin{aligned}\frac{d}{dz}\left(\sum_{i=1}^{\infty}\prod_{j=1}^{i}\frac{\rho}{1+jz}-\frac{\rho}{z}\right)&\leq\frac{d}{dz}\left(\sum_{i=1}^{\infty}\prod_{j=1}^{i}\frac{1.8}{1+jz}-\frac{1.8}{z}\right)\\&=\frac{1.8}{z^2}-\sum_{i=1}^{\infty}\left(\prod_{j=1}^{i}\frac{1}{1+jz}\right)i1.8^{i}<0,\end{aligned}$$

the term $\sum\limits_{i=1}^{\infty}\prod\limits_{j=1}^{i}\frac{\rho}{1+jz}-\frac{\rho}{z}$ monotonically increases with z for any $\rho\in[1.8,\infty)$ and $z\in(0,1)$. Therefore,

$$(3.4)\geq\frac{\Lambda_s}{(1+\zeta_x)(1+\zeta^s)}\frac{z}{\rho+z-1}\left(\sum_{i=1}^{\infty}\prod_{j=1}^{i}\frac{1.8}{1+j}-1.8\right)>0.$$

Here, we can see that the RHS of the inequality is larger than zero, since all terms in the expression are positive.

Case (ii): $\rho\in[1.06,1.8)$. In this segment, we introduce the lower bound equation $f_\upsilon:=\zeta-\upsilon\zeta^s-(\upsilon-1)\zeta\zeta^s$, which is a function of an independent variable υ. Since $\frac{df_\upsilon}{d\upsilon}\leq 0$, it follows that $f_r\geq f_\upsilon$ if $\rho\leq\upsilon$. Furthermore, we have already shown in Case (i) that $f_\upsilon\geq 0$ if $\upsilon=1.8$. Moving forward, we demonstrate that f_υ is monotonically increasing with ρ and monotonically decreasing with z for any $\upsilon\in[1.06,1.8)$. Before demonstrating this, we define a function $g_\upsilon:=\frac{\zeta}{1+\zeta}-\upsilon\frac{\zeta^s}{1+\zeta^s}$. It holds

$$\frac{dg_\upsilon}{d\rho}=\frac{d}{d\rho}\left(\frac{\Lambda_s}{(1+\zeta)(1+\zeta^s)}f_\upsilon\right)=\frac{d}{d\rho}\left(\frac{\sum\limits_{i=1}^{\infty}\prod\limits_{j=1}^{i}\frac{\rho}{1+jz}}{1+\sum\limits_{i=1}^{\infty}\prod\limits_{j=1}^{i}\frac{\rho}{1+jz}}-\upsilon\frac{\sum\limits_{i=1}^{\infty}\prod\limits_{j=1}^{i}\frac{1}{\rho+jz}}{1+\sum\limits_{i=1}^{\infty}\prod\limits_{j=1}^{i}\frac{1}{\rho+jz}}\right)\geq 0.$$

We find

$$\frac{d}{d\rho}\left(\zeta\zeta^{s}\right)$$
$$=\sum_{i=1}^{\infty}\frac{i}{\rho}\prod_{j=1}^{i}\frac{\rho}{1+jz}\cdot\sum_{i=1}^{\infty}\prod_{j=1}^{i}\frac{1}{\rho+jz}-\sum_{i=1}^{\infty}\prod_{j=1}^{i}\frac{\rho}{1+jz}\cdot\sum_{i=1}^{\infty}\sum_{j=1}^{i}\frac{1}{\rho+jz}\prod_{j=1}^{i}\frac{1}{\rho+jz}\geq 0$$

which indicates

$$\frac{d}{d\rho}\frac{\Lambda_s}{(1+\zeta)\left(1+\zeta^{s}\right)}\leq 0,\quad\text{and hence}\quad\frac{df_{\upsilon}}{d\rho}\geq 0.$$

We find

$$\frac{d}{dz}\frac{\zeta}{\zeta^{s}}=\frac{\sum\limits_{i=1}^{\infty}\prod\limits_{j=1}^{i}\frac{\rho}{1+jz}\cdot\sum\limits_{i=1}^{\infty}\prod\limits_{j=1}^{i}\frac{1}{\rho+jz}\sum\limits_{j=1}^{i}\frac{j}{\rho+jz}-\sum\limits_{i=1}^{\infty}\prod\limits_{j=1}^{i}\frac{\rho}{1+jz}\sum\limits_{j=1}^{i}\frac{j}{1+jz}\cdot\sum\limits_{i=1}^{\infty}\prod\limits_{j=1}^{i}\frac{1}{\rho+jz}}{\left(\zeta^{s}\right)^{2}}\leq 0,$$

which indicates

$$\frac{d}{dz}\left(\frac{1}{\zeta^{s}}-\frac{\rho}{\zeta}+1-\rho\right)\leq 0,\quad\text{and hence}\quad\frac{df_r}{dz}\leq 0\quad\text{and}\quad\frac{df_{\upsilon}}{dz}\leq 0.$$

The monotonicity of f_{υ} in ρ and z implies that if we solve for ρ such that $f_{\upsilon}(z=1)=0$ and denote the solution as ε, then for any $\rho\in[\varepsilon,\infty)$ and $z\in(0,1)$, it holds that $f_r\geq f_{\upsilon}\geq 0$. In other words, if we can find a value of ε smaller than 1.06, we can prove Case (ii). To do so, we can recursively calculate $f_{\upsilon}(z=1)=0$ by updating υ to ε. After the fifteenth round, we can find a solution $\varepsilon\leq 1.06$.

Case (iii): $\rho\in[1,1.06)$. In this section, we derive a lower bound for f_r (i.e., (3.6)) and demonstrate that this lower bound is higher than zero for any $\rho\in[1,1.06)$. For (3.4), it holds

$$\begin{aligned}(3.4)&=\frac{\Lambda_s\left(\frac{1}{\zeta^{s}}-\frac{\rho}{\zeta}-(\rho-1)\right)}{\zeta\zeta^{s}\left(1+\zeta\right)\left(1+\zeta^{s}\right)}\\&\geq\frac{\Lambda_s}{\zeta\zeta^{s}\left(1+\zeta\right)\left(1+\zeta^{s}\right)}\left(\frac{1}{\sum\limits_{i=1}^{\infty}\prod\limits_{j=1}^{i}\frac{1}{\rho+j}}-\frac{\rho}{\sum\limits_{i=1}^{\infty}\prod\limits_{j=1}^{i}\frac{\rho}{1+j}}-\rho+1\right)\end{aligned}\tag{3.6}$$

where

$$
\begin{aligned}
&\frac{d}{d\rho}\left(\frac{1}{\sum\limits_{i=1}^{\infty}\prod\limits_{j=1}^{i}\frac{1}{\rho+j}}-\frac{\rho}{\sum\limits_{i=1}^{\infty}\prod\limits_{j=1}^{i}\frac{\rho}{1+j}}-\rho+1\right)\\
&=\frac{\sum\limits_{i=1}^{\infty}\prod\limits_{j=1}^{i}\frac{1}{\rho+j}\sum\limits_{j=1}^{i}\frac{1}{\rho+j}}{\left(\sum\limits_{i=1}^{\infty}\prod\limits_{j=1}^{i}\frac{1}{\rho+j}\right)^2}+\frac{\sum\limits_{i=1}^{\infty}\left(\prod\limits_{j=1}^{i}\frac{\rho}{1+j}\right)i}{\left(\sum\limits_{i=1}^{\infty}\prod\limits_{j=1}^{i}\frac{\rho}{1+j}\right)^2}-\frac{1}{\sum\limits_{i=1}^{\infty}\prod\limits_{j=1}^{i}\frac{\rho}{1+j}}-1\\
&\geq\frac{\sum\limits_{i=1}^{\infty}\prod\limits_{j=1}^{i}\frac{1}{1.06+j}\sum\limits_{j=1}^{i}\frac{1}{1.06+j}}{\left(\sum\limits_{i=1}^{\infty}\prod\limits_{j=1}^{i}\frac{1}{1+j}\right)^2}+\frac{\sum\limits_{i=1}^{\infty}\left(\prod\limits_{j=1}^{i}\frac{1}{1+j}\right)i}{\left(\sum\limits_{i=1}^{\infty}\prod\limits_{j=1}^{i}\frac{1.06}{1+j}\right)^2}-\frac{1}{\sum\limits_{i=1}^{\infty}\prod\limits_{j=1}^{i}\frac{1}{1+j}}-1>0.
\end{aligned}
$$

Hence it holds

$$
(3.6)\geq\frac{\Lambda_s}{\zeta\zeta^s\left(1+\zeta\right)\left(1+\zeta^s\right)}\left(\frac{1}{\sum\limits_{i=1}^{\infty}\prod\limits_{j=1}^{i}\frac{1}{1+j}}-\frac{1}{\sum\limits_{i=1}^{\infty}\prod\limits_{j=1}^{i}\frac{1}{1+j}}-1+1\right)=0.
$$

■

In the single-sided model, users on the server side are equivalent to users queueing with absolutely no patience. For instance, in a demand market, suppliers on the server side will leave immediately without waiting if they cannot be matched upon arrival at the platform. Consequently, the side with a lower arrival rate performing the service can reduce the number of users who choose not to wait if they cannot be matched upon arrival and depart immediately.

3.2.5. Threshold to determine information disclosure

We define an *indifference curve* to determine the preferred information policy. On the indifference curve, $f_x^{(A,B)} = Rev^A - Rev^B \triangleq 0$ signifies that if the market parameters satisfy this condition, information policies A and B have the same expected revenue. This implies that the platform is indifferent to the choice of information policy, as the same expected revenue is attained regardless of the policy implemented. Consequently, it

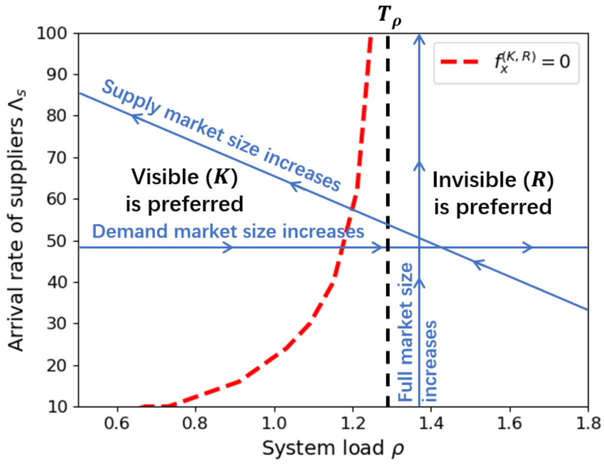

Figure 3.3.: The preferred information policy in a single-sided queueing model: $\Lambda_s \in [10, 100]$ and $\rho \in [0.5, 1.8]$.

determines the preferred information policy, with each policy being preferred on one side of the curve. Let $\zeta := \sum_{i=1}^{\infty} \prod_{j=1}^{i} \frac{\rho}{1+j\delta/\Lambda_s}$. In a single-sided queueing model, the indifference curve $f_x^{(K,R)} = 0$ is given by:

$$\begin{cases} \rho^{t\Lambda_s+1} + \zeta - \rho - \rho\zeta = 0 & \text{if} \quad \rho \neq 1 \\ t\Lambda_s - \zeta = 0 & \text{if} \quad \rho = 1 \end{cases} \tag{3.7}$$

For a fixed service rate Λ_s, if the customer arrival rate is low, it implies that the expected queue length in the system is short, and all ζ, ρ, and t satisfying (3.7) are small. In this case, the visible information policy is preferred, and vice versa. This also implies that when the truncation size is larger than the one satisfying the indifference curve, few customers balk upon entering the system if they see the current queue-length information. As a result, the visible information policy is preferred for higher expected revenue. Conversely, if the expected queue length is long, hiding the information attracts more users to the system, even if some users renege while waiting in the queue, ultimately increasing the expected revenue. Under different arrival rates and system loads, Figure 3.3 provides an example that illustrates the preferred policy through indifference curves.

Proposition 4. *In a demand market, if the system load ρ exceeds a threshold $1 < T_\rho < 2$, then the invisible information policy is preferred.*

Proof. **Value of T_ρ.** The value of T_ρ satisfies the condition $\lim_{\Lambda_s\to\infty} f_x^{(K,R)} = 0$, when ρ is substituted with T_ρ in the function $f_x^{(K,R)}$.

We first prove the threshold $T_\rho > 1$. Then we show that if the arrival rate of suppliers is sufficiently large (i.e., $\Lambda_s \to \infty$) and a fixed ρ, the value of t is too small to satisfy the indifference curve $f_x^{(K,R)} = 0$ for a large ρ (e.g., $\rho \geq 2$). Since the t satisfying $f_x^{(K,R)} = 0$ is monotonically increasing with ρ and Λ_s (refer to Case (i) and Case (iii) of Theorem 5), this indicates that for fixed t and δ, ρ converges to T_ρ (where $1 < T_\rho < 2$) as Λ_s increases.

Lower bound for T_ρ. We suppose $T_\rho < 1$ (i.e., $\rho < 1$) and find a contradiction. The indifference curve $f_x^{(K,R)} = 0$ is

$$\delta t = \frac{\delta}{\Lambda_s}\frac{\ln\left(\rho + (\rho-1)\sum_{i=1}^{\infty}\prod_{j=1}^{i}\frac{\rho}{1+j\delta/\Lambda_s}\right)}{\ln\rho} - \frac{\delta}{\Lambda_s}. \tag{3.8}$$

It holds

$$\begin{aligned}\lim_{\Lambda_s\to\infty}\text{RHS of (3.8)} &= \lim_{\epsilon\to 0}\frac{\epsilon\ln\left(\rho + (\rho-1)\sum_{i=1}^{\infty}\prod_{j=1}^{i}\frac{\rho}{1+j\epsilon}\right)}{\ln\rho}\\ &\leq \lim_{\epsilon\to 0}\frac{\epsilon\ln\left(\rho + (\rho-1)\sum_{i=1}^{\infty}\left(\frac{\rho}{1+\epsilon}\right)^i\right)}{\ln\rho} \overset{\rho<1}{\leq} \lim_{\epsilon\to 0}\frac{\epsilon\ln\frac{\epsilon\rho}{1+\epsilon-\rho}}{\ln\rho} = 0\end{aligned} \tag{3.9}$$

where ϵ is a variable. However, in the LHS of (3.8), the value $\delta t > 0$, which contradicts (3.9).

Upper bound for T_ρ. Since the LHS of (3.8) is a constant value as Λ_s increases sufficiently, we show the RHS of (3.8) increases to infinity if $\rho \geq 2$. It holds

$$\begin{aligned}\lim_{\Lambda_s\to\infty}\text{RHS of (3.8)} &= \lim_{\epsilon\to 0}\frac{\epsilon\ln\left(\rho + (\rho-1)\sum_{i=1}^{\infty}\prod_{j=1}^{i}\frac{\rho}{1+j\epsilon}\right)}{\ln\rho}\\ &\geq \lim_{\epsilon\to 0}\frac{\epsilon\ln\left(\rho + (\rho-1)\sum_{i=1}^{\infty}\left(\frac{\rho}{1+\epsilon}\right)^i\right)}{\ln\rho}\\ &\overset{\rho\geq 2}{\geq} \lim_{\epsilon\to 0}\frac{\epsilon\ln\left(\rho\left(\frac{\rho}{1+\epsilon}-1\right)^{\infty}\Big/(\rho-\epsilon-1)\right)}{\ln\rho} = \infty.\end{aligned}$$

This indicates that the indifference curve $f_x^{(K,R)} = 0$ cannot get satisfied if $\rho \geq 2$ as Λ_s is sufficiently large. ■

Proposition 4 reveals that an invisible information policy is preferred in a demand market with a high system load (e.g., $\rho = 1.7$ in Figure 3.3), regardless of market size. Because the system load is high, i.e., $\rho > T_\rho$, the service rate is lower than the arrival rate of the queue side. The queue length keeps relatively long, and it is preferable to conceal the queue-length information. Theorem 5 illustrates how two different types of larger market sizes affect the preferred information policy.

Theorem 5. *In a demand market, the preferred information policy is determined as follows:*

1. *If one side's market size is large and the arrival rate of customers Λ_d is below a unique threshold T_d, then the visible information policy is preferred, and vice versa.*

2. *If the full market size is large with a fixed system load $\rho < T_\rho$ and the arrival rate of suppliers Λ_s is below a unique threshold T_f, then the invisible information policy is preferred, and vice versa.*

Proof. **Values of T_d and T_f.** The value of T_d satisfies the condition $f_x^{(K,R)} = 0$, when Λ_s is held constant and Λ_d is substituted with T_d in the function $f_x^{(K,R)}$. The value of T_f satisfies the condition $f_x^{(K,R)} = 0$, when ρ is held constant and Λ_s is substituted with T_f in the function $f_x^{(K,R)}$.

We prove the uniqueness of the threshold T_ϖ for each $\varpi \in \{d, f\}$ by establishing the monotonicity of the indifference curve in three cases: (i) arrival rate of customers is larger; (ii) arrival rates of both customers and suppliers are larger. We omit the case that the arrival rate of suppliers is larger since the setting is symmetric to (i).

Case (i). When the arrival rate of customers is larger, we consider that Λ_s remains fixed and ρ increases. The value of t satisfying the indifference curve $f^{(K,R)} = 0$ is

$$t = \ln\left(\rho + (\rho - 1)\sum_{i=1}^{\infty}\prod_{j=1}^{i}\frac{\rho}{1 + j\delta/\Lambda_s}\right) \Big/ (\Lambda_s \ln\rho) - \frac{1}{\Lambda_s}. \tag{3.10}$$

To demonstrate the monotonicity of the indifference curve, we prove that t is monotonically increasing with ρ. It holds

$$\frac{dt}{d\rho} = \frac{d}{d\rho}\frac{\ln\left(\rho + (\rho-1)\sum_{i=1}^{\infty}\prod_{j=1}^{i}\frac{\rho}{1+j}\right)}{\Lambda_s \ln\rho} \geq \frac{d}{d\rho}\frac{\ln\left(\rho + (\rho-1)\frac{\rho}{2}\right)}{\Lambda_s \ln\rho} = \frac{d}{d\rho}\frac{\ln\left(\frac{\rho}{2}+\frac{1}{2}\right)}{\Lambda_s \ln\rho} \geq 0. \tag{3.11}$$

Case (ii). When arrival rates of both customers and suppliers are larger, we consider that both Λ_d and Λ_s increase and a fixed system load ρ. For (3.10), it holds

$$\begin{aligned}\frac{dt}{d\Lambda_s} &= \frac{d}{d\Lambda_s}\left(\frac{1}{\Lambda_s}\left(\ln\left(\rho + (\rho-1)\sum_{i=1}^{\infty}\prod_{j=1}^{i}\frac{\rho}{1+j\delta/\Lambda_s}\right)\Big/\ln\rho - 1\right)\right)\\ &= \frac{1}{\delta\ln\rho}\frac{d}{d\Lambda_s}\left(\frac{\delta}{\Lambda_s}\ln\left(1+\left(1-\frac{1}{\rho}\right)\sum_{i=1}^{\infty}\prod_{j=1}^{i}\frac{\rho}{1+j\delta/\Lambda_s}\right)\right).\end{aligned} \tag{3.12}$$

For simplification in the following equations, we use $z = \delta/\Lambda_s$ and $z \in (0,1)$. Since

$$\begin{aligned}&\frac{d}{dz}\left(z\ln\left(1+\left(1-\frac{1}{\rho}\right)\sum_{i=1}^{\infty}\prod_{j=1}^{i}\frac{\rho}{1+jz}\right)\right)\\ &\begin{cases}\geq \frac{d}{dz}\left(z\ln\left(1+\left(1-\frac{1}{\rho}\right)\frac{\rho}{2}\right)\right)\geq 0 & \text{if } \rho\geq 1\\ < \frac{d}{dz}\left(z\ln\left(1+\left(1-\frac{1}{\rho}\right)\frac{\rho}{2}\right)\right)< 0 & \text{if } \rho< 1\end{cases},\end{aligned} \tag{3.13}$$

this indicates (3.12) ≤ 0. ■

As illustrated in Figure 3.3, there exists a unique threshold that determines the preferred information policy, as stated in the first part of Theorem 5. Essentially, the expected queue length becomes a key determinant of the preferred information policy. A large arrival rate on the queue side results in a long expected queue length, indicating that an invisible policy is preferred. For a large full market size with a relatively low system load (for instance, $\rho = 1.1$ as shown in Figure 3.3), the second part of Theorem 5 establishes a threshold T_f. This threshold, based on the arrival rate of suppliers, indicates whether the queue length will remain relatively long or short, thereby informing the choice of the preferred information policy.

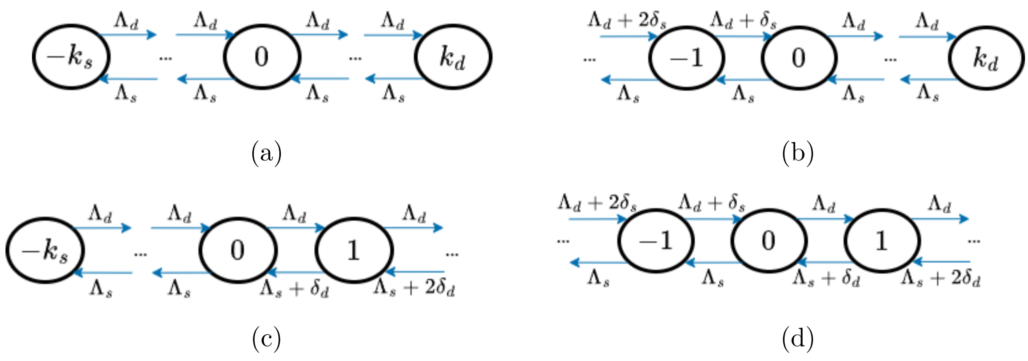

Figure 3.4.: Transitions diagrams of Markov chains under four information policies. Top Left: BV model. Top Right: DV model. Bottom Left: SV model. Bottom Right: BI model.

3.3. Double-sided queue

3.3.1. Model and notation

In this section, we establish a double-sided queueing model to examine the impact of two information policies, visible and invisible, for each side. Consequently, we have four information policies to consider: the *both-visible* (BV) policy, where both sides can see the queue-length information; the *only-demand-visible* (DV) policy and *only-supply-visible* (SV) policy, where only one side can see the queue-length information; and the *both-invisible* (BI) policy, where neither side can see it. We denote the truncation sizes and reneging rates as k_ϖ and δ_ϖ, respectively, where $\varpi \in \{d, s\}$ corresponds to the demand side (customers) and the supply side (suppliers), respectively. When the queue-length is visible, the truncation size can be converted into truncation time, taking into account the service rate of each side. We denote the truncation time by t_ϖ. We represent the set of all four information policies by $M := \{BV, DV, SV, BI\}$.

3.3.2. Markov chain models

Since customers and suppliers are matched based on the first-come-first-served principle, one of the two queues is always empty, enabling the construction of a uni-chain Markov chain for analysis. The transition diagrams for the Markov chains of the double-sided queueing models are provided in Figure 3.4. Without loss of generality, the state of this

Policy	$\ell = BV$	$\ell = DV$	$\ell = SV$	$\ell = BI$
S_ℓ	$\{-k_s, .., k_d\}$	$\{-\infty, .., k_d\}$	$\{-k_s, .., +\infty\}$	$\mathbb{Z}$
$r^\ell_{ij}, j = i+1$	Λ_d	$\max\{\Lambda_d, \Lambda_d - i\delta_s\}$	Λ_d	$\max\{\Lambda_d, \Lambda_d - i\delta_s\}$
$r^\ell_{ij}, j = i-1$	Λ_s	Λ_s	$\max\{\Lambda_s, \Lambda_s + i\delta_d\}$	$\max\{\Lambda_s, \Lambda_s + i\delta_d\}$

Table 3.2.: State space and transition rate of Markov chain.

Markov chain (i.e., i) is defined as the absolute difference between the lengths of the customer and supplier queues. The transition rates are determined by the corresponding arrival rates. For example, if customers are queueing in the market, the transition rate of state i increasing by 1 is the arrival rate of customers Λ_d, whereas it decreasing by 1 is the arrival rate of suppliers Λ_s. Particularly, when the queue-length information is not visible to customers, the transition rate of decreasing by 1 is the arrival rate of suppliers plus the reneging rate of queueing customers, i.e., $\Lambda_s + i\delta_d$. Table 3.2 summarizes the definitions of the state space S_ℓ and the transition rate r^ℓ_{ij} for each $\ell \in M$.

The steady-state distribution of the Markov chain under a BV policy is as follows:

$$\pi_i^{BV} = \begin{cases} \frac{1}{1+\frac{\rho-\rho^{k_d+1}}{1-\rho}+\frac{\rho^{k_s}-1}{\rho^{k_s+1}-\rho^{k_s}}} = \frac{1}{1+\phi_d^{BV}+\phi_s^{BV}} & \text{if } i=0 \\ \rho^i \pi_0^{BV} & \text{if } i>0 \end{cases}$$

for each $i \in S_{BV}$. Here, ϕ_d^{BV} and ϕ_s^{BV} are two auxiliary variables defined as $\phi_d^{BV} := \frac{\rho-\rho^{k_d+1}}{1-\rho}$ and $\phi_s^{BV} := \frac{(1/\rho)-(1/\rho)^{k_s+1}}{1-(1/\rho)} = \frac{\rho^{k_s}-1}{\rho^{k_s+1}-\rho^{k_s}}$. The matching probability of customers or suppliers is defined as the ratio of the sum of their arrival rates while the opposite side is in queue, divided by their own arrival rate. The expressions for ξ_d^{BV} and ξ_s^{BV} are as follows:

$$\xi_d^{BV} = \frac{\Lambda_s \sum_{i=1}^{k_d} \pi_i^{BV} + \Lambda_d \sum_{i=-1}^{-k_s} \pi_i^{BV}}{\Lambda_d} = \frac{\frac{1}{\rho}\phi_d^{BV} + \phi_s^{BV}}{1+\phi_d^{BV}+\phi_s^{BV}}$$

Policy	π_0^ℓ	$\pi_i^\ell, \forall i < 0$	$\pi_i^\ell, \forall i > 0$	ξ_d^ℓ	ξ_s^ℓ
$\ell = BV$	$\frac{1}{1+\phi_d^\ell+\phi_s^\ell}$	$\rho^i \pi_0^\ell$	$\rho^i \pi_0^\ell$	$\frac{\frac{1}{\rho}\phi_d^\ell+\phi_s^\ell}{1+\phi_d^\ell+\phi_s^\ell}$	$\frac{\phi_d^\ell+\rho\phi_s^\ell}{1+\phi_d^\ell+\phi_s^\ell}$
$\ell = DV$	$\frac{1}{1+\phi_d^\ell+\zeta_s^\ell}$	$\prod_{j=-1}^{-i} \frac{1}{\rho - j\delta_s/\Lambda_s} \cdot \pi_0^\ell$	$\rho^i \pi_0^\ell$	$\frac{\frac{1}{\rho}\phi_d^\ell+\zeta_s^\ell}{1+\phi_d^\ell+\zeta_s^\ell}$	$\frac{\phi_d^\ell+\rho\zeta_s^\ell}{1+\phi_d^\ell+\zeta_s^\ell}$
$\ell = SV$	$\frac{1}{1+\zeta_d^\ell+\phi_s^\ell}$	$\rho^i \pi_0^\ell$	$\prod_{j=1}^{i} \frac{\rho}{1+j\delta_d/\Lambda_s} \cdot \pi_0^\ell$	$\frac{\frac{1}{\rho}\zeta_d^\ell+\phi_s^\ell}{1+\zeta_d^\ell+\phi_s^\ell}$	$\frac{\zeta_d^\ell+\rho\phi_s^\ell}{1+\zeta_d^\ell+\phi_s^\ell}$
$\ell = BI$	$\frac{1}{1+\zeta_d^\ell+\zeta_s^\ell}$	$\prod_{j=-1}^{-i} \frac{1}{\rho - j\delta_s/\Lambda_s} \cdot \pi_0^m$	$\prod_{j=1}^{i} \frac{\rho}{1+j\delta_d/\Lambda_s} \cdot \pi_0^\ell$	$\frac{\frac{1}{\rho}\zeta_d^\ell+\zeta_s^\ell}{1+\zeta_d^\ell+\zeta_s^\ell}$	$\frac{\zeta_d^\ell+\rho\zeta_s^\ell}{1+\zeta_d^\ell+\zeta_s^\ell}$

Table 3.3.: Steady-state probability and matching probability for four information policies.

and

$$\xi_s^{BV} = \frac{\Lambda_s \sum_{i=1}^{k_d} \pi_i^{BV} + \Lambda_d \sum_{i=-1}^{-k_s} \pi_i^{BV}}{\Lambda_s} = \frac{\phi_d^{BV} + \rho\phi_s^{BV}}{1 + \phi_d^{BV} + \phi_s^{BV}}.$$

We present the Markov chain steady-state distributions and matching probabilities for the other information policies, i.e., DV, SV and BI, in a similar manner in Table 3.3. Here, ϕ_ϖ^ℓ and ζ_ϖ^ℓ for each $\varpi \in \{d, s\}$ are auxiliary variables defined as $\phi_d^{DV} := \phi_d^{BV}$, $\phi_s^{SV} := \phi_s^{BV}$, $\zeta_d^\ell := \sum_{i=1}^{\infty} \prod_{j=1}^{i} \frac{\rho}{1+j(\delta_d/\Lambda_s)}$ for each $\ell \in \{BI, SV\}$ and $\zeta_s^\ell := \sum_{i=1}^{\infty} \prod_{j=1}^{i} \frac{1/\rho}{1+j(\delta_s/\Lambda_d)} = \sum_{i=1}^{\infty} \prod_{j=1}^{i} \frac{1}{\rho+j(\delta_s/\Lambda_s)}$ for each $\ell \in \{BI, DV\}$. The expected revenue can be expressed as $Rev^\ell := \Lambda_d \sum_{i \in S_\ell^+} \pi_i^\ell + \Lambda_s \sum_{i \in S_\ell^-} \pi_i^\ell$ for each $\ell \in M$, and $S_\ell^+ := \{i | i \in S_\ell, i > 0\}$ and $S_\ell^- := \{i | i \in S_\ell, i < 0\}$.

3.3.3. Indifference curves to determine information policy

We extend the monotonicity results concerning expected revenue and user patience in the double-sided queueing model.

Proposition 6. *The expected revenue increases with truncation size on the side displaying visible information, i.e., for each $(\ell, \varpi) \in \{(BV, d), (BV, s), (DV, d), (SV, s)\}$, we have $Rev^\ell(k_\varpi + 1) > Rev^\ell(k_\varpi)$. It increases with truncation time, i.e., $\frac{dRev^\ell}{dt_\varpi} > 0$.*

It decreases with reneging rate on the side with invisible information, i.e., for each $(\ell, \varpi) \in \{(BI, d), (BI, s), (SV, d), (DV, s)\}$, *we have* $\frac{dRev^\ell}{d\delta_\varpi} < 0$.

Proof. The expected revenue, denoted by Rev^ℓ, can be calculated as $Rev^\ell = \Lambda_s \sum_{i \in S_\ell^+} \pi_i^\ell + \Lambda_d \sum_{i \in S_\ell^-} \pi_i^\ell = \Lambda_s \xi_s^\ell$ for each $\ell \in M$. Table 3.3 summarizes the solution of ξ_s^ℓ, which involves auxiliary variables ϕ_ϖ^ℓ and ζ_ϖ^ℓ where $\varpi \in \{d, s\}$. In the following, we establish the monotonicity of the auxiliary variables ϕ_ϖ^ℓ and ζ_ϖ^ℓ with respect to user patience (i.e., truncation size k_ϖ, truncation time t_ϖ, and reneging rate δ_ϖ for each $\varpi \in \{d, s\}$). Subsequently, we show that the expected revenue is monotonic with respect to the auxiliary variables ϕ_ϖ^ℓ and ζ_ϖ^ℓ, indicating the monotonicity of the expected revenue with respect to user patience.

Note that $1/\left(1 + \phi_d^\ell\right)$ for each $\ell \in \{BV, DV\}$ and $1/\left(1 + \phi_s^\ell\right)$ for each $\ell \in \{BV, SV\}$ have a structure similar to π_0^K. Meanwhile, ζ_d^ℓ for each $\ell \in \{BI, SV\}$ and ζ_s^ℓ for each $\ell \in \{BI, DV\}$ have a structure similar to π_0^R. We define the sign function by

$$sgn(f) := \begin{cases} -1 & \text{if } f < 0 \\ 0 & \text{if } f = 0 \\ 1 & \text{if } f > 0. \end{cases}$$

It is indicated by Proposition 2 that

$$\begin{aligned} sgn\left(\pi_0^K(k+1) - \pi_0^K(k)\right) &= sgn\left(\frac{1}{1 + \phi_\varpi^\ell(k_\varpi + 1)} - \frac{1}{1 + \phi_\varpi^\ell(k_\varpi)}\right) \\ &= -sgn\left(\phi_\varpi^\ell(k_\varpi + 1) - \phi_\varpi^\ell(k_\varpi)\right) < 0 \end{aligned}$$

and

$$sgn\left(\frac{d}{dt}\pi_0^K\right) = sgn\left(\frac{d}{dt_\varpi}\left(1\Big/\left(1 + \phi_\varpi^\ell\right)\right)\right) = -sgn\left(\frac{d}{dt_\varpi}\phi_\varpi^\ell\right) < 0$$

for each $(\ell, \varpi) \in \{(BV, d), (BV, s), (DV, d), (SV, s)\}$. It also indicates that

$$sgn\left(\pi_0^R\right) = sgn\left(\zeta_\varpi^\ell\right) > 0$$

for each $(\ell, \varpi) \in \{(BI, d), (BI, s), (DV, s), (SV, d)\}$.

For the impact of the auxiliary variables ϕ_ϖ^ℓ and ζ_ϖ^ℓ on the expected revenue, it holds

$$sgn\left(\frac{dRev^\ell}{d\phi_\varpi^\ell}\right) = sgn\left(\frac{dRev^\ell}{d\zeta_\varpi^\ell}\right) > 0$$

for each $\ell \in M$. ■

We remark that the indifference curve $f_x^{(A,B)} = 0$ is the same as $f_x^{(B,A)} = 0$ for information policies A and B. In our double-sided queueing model, there are six different indifference curves representing all possible combinations of two different information policies from the four available policies $\left(\text{since } \binom{|M|}{2} = \binom{4}{2} = 6\right)$. For instance, the indifference curve for BV and SV information policies is given by

$$\begin{aligned}
f_x^{(BV,SV)} &= Rev^{BV} - Rev^{SV} = \Lambda_s\left(\frac{\phi_d^{BV} + \rho\phi_s^{BV}}{1 + \phi_d^{BV} + \phi_s^{BV}}\right) - \Lambda_s\left(\frac{\zeta_d^{SV} + \rho\phi_s^{SV}}{1 + \zeta_d^{SV} + \phi_s^{SV}}\right) \\
&= \frac{\Lambda_s + (\Lambda_s - \Lambda_d)\,\phi_s^{BV}}{\left(1 + \phi_d^{BV} + \phi_s^{BV}\right)\left(1 + \zeta_d^{SV} + \phi_s^{SV}\right)}\left(\phi_d^{BV} - \zeta_d^{SV}\right) = 0.
\end{aligned}$$

Simplifying this expression yields

$$\phi_d^{BV} - \zeta_d^{SV} = 0.$$

Since the model is symmetric, we omit the derivation of closed forms for all other indifference curves associated with the four information policies. The closed form for all indifference curves are summarized in Table 3.4.

3.3.4. Preferred information policy to maximize revenue

The preferred information policy is determined by the market size and system load, as illustrated in Figure 3.5.

Proposition 7. *For a double-sided queueing model with a relatively unbalanced system load:*

1. *If the system load ρ is below a unique threshold $\frac{1}{2} < \underline{T_\rho} < 1$, then a DV information policy is preferred for a high arrival rate $\Lambda_d \geq T_l$, while a BI information policy is preferred for a low arrival rate $\Lambda_d < T_l$.*

Indifference curve	Closed form
$f_x^{(BV,BI)} = 0$	$\phi_d^{BV} + \phi_s^{BV} = \zeta_d^{BI} + \zeta_s^{BI}$
$f_x^{(SV,BI)} = 0$	$\phi_s^{SV} = \zeta_s^{BI}$
$f_x^{(BV,SV)} = 0$	$\zeta_d^{SV} = \phi_d^{BV}$
$f_x^{(DV,BI)} = 0$	$\phi_d^{DV} = \zeta_d^{BI}$
$f_x^{(BV,DV)} = 0$	$\zeta_s^{DV} = \phi_s^{BV}$

Note. For any two information policies A and B, the closed form of the indifference curve is obtained by simplifying the equation $Rev^A - Rev^B = 0$.

Table 3.4.: Indifference curves in the double-sided queueing model.

2. *If the system load ρ exceeds a unique threshold $1 < \overline{T_\rho} < 2$, then a SV information policy is preferred for a high arrival rate $\Lambda_d \geq T_l$, while a BI information policy is preferred for a low arrival rate $\Lambda_d < T_l$.*

Proof. **Values of $\underline{T_\rho}$ and $\overline{T_\rho}$.** The value of $\underline{T_\rho}$ satisfies the condition $\lim_{\Lambda_d \to \infty} f_x^{(DV,BV)} = 0$, when ρ is substituted with T_ρ in the function $f_x^{(DV,BV)}$. The value of $\overline{T_\rho}$ satisfies the condition $\lim_{\Lambda_d \to \infty} f_x^{(BV,SV)} = 0$, when ρ is substituted with $\overline{T_\rho}$ in the function $f_x^{(BV,SV)}$. Assuming a constant ρ, if $\rho \leq 1$, then the value of T_l satisfies the condition $f_x^{(DV,BI)} = 0$ when Λ_d is substituted with T_l in the function $f_x^{(DV,BI)}$. Conversely, if $\rho < 1$, it satisfies the condition $f_x^{(BI,SV)} = 0$ when Λ_d is substituted with T_l in the function $f_x^{(BI,SV)}$.

We establish the existence of the threshold values $\underline{T_\rho}$ and $\overline{T_\rho}$ by demonstrating that $\lim_{\substack{\Lambda_s \to \infty \\ \rho = 1}} f_x(BV, BI) > 0$, which proves that the BV policy is preferred for sufficiently large arrival rates on both sides when $\rho = 1$. This result implies that $\underline{T_\rho} < 1$ and $\overline{T_\rho} > 1$. Furthermore, we show that $\lim_{\substack{\Lambda_s \to \infty \\ \rho = 2}} f_x(BV, SV) > 0$, indicating that $\overline{T_\rho} < 2$. Therefore, when the system load is $\rho \geq 2$, the SV policy becomes preferable for a sufficiently large arrival rate. We do not analyze the case where $\underline{T_\rho} > \frac{1}{2}$ as the model is symmetric to the case of $\overline{T_\rho} < 2$.

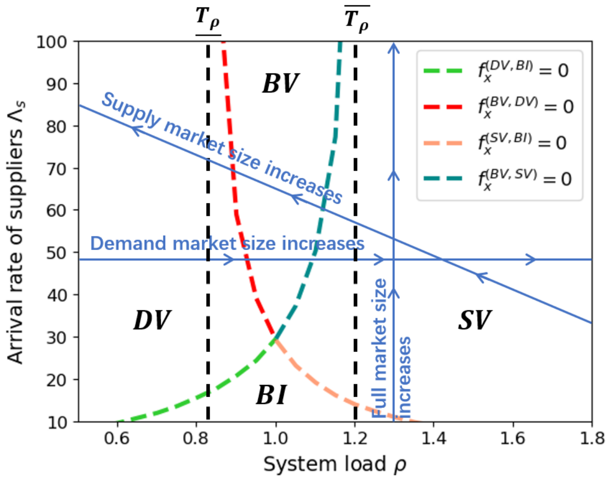

Figure 3.5.: The preferred information policy in a double-sided queueing model: $\Lambda_s \in [10, 100]$ and $\rho \in [0.5, 1.8]$.

Upper bound (resp. lower bound) of $\underline{T_\rho}$ (resp. $\overline{T_\rho}$). With $\rho = 1$, it holds

$$\lim_{\substack{\Lambda_s \to \infty \\ \rho = 1}} f_x(BV, BI) \geq \lim_{\substack{\Lambda_s \to \infty \\ \rho = 1}} \left(t - \frac{1}{2\Lambda_s} \sum_{i=1}^{\infty} 2 \cdot \prod_{j=1}^{i} \frac{1}{1 + j\delta_b/\Lambda_s} \right) \geq 0.$$

Upper bound of $\overline{T_\rho}$. We suppose $\overline{T_\rho} \geq 2$ (i.e., $\rho \geq 2$) and find the contradictory. The difference curve $f_x^{(BV,SV)} = 0$ is

$$\delta_b t_b = \frac{\delta}{\Lambda_s} \frac{\ln \left(\rho + (\rho - 1) \sum_{i=1}^{\infty} \prod_{j=1}^{i} \frac{\rho}{1 + j\delta_b/\Lambda_s} \right)}{\ln \rho} - \frac{\delta_b}{\Lambda_s}$$

which is consistent to (3.8), indicating that the indifference curve $f_x^{(BV,SV)} = 0$ cannot get satisfied if $\rho \geq 2$ as Λ_s increases sufficiently. ■

Proposition 7 provides insights into the preferred information policy for a market with relatively high or low system load (i.e., $\rho \geq \overline{T_\rho}$ and $\rho \leq \underline{T_\rho}$). For a large full market size, the preferred information policy changes from BI to SV in a high system load scenario, as illustrated in Figure 3.5 with $\rho = 1.3$. On the other hand, in a low system load scenario, as shown in Figure 3.5 with $\rho = 0.7$, the preferred information policy changes from BI to DV. This is because, with a larger full market size maintaining an unbalanced system load, the expected queue length on one side increases significantly, while the other side experiences only a minor increase in its expected queue length. This large difference in expected queue lengths leads to a significant difference in the service rate for each other (i.e., the arrival rate of the opposite side), making a differentiated information policy preferable for a large full market size.

The following theorem provides conditions and thresholds to quantitatively determine the preferred information policy, both for one side's market size and for the full market size, particularly when the system load is relatively balanced.

Theorem 8. *In a double-sided model, the preferred information policy is determined as follow:*

1. *For a large market size on one side:*
   a) *If the arrival rate of suppliers Λ_s is below the threshold T_l, then a SV information policy is preferred.*
   b) *If the arrival rate Λ_ϖ of one side $\varpi \in \{d, s\}$ lies between thresholds T_l and T_u and the arrival rate Λ_μ of the other side $\mu \in \{d, s\}, \mu \neq \varpi$ is below the threshold T_b, then a BI information policy is preferred; otherwise, a BV information policy is preferred.*
   c) *If the arrival rate of suppliers Λ_s exceeds the threshold T_u, then a DV information policy is preferred.*
2. *For a large full market size and a fixed system load $\underline{T_\rho} \leq \rho \leq \overline{T_\rho}$:*
   a) *If the arrival rate of suppliers Λ_s is below the threshold T_l, then a BI information policy is preferred.*
   b) *If the arrival rate of suppliers Λ_s lies between thresholds T_l and T_u and the system load ρ is below 1, then a DV information policy is preferred; otherwise, a SV information policy is preferred.*
   c) *If the arrival rate of suppliers Λ_s exceeds the threshold T_u, then a BV information policy is preferred.*

Proof. **Values of T_l, T_u and T_b.** For a larger market size on one side, the value of T_b satisfies the condition $f_x^{(BV,BI)} = 0$ when Λ_d and Λ_s both are substituted with T_b in the function $f_x^{(BV,BI)}$. Assuming a constant Λ_s, if $\Lambda_d \leq T_b$, then the values of T_l

and T_u satisfy the conditions $f_x^{(DV,BI)} = 0$ and $f_x^{(BI,SV)} = 0$ respectively, when Λ_d is substituted with T_l in the function $f_x^{(DV,BI)}$ and with T_u in the function $f_x^{(BI,SV)}$. Conversely, if $\Lambda_d < T_b$, then the values of T_l and T_u satisfy the conditions $f_x^{(DV,BV)} = 0$ and $f_x^{(BV,SV)} = 0$ respectively, when Λ_d is substituted with T_l in the function $f_x^{(DV,BV)}$ and with T_u in the function $f_x^{(BV,SV)}$. For a larger full market size and a fixed system load, assuming a constant Λ_d, if $\rho \leq 1$, then the values of T_l and T_u satisfy the conditions $f_x^{(DV,BI)} = 0$ and $f_x^{(DV,BV)} = 0$ respectively. The is the case when Λ_s is substituted with T_l in the function $f_x^{(DV,BI)}$ and with T_u in the function $f_x^{(DV,BV)}$. Conversely, if $\rho < 1$, then the values of T_l and T_u satisfy the conditions $f_x^{(BI,SV)} = 0$ and $f_x^{(BV,SV)} = 0$ respectively. The is the case when Λ_s is substituted with T_l in the function $f_x^{(BI,SV)}$ and with T_u in the function $f_x^{(BV,SV)}$.

The results for the two different types of larger market sizes exhibit structural symmetry, as the preferred information policy is determined by thresholds on two dimensions. We examined only the scenario where the full market size is larger, as the other cases are symmetrical to this scenario in the model setting. We demonstrate that the system load establishes candidate preferred information policies, and the preferred information policy chosen from the candidates is determined by the threshold on the arrival rate of customers.

The candidate preferred information policy is determined by the system load ρ. Specifically, if $\rho > 1$, the candidate preferred information policy is in $\{BI, SV, BV\}$, while if $\rho < 1$, it is in $\{BI, DV, BV\}$. We only analyze the case of $\rho > 1$ and omit the other since the model setting is symmetric. To establish the candidate preferred information policy, we only need to show two results. First, if the truncation size of suppliers k_d is small, the BI policy has higher expected revenue than the DV policy. Second, if k_d is large, the BV policy has higher expected revenue than the DV policy. Therefore, DV is not a candidate preferred information policy for any k_d. The determination of the preferred information policy is completed by calculating the threshold values T_l, T_u, and T_b based on the corresponding indifference curves, as proven in Theorem 5.

Case (i). If k_d is small and it satisfies $\rho + \rho^2 + .. + \rho^{k_d} \leq \zeta_d^{DV}$, then it holds for the DV policy that $\xi_s^{DV} = 1 + \frac{(\rho-1)\zeta_s^{DV}-1}{1+\zeta_s^{DV}+\rho\left(1-\rho^{k_d}\right)/(1-\rho)} \leq 1$, which indicates

$$(\rho - 1)\zeta_s^{DV} - 1 < 0. \tag{3.14}$$

It holds for the BI policy that

$$\xi_s^{BI} = 1 + \frac{(\rho-1)\zeta_s^{BI} - 1}{1+\zeta_s^{BI}+\zeta_d^{BI}} \overset{(3.14)}{\geq} 1 + \frac{(\rho-1)\zeta_s^{DV} - 1}{1+\zeta_s^{DV} + \rho\left(1-\rho^{k_d}\right)/\left(1-\rho\right)} = \xi_s^{DV}.$$

Case (ii). If k_d is large and it satisfies $\rho+\rho^2+..+\rho^{k_d} > \zeta_d^{DV}$, i.e., $\rho^{k_d} > \frac{\rho-1}{\rho}\zeta_d^{DV}+1$, then we show

$$\frac{\rho^{k_d}-1}{\rho^{k_d+1}-\rho^{k_d}} > \zeta_s^{DV} \tag{3.15}$$

which indicates $\xi_s^{BV} \geq \xi_s^{DV}$. A sufficient and necessary condition for (3.15) is $\rho^{k_d} > \frac{1}{1-(\rho-1)\zeta_s^{DV}}$. To prove it, it is sufficient to show $\frac{\rho-1}{\rho}\zeta_d^{DV}+1 \geq \frac{1}{1-(\rho-1)\zeta_s^{DV}}$ by proving $h \geq 0$ where $h := -\rho\zeta_s^{DV} + \zeta_d^{DV}\zeta_s^{DV} + \zeta_d^{DV}\left(1-\rho\zeta_s^{DV}\right)$. It is obvious that the first term of h, i.e., $-\rho\zeta_s^{DV}$, increases with ρ. For the second term of h, it holds

$$\begin{aligned}
\frac{d\left(\zeta_d^{DV}\zeta_s^{DV}\right)}{d\rho} &= \zeta_s^{DV}\sum_{i=1}^{\infty}\frac{i}{\rho}\prod_{j=1}^{i}\frac{\rho}{1+j\delta_b/\Lambda_s} - \zeta_d^{DV}\sum_{i=1}^{\infty}\frac{i}{\rho+j\delta_b/\Lambda_s}\prod_{j=1}^{i}\frac{1}{\rho+j\delta_b/\Lambda_s} \\
&> \frac{1}{\rho}\left(\zeta_s^{DV}\sum_{i=1}^{\infty}\prod_{j=1}^{i}\frac{\rho}{1+j\delta_b/\Lambda_s}\cdot i - \zeta_d^{DV}\sum_{i=1}^{\infty}\prod_{j=1}^{i}\frac{1}{\rho+j\delta_b/\Lambda_s}\cdot i\right) \overset{\rho>1}{>} 0.
\end{aligned}$$

For the third term of h, it holds

$$\begin{aligned}
\frac{d\left(1-\rho\zeta_s^{DV}\right)}{d\rho} &= \sum_{i=1}^{\infty}\prod_{j=1}^{i}\frac{1}{\rho+j\delta_b/\Lambda_s}\sum_{j=1}^{i}\frac{\rho}{\rho+j\delta_b/\Lambda_s} - \zeta_s^{DV} \\
&= \sum_{i=1}^{\infty}\prod_{j=1}^{i}\frac{1}{\rho+j\delta_b/\Lambda_s}\left(\sum_{j=1}^{i}\frac{\rho}{\rho+j\delta_b/\Lambda_s} - 1\right) \\
&> \sum_{i=1}^{\infty}\prod_{j=1}^{i}\frac{1}{\rho+j}\left(\sum_{j=1}^{i}\frac{\rho}{1+j} - 1\right) \geq 0.
\end{aligned}$$

Since $\frac{dh}{d\rho} \geq 0$ and $h(\rho=1)=0$, we show $h \geq 0$ and prove (3.15). Hence for BV policy, it holds

$$\xi_s^{BV} = \frac{\left(\rho-\rho^{k_d+1}\right)/\left(1-\rho\right) + \rho\frac{\rho^{k_d}-1}{\rho^{k_d+1}-\rho^{k_d}}}{1+\left(\rho-\rho^{k_d+1}\right)/\left(1-\rho\right) + \frac{\rho^{k_d}-1}{\rho^{k_d+1}-\rho^{k_d}}}$$

$$\stackrel{(3.15)}{>} \frac{\left(\rho - \rho^{k_d+1}\right)/(1-\rho) + \rho\zeta_s^{DV}}{1 + \left(\rho - \rho^{k_d+1}\right)/(1-\rho) + \zeta_s^{DV}} = \xi_s^{DV}.$$

■

As depicted in Figure 3.5, when one side of the market, such as customers, is larger, the preferred information policy transitions from DV to either BV or BI – dependent on the arrival rate of suppliers – before ultimately shifting to SV. On the other hand, for a large supply market size, the preferred information policy transitions from SV to either BV or BI – dependent on the arrival rate of customers – before ultimately shifting to DV. The first part of Theorem 8 states these changes using thresholds that are applicable to any system load. For a large full market size maintaining a relatively balanced system load (i.e., close to 1), the preferred information policy transitions first from BI to either DV or SV – dependent on the system load – and eventually to BV when the arrival rates of both customers and suppliers are larger. The second part of Theorem 8 describes these changes using thresholds.

Theorem 8 demonstrates that the theoretical results for the two types of larger market sizes exhibit structural symmetry, as the preferred information policy is determined by thresholds on two dimensions. For example, if the demand market size is larger, the candidate preferred information policies are determined by the arrival rate of suppliers, using the threshold T_b, and the preferred information policy is determined by the arrival rate of customers, using the thresholds T_l and T_u. On the other hand, if the full market size is larger, the candidate preferred information policies are determined by the system load, using the threshold of one, and the preferred information policy is determined by the arrival rate of suppliers, using the thresholds T_l and T_u. Essentially, this is determined by the difference in expected queue lengths due to different arrival rates on both sides. When one side's arrival rate is larger and the other side's arrival rate is fixed, the expected queue length of the former side increases monotonically. As a result, the preferred information policy is to conceal information on the side with a long expected queue length and display information on the side with a short expected queue length (i.e., a differentiated information policy). If both arrival rates are larger while maintaining a fixed system load closed to one, the expected queue lengths of both sides are larger, indicating high service rates on both sides. The system load determines the rate at which the expected queue length increases on both sides when arrival rates are high, as well as whether it is preferable to display information on both sides or only one side for sufficiently high arrival rates on both sides.

3.3.5. Asymmetry in user patience

The asymmetry in user patience within the double-sided queueing model influences the preferred selection of information policy. We introduce a *patience coefficient* α, which represents the ratio of patience parameters for customers and suppliers, i.e., $t_d = \alpha t_s$ and $\delta_d = \frac{1}{\alpha}\delta_s$. An increase in α suggests that customers are more patient than suppliers.

Proposition 9. *For asymmetric user patience, i.e., $\alpha \neq 1$, hiding the information on the side with lower user patience increases expected revenue. Specifically, if the arrival rate of suppliers Λ_s and patience coefficient α satisfy the indifference curves $f_x^{(BV,DV)} = 0$ or $f_x^{(SV,BI)} = 0$ for fixed customer patience (t_d, δ_d) and system load ρ, then $\frac{d\Lambda_s}{d\alpha} \geq 0$.*

Proof. We examine the sign of $\frac{d\Lambda_s}{d\alpha}$ for (Λ_s, α) that satisfies the indifference curve $f_x^{(BV,DV)} = 0$ for fixed (t_d, δ_c) and ρ. We do not discuss the case of (Λ_s, α) that satisfies the indifference curve $f_x^{(SV,BI)} = 0$ since the model setting is symmetric. The indifference curve $f_x^{(BV,DV)} = 0$ holds

$$\sum_{i=1}^{\infty}\prod_{j=1}^{i}\frac{1}{\rho + j\delta_c/(\Lambda_s/\alpha)} = \frac{\rho^{\rho t_d \cdot \Lambda_s/\alpha} - 1}{\rho^{\rho t_d \cdot \Lambda_s/\alpha + 1} - \rho^{\rho t_d \cdot \Lambda_s/\alpha}}$$

which has a unique solution for Λ_s/α to get satisfied for fixed (t_d, δ_c) and ρ. Hence it holds $\frac{d\Lambda_s}{d\alpha} \geq 0$.

■

Proposition 9 states that if suppliers become more impatient while customers' patience remains fixed, then the supply side's preferred information policy changes from visible to invisible. This is because concealing information about the queue length on the side with lower user patience can boost expected revenue by attracting more users to join the queue. This occurs as the truncation size of the suppliers' queue decreases while the expected queue length remains constant. The advantage of DV and BI information policies over BV and SV policies, respectively, increases monotonically with customers' patience in cases of asymmetric user patience.

3.4. Endogenous arrival rate

In Sections 3.2 and 3.3, we examined queueing models featuring exogenously given arrival rates of customers and suppliers, represented by the Poisson rates Λ_d and Λ_s. In real-world scenarios, especially in the context of multiple platforms offering alternative options (e.g., with over one hundred freight exchanges in Europe), potential users might hesitate to join the same service system due to perceived concerns about long-term service quality (Parker et al. 2016). Incorporating a behavioral model that endogenizes agent behavior with both visible and invisible queue lengths presents challenges and may result in an excessively complex general model. Instead of pursuing a model where agent behavior is endogenized, our approach in the multi-platform context involves assessing service quality on each side using the matching probability (Kritikos et al. 2013; Sivakumar et al. 2014). The user's arrival rate is influenced by this matching probability. For clarity, we refer to models with exogenously given user arrival rates as *exogenous* models, and refer to Λ_d and Λ_s as *potential* arrival rates. In the exogenous model, all potential arrivals of customers and suppliers are assumed to effectively enter the service system and exhibit abandonment behaviors driven by the information policy. Conversely, in the *endogenous* model, some potential arrivals of customers and suppliers may refrain from entering the service system due to the perceived platform's long-term service quality, even before exhibiting abandonment behaviors driven by the information policy.

Although it is recognized that user perceptions of service quality can affect arrival rates over the long term, few studies have examined the implications of this endogeneity in a model with multiple platforms. By extending the exogenous model, our endogenous model explores this research question, taking into account the interdependence of matching probability and arrival rate. The endogenous arrival rates of customers (on the demand side) and suppliers (on the supply side) are represented as:

$$\lambda_\varpi := \Lambda_\varpi \xi_\varpi \quad \text{for each} \quad \varpi \in \{d, s\} \tag{3.16}$$

where the linear multiplication of Λ_ϖ and ξ_ϖ is based on the model of Batt and Terwiesch (2015). In the following, we use the symbol n to represent the endogenous arrival assumption. The system load in the endogenous model is denoted by $\rho_n := \lambda_d/\lambda_s$.

Lemma 10. *The system load is determined by the potential arrival rates of customers and suppliers, as indicated by* $\rho_n = \sqrt{\rho} = \sqrt{\Lambda_d/\Lambda_s}$.

Proof. In the exogenous model, $\rho = \Lambda_d/\Lambda_s$. Since the matching rates of both sides are equal, it holds

$$\xi_d^\ell \lambda_d^\ell = \xi_s^\ell \lambda_s^\ell \tag{3.17}$$

for each information policy $\ell \in \{K, R, BV, DV, SV, BI\}$. In the endogenous model under information policy ℓ, we have $\rho_n = \lambda_d^\ell/\lambda_s^\ell = \Lambda_d \xi_d^\ell / \left(\Lambda_s \xi_s^\ell\right) \overset{(3.17)}{=} \frac{\Lambda_d}{\Lambda_s} \Big/ \frac{\lambda_d^\ell}{\lambda_s^\ell} = (\Lambda_d/\Lambda_s)/\rho_n$. ∎

When the potential arrival rates of both sides differ, the side with a higher potential arrival rate experiences a lower matching probability, resulting in a lower system load in the endogenous model. Lemma 10 reveals that in an endogenous model, the system load is determined independently by potential arrival rates. Consequently, we can solve the steady-state probabilities of Markov chains in both single-sided and double-sided endogenous models using system load ρ_n to compare information policies with identical potential arrival rates for customers and suppliers.

3.4.1. Endogenous single-sided queueing model

In the endogenous single-sided queueing model, the value of $\pi_0^{(\ell,n)}$ for each $\ell \in \{K, R\}$ can be determined by solving (3.1)-(3.3) while replacing all variables with those corresponding to the endogenous model and using (3.16). With the value of $\pi_0^{(\ell,n)}$, we can then obtain the value of $\pi_i^{(\ell,n)}$ for any $i \in S_\ell^n$ for each $\ell \in \{K, R\}$ in the steady-state distribution by utilizing (3.1) and (3.2). Specifically, $\pi_0^{(K,n)}$ is the solution to the equation:

$$\pi_0^{(K,n)} \left(1 - \rho_n^{\,t\Lambda_s\left(1-\pi_0^{(K,n)}\right)+1}\right) + \rho_n = 1, \tag{3.18}$$

while $\pi_0^{(R,n)}$ can be obtained by solving the equation:

$$1 + \sum_{i=1}^{\infty} \prod_{j=1}^{i} \frac{\rho_n}{1 + j\delta \Big/ \left(\Lambda_s \left(1 - \pi_0^{(R,n)}\right)\right)} = \frac{1}{\pi_0^{(R,n)}}. \tag{3.19}$$

In the endogenous model, obtaining direct solutions for $\pi_0^{(\ell,n)}$ for each $\ell \in \{K, R\}$ using (3.18) and (3.19) is challenging due to the presence of transcendental terms. The results presented below demonstrate the monotonic relationship between match probability and potential user arrival rate under both visible and invisible information policies.

Lemma 11. *In an endogenous K model,* $\frac{d\xi_s^{(K,n)}}{dt} > 0$ *(resp.* $\frac{d\pi_0^{(K,n)}}{dt} < 0$*).*

Proof. In an endogenous K model, $\xi_s^{(K,n)} = \frac{\rho_n - {\rho_n}^{\Lambda_s \xi_s^{(K,n)} t+1}}{1-{\rho_n}^{\Lambda_s \xi_s^{(K,n)} t+1}}$. Define $h_p := \frac{\rho_n - {\rho_n}^{\Lambda_s \xi_s^{(K,n)} t+1}}{1-{\rho_n}^{\Lambda_s \xi_s^{(K,n)} t+1}} - \xi_s^{(K,n)}$. By applying the implicit function theorem, it holds that $\frac{d\xi_s^{(K,n)}}{dt} = -\frac{dh_p}{dt} \Big/ \frac{dh_p}{d\xi_s^{(K,n)}}$ where $\frac{dh_p}{dt} > 0$ is obvious. For $\frac{dh_p}{d\xi_s^{(K,n)}}$, it holds

$$\frac{dh_p}{d\xi_s^{(K,n)}} = \frac{(\rho_n - 1)\left({\rho_n}^{\Lambda_s \xi_s^{(K,n)} t+1} \Lambda_s t \ln \rho_n\right)}{\left(1-{\rho_n}^{\Lambda_s \xi_s^{(K,n)} t+1}\right)^2} - 1 < \frac{(\rho_n - 1)\Lambda_s t \ln \rho_n}{{\rho_n}^{\Lambda_s t+1} + 1/{\rho_n}^{\Lambda_s t+1} - 2} - 1 \leq 0.$$

Hence, we can show that $\frac{d\xi_s^{(K,n)}}{dt} > 0$ and, as $\pi_0^{(K,n)} = 1 - \xi_s^{(K,n)}$, we can infer that $\frac{d\pi_0^{(K,n)}}{dt} < 0$. ∎

Lemma 12. *In an endogenous R model,* $\frac{d\xi_s^{(R,n)}}{d\delta} < 0$ *(resp.* $\frac{d\pi_0^{(R,n)}}{d\delta} > 0$*).*

Proof. In an endogenous R model, $(1-\xi_s^{(R,n)})\left(1+\sum_{i=1}^{\infty}\prod_{j=1}^{i}\frac{\rho_n}{1+j\delta/(\Lambda_s\xi_s^{(R,n)})}\right) = 1$. Define $f_p(\xi_s^{(R,n)}, \delta) := (1-\xi_s^{(R,n)})\left(1+\sum_{i=1}^{\infty}\prod_{j=1}^{i}\frac{\rho_n}{1+j\delta/(\Lambda_s\xi_s^{(R,n)})}\right) - 1$. By applying the implicit function theorem, it holds that $\frac{d\xi_s^{(R,n)}}{d\delta} = -\frac{df_p}{d\delta} \Big/ \frac{df_p}{d\xi_s^{(R,n)}}$ where $\frac{df_p}{d\delta} < 0$ is obvious. For $\frac{df_p}{d\delta}$, it holds

$$\begin{aligned}
\frac{df_p}{d\xi_s^{(R,n)}} =& -1 - \sum_{i=1}^{\infty}\prod_{j=1}^{i}\frac{\rho_n}{1+j\delta/(\Lambda_s\xi_s^{(R,n)})} + \left(1-\xi_s^{(R,n)}\right)\frac{d}{d\xi_s^{(R,n)}}\sum_{i=1}^{\infty}\prod_{j=1}^{i}\frac{\rho_n}{1+j\delta/(\Lambda_s\xi_s^{(R,n)})} \\
=& -1 - \sum_{i=1}^{\infty}\prod_{j=1}^{i}\frac{\rho_n}{1+j\delta/(\Lambda_s\xi_s^{(R,n)})} \\
&+ \left(1-\xi_s^{(R,n)}\right)\sum_{i=1}^{\infty}\exp\left(\log\prod_{j=1}^{i}\frac{\rho_n}{1+j\delta/(\Lambda_s\xi_s^{(R,n)})}\right) \\
=& -1 - \sum_{i=1}^{\infty}\prod_{j=1}^{i}\frac{\rho_n}{1+j\delta/(\Lambda_s\xi_s^{(R,n)})}
\end{aligned}$$

$$+\left(\frac{1}{\xi_s^{(R,n)}}-1\right)\sum_{i=1}^{\infty}\prod_{j=1}^{i}\frac{\rho_n}{1+j\delta/(\Lambda_s\xi_s^{(R,n)})}\sum_{j=1}^{i}\frac{j\delta/\Lambda_s}{1+j\delta/\left(\Lambda_s\xi_s^{(R,n)}\right)}. \tag{3.20}$$

If $\frac{1}{2}\leq\xi_s^{(R,n)}<1$, it is obvious that $\frac{df_p}{d\xi_s^{(R,n)}}<0$ since every term in (3.20) is negative. If $0<\xi_s^{(R,n)}<\frac{1}{2}$, it holds

$$\begin{aligned}(3.20)<&-1-\sum_{i=1}^{\infty}\prod_{j=1}^{i}\frac{\rho_n}{1+j\delta/(\Lambda_s\xi_s^{(R,n)})}\\&+\frac{\sum_{i=1}^{\infty}\prod_{j=1}^{i}\frac{\rho_n}{1+j\delta/(\Lambda_s\xi_s^{(R,n)})}\sum_{j=1}^{i}\frac{j\delta/(\Lambda_s\xi_s^{(R,n)})}{1+j\delta/\left(\Lambda_s\xi_s^{(R,n)}\right)}}{\sum_{i=1}^{\infty}\prod_{j=1}^{i}\frac{\rho_n}{1+j\delta/(\Lambda_s\xi_s^{(R,n)})}}\end{aligned} \tag{3.21}$$

where $\sum_{i=1}^{\infty}\prod_{j=1}^{i}\frac{\rho_n}{1+j\delta/(\Lambda_s\xi_s^{(R,n)})}=\frac{\xi_s^{(R,n)}}{1-\xi_s^{(R,n)}}\leq 1$ indicating $\rho_n<1$. We denote $y:=\delta/\left(\Lambda_s\xi_s^{(R,n)}\right)$ for simplification in the following equations. By solving $\sum_{i=1}^{\infty}\prod_{j=1}^{i}\frac{\rho_n}{1+jy}=1$ where $y\in(0,1)$, it holds $\frac{\rho_n}{1+jy}\leq\frac{1}{2}$ for any $j\geq 2$. To prove (3.21) ≤ 0, it is sufficient to show

$$\sum_{i=1}^{\infty}\prod_{j=1}^{i}\frac{\rho_n}{1+jy}-\sum_{i=1}^{\infty}\prod_{j=1}^{i}\frac{\rho_n}{1+jy}\sum_{j=1}^{i}\frac{jy}{1+jy}\geq 0 \tag{3.22}$$

for any $y\in(0,1)$ and $\rho_n\in(0,1)$.

In the following analysis, we demonstrate that (3.22) ≥ 0 for any $\rho_n\in(0,1)$ and $y\in(0,1)$. To do this, we seek different ad-hoc intervals corresponding to different degrees of relaxation for (3.22). We first obtain a lower bound equation of (3.22) (i.e., (3.25)) and solve it to show (3.22) ≥ 0 for any $\rho_n\in(0,0.393]$ and $y\in(0,1)$. Next, we demonstrate (3.22) ≥ 0 for any $\rho_n\in(0.393,1)$ by discussing three cases: (i) $y\in(0,0.2665]$; (ii) $y\in(0.2665,\frac{1}{\sqrt{2}}]$; (iii) $y\in(\frac{1}{\sqrt{2}},1)$. The magnitude of these values does not affect the generality of our conclusions.

For (3.22), it holds

$$(3.22)=\frac{\rho_n}{1+y}-\frac{\rho_n}{1+y}\frac{y}{1+y}-\sum_{i=2}^{N}\prod_{j=1}^{i}\frac{\rho_n}{1+jy}\sum_{j=1}^{i}\frac{jy}{1+jy}+1$$

$$- \sum_{i=N+1}^{\infty} \prod_{j=1}^{i} \frac{\rho_n}{1+jy} \left(\sum_{j=1}^{i} \frac{jy}{1+jy} - 1 \right) \tag{3.23}$$

$$\geq \frac{\rho_n}{2} - \sum_{i=2}^{N} {\rho_n}^i \left(\sum_{j=1}^{i} \frac{j}{1+j} - 1 \right)$$

$$- {\rho_n}^{N+1} \left(\frac{1+(N+2)}{1-\rho_n} \left(\sum_{j=1}^{N+1} \frac{j}{1+j} - 1 \right) + \frac{(1+(N+2))\rho_n}{(1-\rho_n)^2} \right) \tag{3.24}$$

for any $N \geq 2$ since we get the lower bound (3.24) by decreasing the value of $\frac{\rho_n}{1+y} - \frac{\rho_n}{1+y}\frac{y}{1+y}$ and increasing the values of $\sum_{i=2}^{N} \prod_{j=1}^{i} \frac{\rho_n}{1+jy} \left(\sum_{j=1}^{i} \frac{jy}{1+jy} - 1 \right)$ and $\sum_{i=N+1}^{\infty} \prod_{j=1}^{i} \frac{\rho_n}{1+jy} \left(\sum_{j=1}^{i} \frac{jy}{1+jy} - 1 \right)$ in (3.23). The lower bound (3.24) becomes tighter if N increases. Hence, for one case $N = 8$, it holds

$$(3.24) \overset{N=8 \text{ in } (3.24)}{\geq} \frac{\rho_n}{2} - \sum_{i=2}^{8} {\rho_n}^i \left(\sum_{j=1}^{i} \frac{j}{1+j} - 1 \right)$$

$$- {\rho_n}^9 \left(\frac{11}{1-\rho_n} \left(\sum_{j=1}^{9} \frac{j}{1+j} - 1 \right) + \frac{11\rho_n}{(1-\rho_n)^2} \right). \tag{3.25}$$

By solving (3.25) ≥ 0, it holds $\rho_n \leq 0.393$. This indicates that for any $\rho_n \in (0, 0.393]$ and $y \in (0, 1)$, (3.22) ≥ 0. Next, we show for any $\rho_n \in (0.393, 1)$ and $y \in (0, 1)$, (3.22) ≥ 0.

Case (i): $y \in (0, 0.2665]$. Note that the value 0.2665 is the solution of $1/(1+y) + 1/(1+2y) + 1/(1+3y) = 2$. Hence it holds

$$(3.22) = \frac{\rho_n}{1+y} \left(\frac{1}{1+y} + \sum_{i=2}^{\infty} \prod_{j=2}^{i} \frac{\rho_n}{1+jy} \left(\sum_{j=1}^{i} \frac{1}{1+jy} - i \right) \right) \tag{3.26}$$

$$\geq \frac{\rho_n}{1+y} \left(\frac{1}{1+y} + \sum_{i=2}^{3} \prod_{j=2}^{i} \frac{0.393}{1+jy} \left(\sum_{j=1}^{i} \frac{1}{1+jy} - i \right) - \sum_{i=4}^{\infty} \left(\frac{1}{2} \right)^{i-1} (i-1) \right)$$

$$\overset{y \leq 0.2665}{\geq} \frac{\rho_n}{1+y} \left(\frac{1}{1+0.2665} + \sum_{i=2}^{3} \left(\prod_{j=2}^{i} \frac{0.393}{1+0.2665j} \right) \right.$$

$$\left. \left(\sum_{j=1}^{i} \frac{1}{1+0.2665j} - i \right) - 1 \right) > 0.$$

Case (ii): $y \in (0.2665, \frac{1}{\sqrt{2}}]$**.** Note that the value $\frac{1}{\sqrt{2}}$ is the solution of $1/(1+y)+1/(1+2y)=2$. Hence it holds

$$
\begin{aligned}
(3.26) \geq & \frac{\rho_n}{1+y}\left(\frac{1}{1+y}+\frac{0.393}{1+2y}\left(\frac{1}{1+y}+\frac{1}{1+2y}-1\right)-\sum_{i=3}^{9}\left(\frac{1}{2}\right)^{i-1}\left(i-\sum_{j=1}^{i}\frac{1}{1+jy}\right)\right.\\
&\left.-\sum_{i=9}^{\infty}\left(\frac{1}{2}\right)^{i-1}\left(i-1-\sum_{j=1}^{9}\frac{1}{1+\frac{1}{\sqrt{2}}j}\right)\right)\\
\geq & \frac{\rho_n}{1+y}\left(\frac{1}{1+y}+\frac{0.393}{1+2y}\left(\frac{1}{1+y}+\frac{1}{1+2y}-1\right)\right.\\
&\left.-\sum_{i=3}^{9}\left(\frac{1}{2}\right)^{i-1}\left(i-\sum_{j=1}^{i}\frac{1}{1+jy}\right)-0.03\right). \qquad (3.27)
\end{aligned}
$$

By solving $(3.27) \geq 0$, it holds $y \leq 0.584$. This indicates for $\rho_n \in (0.393, 1)$ and $y \in (0, 0.584]$, $(3.22) \geq 0$. We then show for any $y \in (0.584, \frac{1}{\sqrt{2}}]$, $(3.22) \geq 0$. For (3.26), it holds

$$
\begin{aligned}
(3.26) \geq & \frac{\rho_n}{1+y}\left(\frac{1}{1+y}+\frac{0.393}{1+2y}\left(\frac{1}{1+y}+\frac{1}{1+2y}-1\right)\right.\\
&\left.-\sum_{i=3}^{5}\prod_{j=2}^{i}\frac{1}{1+0.584j}\left(i-\sum_{j=1}^{i}\frac{1}{1+jy}\right)-\sum_{i=6}^{\infty}\left(i-1-\sum_{j=1}^{6}\frac{1}{1+\frac{1}{\sqrt{2}}j}\right)\right)\\
\overset{y\leq\frac{1}{\sqrt{2}}}{\geq} & \frac{\rho_n}{1+y}\left(\frac{1}{1+\frac{1}{\sqrt{2}}}+\frac{0.393}{1+2\cdot\frac{1}{\sqrt{2}}}\left(\frac{1}{1+\frac{1}{\sqrt{2}}}+\frac{1}{1+2\cdot\frac{1}{\sqrt{2}}}-1\right)\right.\\
&\left.-\sum_{i=3}^{5}\prod_{j=2}^{i}\frac{1}{1+0.584j}\left(i-\sum_{j=1}^{i}\frac{1}{1+\frac{1}{\sqrt{2}}j}\right)-0.251\right)\geq 0.
\end{aligned}
$$

Case (iii): $y \in (\frac{1}{\sqrt{2}}, 1)$**.** For (3.26), it holds

$$
(3.26) \geq \frac{\rho_n}{1+y}\left(\frac{1}{1+y}-\sum_{i=2}^{6}\prod_{j=2}^{i}\frac{1}{1+\frac{1}{\sqrt{2}}j}-\sum_{i=7}^{\infty}\left(i-1-\sum_{j=1}^{7}\frac{1}{1+\frac{1}{\sqrt{2}}j}\right)\right)\overset{y<1}{>}0.
$$

■

By replacing all variables with those corresponding to the endogenous single-sided queueing model, the conclusions of Proposition 2-4 and Theorem 5 apply. We provide extended analytical results for endogenous single-sided models in the following.

Proposition 13. *In the endogenous single-sided model under the visible information policy, the expected revenue increases with increasing truncation size, i.e.,* $Rev^{(K,n)}(k_n + 1) > Rev^{(K,n)}(k_n)$*. It increases with increasing truncation time, i.e.,* $\frac{dRev^{(K,n)}}{dt} > 0$*. Under the invisible information policy, it decreases with the reneging rate, i.e.,* $\frac{dRev^{(R,n)}}{d\delta} < 0$*.*

Proof. **Endogenous K model.** Since $\pi_0^{(K,n)} = \frac{1-\rho_n}{1-{\rho_n}^{k_n+1}}$, $\pi_i^{(K,n)} = {\rho_n}^i \pi_0^{(K,n)}$ and $Rev^{(K,n)} = \Lambda_s \left(1 - \pi_{k_n}^{(K,n)}\right)^2 = \Lambda_s \left(\frac{1-{\rho_n}^{k_n}}{1-{\rho_n}^{k_n+1}}\right)^2$ where $k_n := \lceil t\lambda_d^K \rceil$ is an integer, the revenue increment in k_n is

$$\begin{aligned} Rev^{(K,n)}(k_n+1) - Rev^{(K,n)}(k_n) &= \Lambda_s \left(2 - \pi_{k_n+1}^{(K,n)} - \pi_{k_n}^{(K,n)}\right)\left(\pi_{k_n}^{(K,n)} - \pi_{k_n+1}^{(K,n)}\right) \\ &= \frac{\Lambda_s \left(2 - \pi_{k_n+1}^{(K,n)} - \pi_{k_n}^{(K,n)}\right)\left({\rho_n}^{k_n}(\rho_n - 1)^2\right)}{\left(1-{\rho_n}^{k_n+2}\right)\left(1-{\rho_n}^{k_n+1}\right)} > 0. \end{aligned}$$

We also show that $\frac{dk_n}{dt} = \frac{d\left(\Lambda_s \xi_s^{(K,n)} t\right)}{dt} = \Lambda_d \left(\frac{d\xi_s^{(K,n)}}{dt} + \xi_s^{(K,n)}\right) > 0$, as we have already shown in Lemma 11 that $\frac{d\xi_s^{(K,n)}}{dt} > 0$. As $\frac{dk_n}{dt} \geq 0$ for fixed potential arrival rates of customers and suppliers, it implies $\frac{dRev^{(K,n)}}{dt} \geq 0$.

Endogenous R model. Since $\pi_i^{(R,n)} = \prod_{j=1}^{i} \frac{\rho_n}{1+j\delta/\left(\Lambda_s\xi_s^{(R,n)}\right)} \pi_0^{(R,n)}$ and $\pi_0^{(R,n)} = \frac{1}{1+\zeta_n}$, the first derivative of $Rev^{(R,n)}$ in δ is

$$\frac{dRev^{(R,n)}}{d\delta} = 2\Lambda_s \xi_s^{(R,n)} \frac{d(1-\pi_0^{(R,n)})}{d\delta} = -2\Lambda_s \xi_s^{(R,n)} \frac{d\pi_0^{(R,n)}}{d\delta} < 0 \qquad (3.28)$$

where in the last step of (3.28), $\frac{d\pi_0^{(R,n)}}{d\delta} > 0$ is shown in Lemma 12. ∎

Proposition 14. *In an endogenous single-sided model, queueing the side with a higher potential arrival rate has a higher expected revenue. Specifically, for each $\ell \in \{K, R\}$, if the system load satisfies $\rho_n \geq 1$, then the expected revenue in a demand market is higher than or equal to that in a supply market, i.e.,* $Rev_d^{(\ell,n)} \geq Rev_s^{(\ell,n)}$*. Otherwise, if $\rho_n < 1$, then* $Rev_d^{(\ell,n)} < Rev_s^{(\ell,n)}$*.*

Proof. We replace all the variables in the proof of Proposition 3 by those in the endogenous model, and derive the important steps that align with the original ones. We discuss the case where the arrival rate of customers is higher than that of suppliers, i.e., $\lambda_d^\ell \geq \lambda_s^\ell$ for each $\ell \in \{K, R\}$ and $\rho_n \geq 1$. We omit the case where $\lambda_d^\ell < \lambda_s^\ell$, as the model setting is symmetric. We compare the expected revenues of endogenous single-sided models with different queue sides.

Endogenous K model. The expected revenues of queueing different sides are

$$Rev_d^{(K,n)} - Rev_s^{(K,n)} = \lambda_d^K \left(\frac{1 - {\rho_n}^{k_n}}{1 - {\rho_n}^{\rho_n k_n + 1}} - \frac{1 - {\rho_n}^{\lceil k_n^s / \rho_n \rceil}}{1 - {\rho_n}^{\lceil k_n^s / \rho_n \rceil + 1}} \right) \geq 0.$$

Endogenous R model. The difference between the expected revenues when queueing on different sides is

$$\begin{aligned} Rev_d^{(R,n)} - Rev_s^{(R,n)} &\geq \min\left\{\lambda_s^R, \lambda_s^{(R,qs)}\right\} \left(\frac{\zeta_n}{1 + \zeta_n} - \rho_n \frac{\zeta_n^s}{1 + \zeta_n^s} \right) \\ &= \frac{\min\{\lambda_s^R, \lambda_s^{(R,qs)}\}}{(1 + \zeta_n)(1 + \zeta_n^s)} f_r^n \geq 0 \end{aligned}$$

where $\lambda_s^{(R,qs)}$ is the endogenous arrival rate of suppliers in a supplier market and $f_r^n := \zeta_n - \rho_n \zeta_n^s - (\rho_n - 1)\zeta_n \zeta_n^s$. We omit the proof for demonstrating $f_r^n \geq 0$, as all steps follow the same approach used in the proof of Proposition 3. ■

Proposition 15. *In a demand market and endogenous arrival rate, if the system load ρ_n exceeds a threshold $1 < T_\rho < 2$, then the invisible information policy is preferred.*

Proof. The value of T_ρ satisfies the condition $\lim\limits_{\Lambda_s \to \infty} f_n^{(K,R)} = 0$, when ρ_n is substituted with T_ρ in the function $f_x^{(K,R)}$.

We show that if the potential arrival rate of suppliers is sufficiently large (i.e., $\Lambda_s \to \infty$) and a fixed ρ_n, the value of t is too small to satisfy the indifference curve $f_n^{(K,R)} = 0$ for a large ρ_n (e.g., $\rho_n \geq 2$). It holds

$$\delta t = \lim_{\Lambda_s \to \infty} \frac{\delta}{\lambda_s^K} \frac{\ln\left(\rho_n + (\rho_n - 1) \sum\limits_{i=1}^{\infty} \prod\limits_{j=1}^{i} \frac{\rho_n}{1 + j\delta/\lambda_s^R}\right)}{\ln \rho_n} - \frac{\delta}{\lambda_s^K}$$

$$= \lim_{\epsilon \to 0} \frac{\epsilon \ln \left(\rho_n + (\rho_n - 1) \sum\limits_{i=1}^{\infty} \prod\limits_{j=1}^{i} \frac{\rho_n}{1+j\epsilon} \right)}{\ln \rho_n} \overset{\rho \geq 2}{=} \infty.$$

We omit the proof of demonstrating that the threshold $T_\rho > 1$ in the endogenous model, as all steps follow the same approach used in the proof of Proposition 4. ∎

Theorem 16. *In a demand market and endogenous arrival rate, the preferred information policy is determined as follow:*

1. *If one side's market size is large and the potential arrival rate of customers Λ_d is below a unique threshold T_d, then the visible information policy is preferred, and vice versa.*

2. *If the full market size is large with a fixed system load $\rho_n < T_\rho$ and the arrival rate of suppliers Λ_s is below a unique threshold T_f, then the invisible information policy is preferred, and vice versa.*

Proof. The value of T_d satisfies the condition $f_n^{(K,R)} = 0$, when Λ_s is held constant and Λ_d is substituted with T_d in the function $f_n^{(K,R)}$. The value of T_f satisfies the condition $f_n^{(K,R)} = 0$, when ρ_n is held constant and Λ_s is substituted with T_f in the function $f_n^{(K,R)}$.

We prove the uniqueness of the threshold T_ϖ for each $\varpi \in \{d, f\}$ by establishing the monotonicity of the indifference curve in three cases: (i) potential arrival rate of customers is larger; (ii) potential arrival rates of both customers and suppliers are larger. We omit the case that the potential arrival rate of suppliers is larger since the setting is symmetric to (i).

Case (i). When the potential arrival rate of customers is larger, we consider that Λ_s remains fixed and ρ_n increases. The value of t satisfying the indifference curve $f_n^{(K,R)} = 0$ is

$$t = \ln \left(\rho_n + (\rho_n - 1) \sum_{i=1}^{\infty} \prod_{j=1}^{i} \frac{\rho_n}{1 + j\delta/\lambda_s^R} \right) \Big/ \left(\lambda_s^K \ln \rho_n \right) - \frac{1}{\lambda_s^K}. \tag{3.29}$$

It holds

$$\frac{dt}{d\rho_n} \geq \frac{d}{d\rho_n}\left(\frac{\ln\left(\rho_n + (\rho_n - 1)\sum_{i=1}^{\infty}\prod_{j=1}^{i}\frac{\rho_n}{1+j}\right)}{\Lambda_s \ln \rho_n} - \frac{1}{\lambda_s^K}\right)$$

$$= \frac{1}{\Lambda_s}\left(\frac{d}{d\rho_n}\frac{\ln\left(\frac{\rho_n}{2}+\frac{1}{2}\right)}{\ln \rho_n} - \frac{d\frac{1}{\xi_s^{(K,n)}}}{d\rho_n}\right) \overset{(3.11),\ \textit{Lemma}\ 12}{\geq} 0.$$

Case (ii). When potential arrival rates of both customers and suppliers are larger, we consider that both Λ_d and Λ_s increase and a fixed system load ρ_n. For (3.29), it holds

$$\frac{dt}{d\Lambda_s} = \frac{d}{d\Lambda_s}\left(\frac{\ln\left(\rho_n + (\rho_n - 1)\sum_{i=1}^{\infty}\prod_{j=1}^{i}\frac{\rho_n}{1+j\delta/\lambda_s^R}\right)}{\lambda_s^K \ln \rho_n} - \frac{1}{\lambda_s^K}\right)$$

$$= \frac{1}{\delta \ln \rho_n}\frac{d}{d\Lambda_s}\left(\frac{\delta}{\lambda_s^K}\cdot \ln\left(1 + \left(1 - \frac{1}{\rho_n}\right)\sum_{i=1}^{\infty}\prod_{j=1}^{i}\frac{\rho_n}{1+j\delta/\lambda_s^R}\right)\right)$$

$$\overset{(3.13)}{\leq} \frac{1}{\delta \ln \rho_n}\frac{d}{d\Lambda_s}\left(\frac{\delta}{\lambda_s^K}\ln\left(\frac{1}{2}+\frac{\rho_n}{2}\right)\right) \overset{\textit{Lemma}\ 11}{\leq} 0.$$

■

3.4.2. Endogenous double-sided queueing model

The steady-state distribution and matching probability under the four proposed information policies can be obtained by replacing all variables in Table 3.3 with those corresponding to the endogenous models. Close forms for all indifference curves of endogenous models are summarized in Table 3.5. In the endogenous double-sided queueing model, the information policy not only influences the matching probability and user arrival rate, but also affects the truncation size of both sides of the queue by altering the respective service rates on each side, and consequently, the respective queue lengths. Despite the complexity and difficulty in tracing this endogeneity within the service system, we contend that the recommendation of the preferred information policy in the double-sided queueing model is qualitatively consistent with that in the exogenous model. By replacing all variables with those corresponding to the endogenous double-sided queueing

Indifference curve	Closed form
$f_n^{(BV,BI)}=0$	$\phi_d^{(BV,n)}+\phi_s^{(BV,n)}=\zeta_d^{(BI,n)}+\zeta_s^{(BI,n)}$
$f_n^{(SV,BI)}=0$	$\frac{\zeta_d^{(SV,n)}+\rho_n\phi_s^{(SV,n)}}{1+\zeta_d^{(SV,n)}+\phi_s^{(SV,n)}}=\frac{\zeta_d^{(BI,n)}+\rho_n\zeta_s^{(BI,n)}}{1+\zeta_d^{(BI,n)}+\zeta_s^{(BI,n)}}$
$f_n^{(BV,SV)}=0$	$\frac{\phi_d^{(BV,n)}+\rho_n\phi_s^{(BV,n)}}{1+\phi_d^{(BV,n)}+\phi_s^{(BV,n)}}=\frac{\zeta_d^{(SV,n)}+\rho_n\phi_s^{(SV,n)}}{1+\zeta_d^{(SV,n)}+\phi_s^{(SV,n)}}$
$f_n^{(DV,BI)}=0$	$\frac{\phi_d^{(DV,n)}+\rho_n\zeta_s^{(DV,n)}}{1+\phi_d^{(DV,n)}+\zeta_s^{(DV,n)}}=\frac{\zeta_d^{(BI,n)}+\rho_n\zeta_s^{(BI,n)}}{1+\zeta_d^{(BI,n)}+\zeta_s^{(BI,n)}}$
$f_n^{(BV,DV)}=0$	$\frac{\phi_d^{(BV,n)}+\rho_n\phi_s^{(BV,n)}}{1+\phi_d^{(BV,n)}+\phi_s^{(BV,n)}}=\frac{\phi_d^{(DV,n)}+\rho_n\zeta_s^{(DV,n)}}{1+\phi_d^{(DV,n)}+\zeta_s^{(DV,n)}}$

Note. For any two information policies A and B, the closed form of the indifference curve is obtained by simplifying the equation $Rev^{(A,n)} - Rev^{(B,n)} = 0$ in the endogenous model.

Table 3.5.: Indifference curves in the double-sided queueing model with endogenous arrival rates.

model, the conclusions of Proposition 6-9 and Theorem 8 apply. We provide extended analytical results for endogenous double-sided models in the following.

Proposition 17. *In an endogenous double-sided model, the expected revenue increases with truncation size on the side displaying visible information, i.e., for each* $(\ell,\varpi)\in\{(BV,d),(BV,s),(DV,d),(SV,s)\}$*, we have* $Rev^{(\ell,n)}(k_\varpi^n+1) > Rev^{(\ell,n)}(k_\varpi^n)$*. It increases with truncation time, i.e.,* $\frac{dRev^{(\ell,n)}}{dt_\varpi} > 0$*. It decreases with reneging rate on the side with invisible information, i.e., for each* $(\ell,\varpi)\in\{(BI,d),(BI,s),(SV,d),(DV,s)\}$*, we have* $\frac{dRev^{(\ell,n)}}{d\delta_\varpi} < 0$*.*

Proof. In the endogenous double-sided models, we present the Markov chain steady-state distributions and matching probabilities for four information policies in Table 3.6, where auxiliary variables are defined by

$$\phi_d^{(\ell,n)} := \frac{\rho_n - {\rho_n}^{k_d^{(\ell,n)}+1}}{1-\rho_n} \qquad \text{for each} \quad \ell\in\{DV,BV\}$$

$$\phi_s^{(\ell,n)} := \frac{(1/\rho_n) - (1/\rho_n)^{k_s^{(\ell,n)}+1}}{1-(1/\rho_n)} = \frac{{\rho_n}^{k_s^{(\ell,n)}} - 1}{{\rho_n}^{k_s^{(\ell,n)}+1} - {\rho_n}^{k_s^{(\ell,n)}}} \qquad \text{for each} \quad \ell\in\{SV,BV\}$$

$$\zeta_d^{(\ell,n)} := \sum_{i=1}^{\infty}\prod_{j=1}^{i}\frac{\rho_n}{1+j(\delta_d/\lambda_s^{\ell})} \qquad \text{for each} \quad \ell\in\{SV,BI\}$$

Model	π_0^m	π_i^m, $\forall i < 0$	π_i^m, $\forall i > 0$
$m = (BV, n)$	$\frac{1}{1+\phi_d^m+\phi_s^m}$	$\rho^i \pi_0^m$	$\rho^i \pi_0^m$
$m = (DV, n)$	$\frac{1}{1+\phi_d^m+\zeta_s^m}$	$\prod_{j=-1}^{-i} \frac{1}{\rho - j\delta_s/\Lambda_s} \cdot \pi_0^m$	$\rho^i \pi_0^m$
$m = (SV, n)$	$\frac{1}{1+\zeta_d^m+\phi_s^m}$	$\rho^i \pi_0^m$	$\prod_{j=1}^{i} \frac{\rho}{1+j\delta_d/\Lambda_s} \cdot \pi_0^m$
$m = (BI, n)$	$\frac{1}{1+\zeta_d^m+\zeta_s^m}$	$\prod_{j=-1}^{-i} \frac{1}{\rho - j\delta_s/\Lambda_s} \cdot \pi_0^m$	$\prod_{j=1}^{i} \frac{\rho}{1+j\delta_d/\Lambda_s} \cdot \pi_0^m$

ξ_d^m	ξ_s^m
$\frac{\frac{1}{\rho}\phi_d^m+\phi_s^m}{1+\phi_d^m+\phi_s^m}$	$\frac{\phi_d^m+\rho\phi_s^m}{1+\phi_d^m+\phi_s^m}$
$\frac{\frac{1}{\rho}\phi_d^m+\zeta_s^m}{1+\phi_d^m+\zeta_s^m}$	$\frac{\phi_d^m+\rho\zeta_s^m}{1+\phi_d^m+\zeta_s^m}$
$\frac{\frac{1}{\rho}\zeta_d^m+\phi_s^m}{1+\zeta_d^m+\phi_s^m}$	$\frac{\zeta_d^m+\rho\phi_s^m}{1+\zeta_d^m+\phi_s^m}$
$\frac{\frac{1}{\rho}\zeta_d^m+\zeta_s^m}{1+\zeta_d^m+\zeta_s^m}$	$\frac{\zeta_d^m+\rho\zeta_s^m}{1+\zeta_d^m+\zeta_s^m}$

Table 3.6.: Steady-state probability and matching probability for four information policies in an endogenous model where $m = (\ell, n)$ and $\ell \in M$.

$$\zeta_s^{(\ell,n)} := \sum_{i=1}^{\infty} \prod_{j=1}^{i} \frac{1/\rho_n}{1 + j(\delta_s/\lambda_d^\ell)} = \sum_{i=1}^{\infty} \prod_{j=1}^{i} \frac{1}{\rho_n + j(\delta_s/\lambda_s^\ell)} \qquad \text{for each} \quad \ell \in \{DV, BI\}$$

where $k_s^{(\ell,n)} := \lceil t_s \lambda_d^\ell \rceil$ and $k_d^{(\ell,n)} := \lceil t_d \lambda_s^\ell \rceil$. We note that the definitions of these auxiliary variables are symmetric to those corresponding to exogenous models. Additionally, $1/\left(1 + \phi_d^{(\ell,n)}\right)$ for each $\ell \in \{BV, DV\}$ and $1/\left(1 + \phi_s^{(\ell,n)}\right)$ for each $\ell \in \{BV, SV\}$ have a structure similar to $\pi_0^{(K,n)}$. Meanwhile, $\zeta_d^{(\ell,n)}$ for each $\ell \in \{BI, SV\}$ and $\zeta_s^{(\ell,n)}$ for each $\ell \in \{BI, DV\}$ have a structure similar to $\pi_0^{(R,n)}$. We omit the following steps, as they follow the same approach used in the proof of Proposition 6. ■

Proposition 18. *For an endogenous double-sided queueing model with a relatively unbalanced system load:*

1. *If the system load ρ_n is below a unique threshold $\frac{1}{2} < \underline{T_\rho} < 1$, then a DV information policy is preferred for a high potential arrival rate $\Lambda_d \geq T_l$, while a BI information policy is preferred for a low potential arrival rate $\Lambda_d < T_l$.*

2. *If the system load ρ_n exceeds a unique threshold $1 < \overline{T_\rho} < 2$, then a SV information policy is preferred for a high potential arrival rate $\Lambda_d \geq T_l$, while a BI information policy is preferred for a low potential arrival rate $\Lambda_d < T_l$.*

Proof. The value of $\underline{T_\rho}$ satisfies the condition $\lim_{\Lambda_d \to \infty} f_n^{(DV,BV)} = 0$, when ρ_n is substituted with T_ρ in the function $f_n^{(DV,BV)}$. The value of $\overline{T_\rho}$ satisfies the condition $\lim_{\Lambda_d \to \infty} f_n^{(BV,SV)} = 0$, when ρ_n is substituted with $\overline{T_\rho}$ in the function $f_n^{(BV,SV)}$. Assuming a constant ρ_n, if $\rho_n \leq 1$, then the value of T_l satisfies the condition $f_n^{(DV,BI)} = 0$ when Λ_d is substituted with T_l in the function $f_n^{(DV,BI)}$. Conversely, if $\rho_n < 1$, it satisfies the condition $f_n^{(BI,SV)} = 0$ when Λ_d is substituted with T_l in the function $f_n^{(BI,SV)}$.

Upper bound (resp. lower bound) of $\underline{T_\rho}$ (resp. $\overline{T_\rho}$). With $\rho_n = 1$, it holds

$$\lim_{\substack{\Lambda_s \to \infty \\ \rho_n = 1}} f_n(BV, BI) \geq \lim_{\substack{\Lambda_s \to \infty \\ \rho_n = 1}} \left(t - \frac{1}{2\Lambda_s} \sum_{i=1}^{\infty} 2 \cdot \prod_{j=1}^{i} \frac{1}{1 + j\delta_b/\Lambda_s} \right) \geq 0.$$

Upper bound of $\overline{T_\rho}$. We suppose $\overline{T_\rho} \geq 2$ (i.e., $\rho_n \geq 2$) and find the contradictory. The difference curve $f_n^{(BV,SV)} = 0$ is

$$\begin{aligned} \delta_b t_b = & \frac{\delta_b}{\lambda_s^{BV} + \lambda_d^{BV} - \lambda_d^{SV}} \frac{\ln \left(\rho_n + (\rho_n - 1) \sum_{i=1}^{\infty} \prod_{j=1}^{i} \frac{\rho_n}{1 + j\delta_b/\lambda_s^{SV}} \right)}{\ln \rho_n} \\ & - \frac{\delta_b}{\lambda_s^{BV} + \lambda_d^{BV} - \lambda_d^{SV}} \end{aligned} \tag{3.30}$$

where it holds $\lim_{\substack{\Lambda_s \to \infty \\ \rho_n \geq 2}} \left(\frac{\delta_b}{\lambda_s^{BV} + \lambda_d^{BV} - \lambda_d^{SV}} \right) = 0$ and $\lim_{\substack{\Lambda_s \to \infty \\ \rho_n \geq 2}} \frac{\delta_b}{\lambda_s^{SV}} = 0$. Hence it holds

$$\lim_{\substack{\Lambda_s \to \infty \\ \rho_n \geq 2}} \text{RHS of (3.30)} = \lim_{\epsilon \to 0} \frac{\epsilon \ln \left(\rho_n + (\rho_n - 1) \sum_{i=1}^{\infty} \prod_{j=1}^{i} \frac{\rho_n}{1 + j\epsilon} \right)}{\ln \rho_n} = \infty$$

while the LHS of (3.30) is constant. ■

Theorem 19. *In an endogenous double-sided model, the preferred information policy is determined as follow:*

1. *For a larger market size on one side:*

   a) *If the potential arrival rate of suppliers* Λ_s *is below the threshold* T_l*, then a* SV *information policy is preferred.*

   b) *If the potential arrival rate* Λ_ϖ *of one side* $\varpi \in \{d, s\}$ *lies between thresholds* T_l *and* T_u *and the potential arrival rate* Λ_μ *of the other side* $\mu \in \{d, s\}, \mu \neq \varpi$ *is below the threshold* T_b*, then a* BI *information policy is preferred; otherwise, a* BV *information policy is preferred.*

   c) *If the potential arrival rate of suppliers* Λ_s *exceeds the threshold* T_u*, then a* DV *information policy is preferred.*

2. *For a larger full market size and a fixed system load* $\underline{T_\rho} \leq \rho_n \leq \overline{T_\rho}$*:*

   a) *If the potential arrival rate of suppliers* Λ_s *is below the threshold* T_l*, then a* BI *information policy is preferred.*

   b) *If the potential arrival rate of suppliers* Λ_s *lies between thresholds* T_l *and* T_u *and the system load* ρ_n *is below* 1*, then a* DV *information policy is preferred; otherwise, a* SV *information policy is preferred.*

   c) *If the potential arrival rate of suppliers* Λ_s *exceeds the threshold* T_u*, then a* BV *information policy is preferred.*

Proof. For a larger market size on one side, the value of T_b satisfies the condition $f_n^{(BV,BI)} = 0$ when Λ_d and Λ_s both are substituted with T_b in the function $f_n^{(BV,BI)}$. Assuming a constant Λ_s, if $\Lambda_d \leq T_b$, then the values of T_l and T_u satisfy the conditions $f_n^{(DV,BI)} = 0$ and $f_n^{(BI,SV)} = 0$ respectively, when Λ_d is substituted with T_l in the function $f_n^{(DV,BI)}$ and with T_u in the function $f_n^{(BI,SV)}$. Conversely, if $\Lambda_d < T_b$, then the values of T_l and T_u satisfy the conditions $f_n^{(DV,BV)} = 0$ and $f_n^{(BV,SV)} = 0$ respectively, when Λ_d is substituted with T_l in the function $f_n^{(DV,BV)}$ and with T_u in the function $f_n^{(BV,SV)}$. For a larger full market size and a fixed system load, assuming a constant Λ_d, if $\rho_n \leq 1$, then the values of T_l and T_u satisfy the conditions $f_n^{(DV,BI)} = 0$ and $f_n^{(DV,BV)} = 0$ respectively. The is the case when Λ_s is substituted with T_l in the function $f_n^{(DV,BI)}$ and with T_u in the function $f_n^{(DV,BV)}$. Conversely, if $\rho_n < 1$, then the values of T_l and T_u satisfy the conditions $f_n^{(BI,SV)} = 0$ and $f_n^{(BV,SV)} = 0$ respectively. The is the case when Λ_s is substituted with T_l in the function $f_n^{(BI,SV)}$ and with T_u in the function $f_n^{(BV,SV)}$.

We follow the same steps as those presented in the proof of Theorem 8. We demonstrate that as the full market size is larger, the system load establishes candidate preferred information policies. For example, if $\rho_n > 1$, the candidate preferred information policy is in $\{BI, SV, BV\}$. To demonstrate this, we discuss two cases. Case (i): if the truncation size of suppliers $k_d^{(DV,n)}$ is small and satisfies $\rho_n + {\rho_n}^2 + .. + {\rho_n}^{k_d^{(DV,n)}} \leq \zeta_d^{(DV,n)}$, then the BI policy has higher expected revenue than the DV policy. Case (ii): if the truncation size of suppliers $k_d^{(DV,n)}$ is large and satisfies $\rho_n + {\rho_n}^2 + .. + {\rho_n}^{k_d^{(DV,n)}} > \zeta_d^{(DV,n)}$, then the BV policy has higher expected revenue than the DV policy. Therefore, DV is not a candidate preferred information policy for any value of $k_d^{(DV,n)}$. ■

Proposition 20. *For asymmetric user patience in an endogenous model, i.e., $\alpha \neq 1$, hiding the information on the side with lower user patience increases expected revenue. Specifically, if the potential arrival rate of suppliers Λ_s and patience coefficient α satisfy the indifference curves $f_n^{(BV,DV)} = 0$ or $f_n^{(SV,BI)} = 0$ for fixed customer patience (t_d, δ_d) and system load ρ_n, then $\frac{d\Lambda_s}{d\alpha} \geq 0$.*

Proof. There exists a unique solution for $\left(\lambda_s^{BV}/\alpha, \lambda_s^{DV}/\alpha\right)$ that satisfies the indifference curve $f_n^{(BV,DV)} = 0$ for fixed (t_d, δ_c) and ρ_n. Since the effective arrival rate is weakly increasing with the potential arrival rate, i.e., $\frac{d\lambda_s^{BV}}{d\Lambda_s} \geq 0$ and $\frac{d\lambda_s^{DV}}{d\Lambda_s} \geq 0$, it follows that $\frac{d\Lambda_s}{d\alpha} \geq 0$. ■

3.4.3. Impact of endogeneity

We define the *relative revenue difference* between different information policies. In the exogenous model, the relative revenue difference is denoted by $v := \frac{a-b}{a}$, where

$$a := \begin{cases} \max\left\{Rev^K, Rev^R\right\} \\ \max\left\{Rev^A | A \in M\right\} \end{cases} \quad \text{and} \quad b := \begin{cases} \min\left\{Rev^K, Rev^R\right\} & \text{single-sided} \\ \min\left\{Rev^A | A \in M\right\} & \text{double-sided.} \end{cases} \tag{3.31}$$

In the endogenous model, the relative revenue difference is denoted by $v_n := \frac{a_n - b_n}{a_n}$, where all variables are replaced with those corresponding to the endogenous models. Specifically, Rev^B is replaced with $Rev^{(B,n)}$ for an information policy $B \in \{K, R\} \cup M$ in (3.31). This metric quantifies the varying effects of different information policies on the platform's revenue, highlighting the significance of information design for the platform's performance.

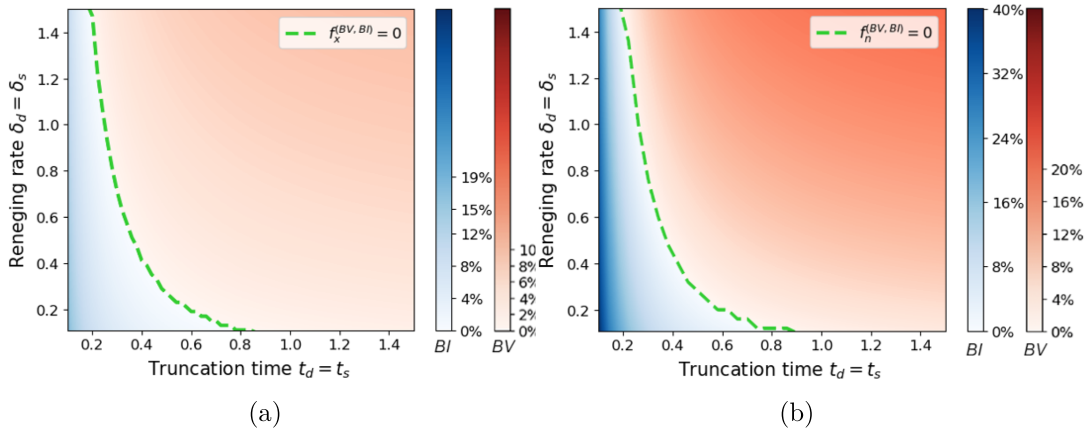

Figure 3.6.: Comparisons of information policies in terms of relative revenue difference: $\Lambda_d = \Lambda_s = 20$. Left: Exogenous model. Right: Endogenous model.

Figure 3.6 provides an example of comparing information policies in terms of relative revenue difference for a balanced market (i.e., $\Lambda_d = \Lambda_s$) with symmetric user patience (i.e., $t_d = t_s$ and $\delta_d = \delta_s$). It shows that the BV policy is preferred for (t_d, δ_d) values above the indifference curve, while the BI policy is preferred otherwise. The relative revenue advantage of the preferred information policy in the market increases as the market parameters move further away from the indifference curve. For instance, in the region of Figure 3.6 where both t_d and δ_d are larger, the BV policy is darker, indicating a larger relative revenue difference and a greater relative advantage among the different information policies. This occurs when the user's patience level varies significantly between information policies, and the user is sensitive to the displayed queue-length information.

Proposition 21. *The relative revenue difference is larger in the endogenous model.*

Proof. We compare exogenous and endogenous models under ceteris paribus, considering the shift in the indifference curve. Specifically, we consider those market parameters that maintain the same preferred and least preferred information policies in both models.

Single-sided queueing model. The market with the same preferred information policy in both exogenous and endogenous models has either large or small values for both k and δ. Thus, we consider four cases: (i) $\rho \geq 1$ and both k and δ are large, (ii) $\rho \geq 1$ and both k and δ are small, (iii) $\rho < 1$ and both k and δ are large, and (iv) $\rho < 1$

and both k and δ are small. The ratio of the relative revenue differences between the information policies of the endogenous model and the exogenous model is

$$\begin{aligned}
\frac{v_n}{v} =& \frac{Rev^{(K,n)} - Rev^{(R,n)}}{Rev^K - Rev^R} \cdot \frac{\max\left\{Rev^K, Rev^R\right\}}{\max\left\{Rev^{(K,n)}, Rev^{(R,n)}\right\}} \\
\geq& \left(2 - \pi_0^{(K,n)} - \pi_0^{(R,n)}\right) \cdot \left|\frac{\pi_0^{(K,n)} - \pi_0^{(R,n)}}{\pi_0^K - \pi_0^R}\right| \qquad (3.32) \\
=& \left(2 - \frac{1-\rho_n}{1-{\rho_n}^{k_n+1}} - \frac{1}{1+\zeta_n}\right) \cdot \left|\frac{{\rho_n}^{k_n+1} - \rho_n + (1-\rho_n)\,\zeta_n}{\rho^{k+1} - \rho + (1-\rho)\,\zeta}\right. \\
& \left. \cdot \frac{\left(1-\rho^{k+1}\right)(1+\zeta)}{\left(1-{\rho_n}^{k_n+1}\right)(1+\zeta_n)}\right|. \qquad (3.33)
\end{aligned}$$

We show the ratio $\frac{v_n}{v} \geq 1$ in the above four cases.

Case (i). If $\rho \geq 1$ and k, k_n and δ are large, then

$$\begin{aligned}
(3.33) =& \left(2 - O\left(\left(\frac{1}{\rho_n}\right)^{k_n}\right) - \pi_0^{(R,n)}\right) \\
& \cdot \left|O\left(\max\left\{\left(\frac{1}{\rho_n}\right)^{k+1}, \frac{\zeta_n}{\zeta}\right\}\right) O\left({\rho_n}^{k+1}\frac{\zeta}{\zeta_n}\right)\right| \geq 1
\end{aligned}$$

where $\frac{\zeta}{\zeta_n} > 0$ is upper bounded by a constant and k and k_n are large.

Case (ii). If $\rho \geq 1$ and k, k_n and δ are small, then

$$(3.33) = \left(2 - \frac{1-\rho_n}{1-{\rho_n}^{k_n+1}}\right) \left|\frac{{\rho_n}^{k_n+1} - {\rho_n}^{\infty}}{\rho^{k+1} - \rho^{\infty}} \cdot \frac{\rho^{\infty} - 1}{{\rho_n}^{\infty} - 1} \cdot \frac{\rho^{k+1} - 1}{{\rho_n}^{k_n+1} - 1} \cdot \frac{1-\rho_n}{1-\rho}\right| \geq 1.$$

Case (iii). If $\rho < 1$ and k, k_n and δ are large, recall that we denote $z = \delta/\Lambda_s$ and $z \in (0,1)$, it holds

$$\begin{aligned}
(3.33) =& \left(1 + \rho_n - \frac{1}{1+\zeta_n}\right) \cdot \frac{\rho_n - (1-\rho_n)\,\zeta_n}{\rho - (1-\rho)\,\zeta} \cdot \frac{1+\zeta}{1+\zeta_n} \\
\geq& \left(\rho_n + \frac{\sum_{i=1}^{\infty}\prod_{j=1}^{i}\frac{\rho_n}{1+jz}}{1 + \sum_{i=1}^{\infty}\prod_{j=1}^{i}\frac{\rho_n}{1+jz}}\right) \cdot \frac{1}{\rho_n} \cdot \frac{1 + \sum_{i=1}^{\infty}\prod_{j=1}^{i}\frac{{\rho_n}^2}{1+jz}}{1 + \sum_{i=1}^{\infty}\prod_{j=1}^{i}\frac{\rho_n}{1+jz}} \qquad (3.34)
\end{aligned}$$

where we use the fact that $\frac{\rho_n-(1-\rho_n)\zeta_n}{\rho-(1-\rho)\zeta} \geq \frac{\rho_n-(1-\rho_n)\sum_{i=1}^{\infty}\prod_{j=1}^{i}\frac{\rho_n}{1+jz}}{{\rho_n}^2-(1-{\rho_n}^2)\sum_{i=1}^{\infty}\prod_{j=1}^{i}\frac{{\rho_n}^2}{1+jz}} \geq \frac{1}{\rho_n}$ (indicated by $\frac{d}{dz}\frac{\sum_{i=1}^{\infty}\prod_{j=1}^{i}\frac{\rho_n}{1+jz}}{\sum_{i=1}^{\infty}\prod_{j=1}^{i}\frac{{\rho_n}^2}{1+jz}} \leq 0$ and hence $\frac{\sum_{i=1}^{\infty}\prod_{j=1}^{i}\frac{\rho_n}{1+jz}}{\sum_{i=1}^{\infty}\prod_{j=1}^{i}\frac{{\rho_n}^2}{1+jz}} \leq \frac{\sum_{i=1}^{\infty}{\rho_n}^i}{\sum_{i=1}^{\infty}{\rho_n}^{2i}} \leq 1+\frac{1}{\rho_n}$). Hence to show (3.34) ≥ 1, it is equivalent to showing

$$\left(\left(1+\frac{1}{\rho_n}\right)\left(1+\sum_{i=1}^{\infty}\prod_{j=1}^{i}\frac{\rho_n}{1+jz}\right)-\frac{1}{\rho_n}\right)\left(1+\sum_{i=1}^{\infty}\prod_{j=1}^{i}\frac{{\rho_n}^2}{1+jz}\right) \geq \left(1+\sum_{i=1}^{\infty}\prod_{j=1}^{i}\frac{\rho_n}{1+jz}\right)^2$$

which is proven since

$$\begin{aligned}\left(\frac{1}{\rho_n}-1\right)+\sum_{i=1}^{\infty}\prod_{j=1}^{i}\frac{{\rho_n}^2}{1+jz}\Big/\sum_{i=1}^{\infty}\prod_{j=1}^{i}\frac{\rho_n}{1+jz}+\left(1+\frac{1}{\rho_n}\right)\sum_{i=1}^{\infty}\prod_{j=1}^{i}\frac{{\rho_n}^2}{1+jz}-\sum_{i=1}^{\infty}\prod_{j=1}^{i}\frac{\rho_n}{1+jz}\\ \geq \frac{1-\rho_n}{\rho_n}+\frac{1}{1+\rho_n}+\left(1+\frac{1}{\rho_n}\right)\sum_{i=1}^{\infty}\prod_{j=1}^{i}\frac{{\rho_n}^2}{1+jz}-\sum_{i=1}^{\infty}\prod_{j=1}^{i}\frac{\rho_n}{1+jz} \geq 0.\end{aligned}$$

Case (iv). If $\rho < 1$ and k, k_n and δ are small, then

$$\begin{aligned}(3.33) &= \left(2-\frac{1-\rho_n}{1-{\rho_n}^{k_n+1}}-\frac{1}{1+\frac{\rho_n}{1-\rho_n}}\right)\\ &\quad\left|\frac{{\rho_n}^{k_n+1}-\rho_n+(1-\rho_n)\frac{\rho_n}{1-\rho_n}}{\rho^{k+1}-\rho+(1-\rho)\frac{\rho}{1-\rho}}\frac{\left(1-\rho^{k+1}\right)\left(\frac{\rho}{1-\rho}+1\right)}{(1-{\rho_n}^{k_n+1})\left(\frac{\rho_n}{1-\rho_n}+1\right)}\right|\\ &= \left(1-\frac{1-\rho_n}{1-{\rho_n}^{k_n+1}}+\rho_n\right)\left|\frac{{\rho_n}^{k_n+1}}{{\rho_n}^{2k+2}}\frac{1-{\rho_n}^{2k+2}}{1-{\rho_n}^{k_n+1}}\frac{1-\rho_n}{1-{\rho_n}^2}\right|\\ &\geq \frac{2-{\rho_n}^{k_n}-{\rho_n}^{k_n+1}}{1-{\rho_n}^{k_n+1}}\left|\frac{1+{\rho_n}^{k+1}}{\rho_n^k+{\rho_n}^{k+1}}\right| \geq \frac{2\left(1-{\rho_n}^{k_n}\right)}{1-{\rho_n}^{k_n}}\left|\frac{1+{\rho_n}^{k+1}}{\rho_n^k+{\rho_n}^{k+1}}\right| \geq 1.\end{aligned}$$

Double-sided queueing model. The same preferred and least preferred information policies for both exogenous and endogenous models in a double-sided queueing model can be categorized into four cases: (i) If both user patience t_b and δ_b are large, then the *BV* policy is the preferred one, and the *BI* policy is the least preferred; (ii) If both user patience t_b and δ_b are small, then the *BI* policy is the preferred one, and the *BV* policy is the least preferred; (iii) If the system load $\rho > 1$ is large, then the SV policy is preferred, and the DV policy is the least preferred; (iv) If the system load $\rho < 1$ is small, then the DV policy is preferred, and the SV policy is the least preferred. For Case (i) and (ii), the ratio $\frac{v_n}{v}$ can be calculated as:

$$\begin{aligned} \frac{v_n}{v} &= \frac{Rev^{(BV,n)} - Rev^{(BI,n)}}{Rev^{BV} - Rev^{BI}} \frac{\max\left\{Rev^{BV}, Rev^{BI}\right\}}{\max\left\{Rev^{(BV,n)}, Rev^{(BI,n)}\right\}} \\ &\geq \left(2 - \pi_0^{(BV,n)} - \pi_0^{(BI,n)}\right) \left| \frac{\pi_0^{(BV,n)} - \pi_0^{(BI,n)}}{\pi_0^{BV} - \pi_0^{BI}} \right| \geq 1 \end{aligned}$$

and for Case (iii) and (iv), the ratio $\frac{v_n}{v}$ is

$$\begin{aligned} \frac{v_n}{v} &= \frac{Rev^{(SV,n)} - Rev^{(DV,n)}}{Rev^{SV} - Rev^{DV}} \frac{\max\left\{Rev^{SV}, Rev^{DV}\right\}}{\max\left\{Rev^{(SV,n)}, Rev^{(DV,n)}\right\}} \\ &\geq \left(2 - \pi_0^{(SV,n)} - \pi_0^{(DV,n)}\right) \left| \frac{\pi_0^{(SV,n)} - \pi_0^{(DV,n)}}{\pi_0^{SV} - \pi_0^{DV}} \right| \geq 1. \end{aligned}$$

These ratios align with (3.32) as demonstrated in the single-sided queueing model analysis above. The analysis of these cases is omitted as they can be shown by referring to the above analysis. ■

Comparing Figure 3.6(a) and (b), it becomes evident that the endogenous model exhibits a larger relative revenue difference between different information policies than the exogenous model, due to the scale effect. In this model, a side with a higher potential arrival rate has a lower matching probability than the one with a lower potential arrival rate. As a result, the gap in demand and supply arrival rates narrows in the endogenous model, leading to a smaller absolute difference in expected revenue between information policies. In other words, the long-term influence of matching probability on effective arrival rates decreases the absolute revenue difference between information policies, while heightening the relative revenue difference. We introduce the following theorem to demonstrate that, in a sufficiently large market, there exists a lower bound on the increase in the difference between information policies stemming from the scale effect.

Theorem 22. *For a sufficiently large balanced market, the relative revenue difference between information policies is asymptotically twice as large in the endogenous model as* *in the exogenous model. Specifically, we have* $\lim\limits_{\substack{\Lambda_d\to\infty\\ \rho=1}} \frac{v_n}{v} = 2$*. In an unbalanced market, the asymptotic difference is strictly greater than two, i.e.,* $\lim\limits_{\substack{\Lambda_d\to\infty\\ \rho\neq 1}} \frac{v_n}{v} > 2$*.*

Proof. **Single-sided queueing model.** To analyze the ratio $\frac{v_n}{v}$, we only consider the case where the K model has a higher expected revenue in both exogenous and endogenous models. We omit the case where the R model has a higher expected revenue since the model setting is symmetric. The ratio $\frac{v_n}{v}$ is

$$\begin{aligned}\frac{v_n}{v} &= \frac{Rev^{(K,n)} - Rev^{(R,n)}}{Rev^K - Rev^R} \cdot \frac{\max\left\{Rev^K, Rev^R\right\}}{\max\left\{Rev^{(K,n)}, Rev^{(R,n)}\right\}} \\ &= \left(\xi_s^{(K,n)} + \xi_s^{(R,n)}\right) \frac{\xi_s^{(K,n)} - \xi_s^{(R,n)}}{\xi_s^K - \xi_s^R} \cdot \frac{\xi_s^K}{\left(\xi_s^{(K,n)}\right)^2}. \end{aligned} \tag{3.35}$$

Balanced market. For (3.35), if arrival rates of both customers and suppliers are sufficiently large, then it holds

$$\lim_{\substack{\Lambda_s\to\infty\\ \rho=1}} \frac{v_n}{v} = \lim_{\substack{\Lambda_s\to\infty\\ \rho=1}} 2\cdot \frac{\pi_0^{(K,n)} - \pi_0^{(R,n)}}{\pi_0^K - \pi_0^R} = \lim_{\substack{\Lambda_s\to\infty\\ \rho=1}} 2\cdot \frac{1+\sum\limits_{i=1}^{\infty}\prod\limits_{j=1}^{i}\frac{1}{1+j\delta/\Lambda_s}}{1+\sum\limits_{i=1}^{\infty}\prod\limits_{j=1}^{i}\frac{1}{1+j\delta/\left(\Lambda_s\left(1-\pi_0^{(R,n)}\right)\right)}} = 2$$

where $\lim\limits_{\substack{\Lambda_s\to\infty\\ \rho=1}} \xi_s^{(\ell,n)} = 1$ for each $\ell \in \{K, R\}$.

Unbalanced market. For a fixed system load $\rho < 1$ (i.e., $\Lambda_d < \Lambda_s$) in a demand market, if arrival rates of both customers and suppliers are sufficiently large, indicating that Λ_s approaches infinity, we have $\lim\limits_{\Lambda_s\to\infty} \xi_d^\ell = \lim\limits_{\Lambda_s\to\infty} \xi_d^{(\ell,n)} = \frac{\min\{\Lambda_d,\Lambda_s\}}{\Lambda_d} = 1$ and $\lim\limits_{\Lambda_s\to\infty} \xi_s^\ell = \lim\limits_{\Lambda_s\to\infty} \xi_s^{(\ell,n)} = \frac{\min\{\Lambda_d,\Lambda_s\}}{\Lambda_s} = \frac{\Lambda_d}{\Lambda_s}$ for each $\ell \in \{K, R\}$. Hence, for (3.35), we get

$$\lim_{\substack{\Lambda_s\to\infty\\ \rho<1}} \frac{v_n}{v} = 2\left|\frac{\left(1\Big/\left(\rho_n + \sum\limits_{i=1}^{\infty}\prod\limits_{j=1}^{i}\frac{1}{1+j\delta/\left(\Lambda_s\left(1-\pi_0^{(R,n)}\right)\right)}\right)\right) - \left(1-\frac{\Lambda_d}{\Lambda_s}\right)}{\left(1\Big/\left(\rho + \sum\limits_{i=1}^{\infty}\prod\limits_{j=1}^{i}\frac{1}{1+j\delta/\Lambda_s}\right)\right) - \left(1-\frac{\Lambda_d}{\Lambda_s}\right)}\right| \geq 2.$$

We do not analyze the case where $\Lambda_d > \Lambda_s$ since the model setting is symmetric.

Double-sided queueing model. *Balanced market.* In a balanced double-sided market with a sufficiently large arrival rates on both sides, the BV policy is the preferred information policy while the BI policy is the least preferred information policy. The ratio $\frac{v_n}{v}$ is

$$\begin{aligned}\frac{v_n}{v} &= \frac{Rev^{(BV,n)} - Rev^{(BI,n)}}{Rev^{BV} - Rev^{BI}} \cdot \frac{Rev^{BV}}{Rev^{(BV,n)}}\\ &= \left(2 - \frac{1}{1 + k_d^{(BV,n)} + k_s^{(BV,n)}} - \frac{1}{1 + \zeta_d^{(BI,n)} + \zeta_s^{(BI,n)}}\right)\\ &\frac{\zeta_d^{(BI,n)} + \zeta_s^{(BI,n)} - k_d^{(BV,n)} - k_s^{(BV,n)}}{\zeta_d^{BI} + \zeta_s^{BI} - k_d - k_s} \cdot \frac{t_b + t_b}{t_b\xi_s^{(BV,n)} + t_b\xi_d^{(BV,n)}} \frac{1 + \zeta_d^{BI} + \zeta_s^{BI}}{1 + \zeta_d^{(BI,n)} + \zeta_s^{(BI,n)}}.\end{aligned} \tag{3.36}$$

Since in a balanced market $\lim\limits_{\substack{\Lambda_s \to \infty \\ \rho=1}} \xi_s^{(\ell,n)} = 1$ for each $\ell \in \{BV, BI\}$, it holds

$$\lim_{\substack{\Lambda_s \to \infty \\ \rho=1}} \lambda_d^\ell = \Lambda_d. \tag{3.37}$$

Hence it holds

$$\lim_{\substack{\Lambda_s \to \infty \\ \rho=1}} \frac{v_n}{v} \overset{(3.37)}{=} \lim_{\substack{\Lambda_s \to \infty \\ \rho=1}} \frac{2t_b\Lambda_s + 2t_b\Lambda_d + 1}{t_b\Lambda_s + t_b\Lambda_d + 1} = 2.$$

Unbalanced market. If $\Lambda_s > \Lambda_d$ (i.e., $\rho < 1$) and a fixed $\rho > \underline{T_\rho}$ (defined in Proposition 7), then it holds

$$\lim_{\substack{\Lambda_s \to \infty \\ \rho<1}} \lambda_s^\ell = \Lambda_s \xi_s^{(\ell,n)} = \Lambda_d \quad \text{and} \quad \lim_{\substack{\Lambda_s \to \infty \\ \rho<1}} \lambda_d^\ell = \Lambda_d \tag{3.38}$$

for each $\ell \in \{BV, BI\}$. Hence for (3.36), it holds

$$\lim_{\substack{\Lambda_s \to \infty \\ \rho<1}} \frac{v_n}{v} \overset{(3.38)}{=} \lim_{\substack{\Lambda_s \to \infty \\ \rho=1}} \left(2\left|\frac{2}{1+\rho_n}\right|\left|\frac{\zeta_d^{(BI,n)} + \zeta_s^{(BI,n)} - 2t_b\Lambda_d}{\zeta_d^{BI} + \zeta_s^{BI} - 2t_b\Lambda_d} \cdot \frac{1 + \zeta_d^{BI} + \zeta_s^{BI}}{1 + \zeta_d^{(BI,n)} + \zeta_s^{(BI,n)}}\right|\right) > 2.$$

The case where $\rho \leq \underline{T_\rho}$ has been omitted. Here, the DV policy is preferred and the SV policy is the least preferred, and the ratio $\frac{v_n}{v}$ is symmetric to (3.36). We also omit the case of $\Lambda_s < \Lambda_d$ since the model setting is symmetric. ∎

Both Proposition 21 and Theorem 22 suggest that a higher matching probability has two effects: it increases effective arrival rates by stimulating more long-run arrivals, leading to higher revenue, and it increases the difference between information policies through a scale effect.

3.5. Conclusions

We examine different user abandonment behaviors associated with different information disclosure policies and evaluate their impact on platform revenue. Our queueing-theoretical results offer an explanation for why platforms prefer specific information policies in practice. Additionally, we demonstrate that the significance of information design becomes more pronounced in the context of multiple platforms. Dissatisfied users may churn in the long run if they perceive low service quality. For example, with over 100 platforms operating in Europe's online freight exchange market (Hänel 2021) information design becomes even more important than in markets with a monopolistic platform provider.

In chapter 4, we investigate the joint effects of pricing policy and information design. The analysis of information policy provides a valuable foundation for such extensions. Note, that prices are often determined exogenously and our results are valuable in their own right. Another avenue to explore considers the heterogeneity of user requests. In our model, we conducted an analysis of a market segment with homogeneous supply and demand to obtain insights into the strategic implications of information design. Moving forward, we could examine platforms with heterogeneous customer demands and supplier capacities.

4. Joint Effect of Pricing and Information Design

Abstract: Online service platforms, such as ride-hailing and freight exchanges, generate net revenues from commissions. Pricing and queue-length information are strategically used to attract users and maximize profit after considering platform costs. Dynamic pricing based on queue length can increase net revenue but might decrease user loyalty, incurring extra costs. Disclosing the queue length impacts customer balking behavior which influences user arrival rates. When displayed, customers balk at entering if they perceive the queue as too long. If concealed, balking is probabilistic, driven by the customers' uncertainty about the waiting time. Using an $M/M/1$ queueing model, we examine different pricing and information disclosure policies to maximize the expected profit of the platform. Optimizing the underlying semi-Markov decision process requires solving a non-convex quadratically constrained quadratic program. Through uniformization, we derive optimality equations and compare optimal prices, profits, and throughput. We identify unique thresholds for pricing and information policies. The preferred pricing policy depends on the extra cost of implementing dynamic pricing versus a static price. If this cost is low, then dynamic pricing is preferred; otherwise, a static pricing policy is preferred. The preferred information policy depends on the user's sensitivity to queue-length information. Our results reveal that pricing and information policies are complementary. Specifically, both dynamic pricing and visible information policies increase expected profit, while static pricing and invisible information policies increase throughput.

4.1. Introduction

Online service platforms function as intermediaries, connecting customers (representing the demand) and suppliers (representing the supply) on digital marketplaces. Their gross

Table 4.1.: Different strategies of pricing policy and service delay information policy utilized by platforms, sourced from their official websites, documentation, and mobile applications, with updates in Sep. 2023.

Strategy	Examples of platforms
$S\&V$	Amazon Prime Now, Fiverr, ...
$S\&I$	Grubhub, Timocom, Wtransnet, Trans EU, ...
$D\&V$	Uber, Lyft, Uber Freight, Full Truck Alliance, Shipt, Uber Eats, ...
$D\&I$	Instacart, Upwork, ...

revenue comes from customer payments, collected for the services rendered. Platforms then compensate suppliers for the services they provide. Notable examples of such platforms span various sectors: (i) ride-sharing platforms, including Uber, Lyft, DiDi, and Grab; (ii) food delivery platforms like DoorDash, Grubhub, and Uber Eats; (iii) freight exchanges such as Timocom, Raaltrans, Full Truck Alliance, and Uber Freight; (iv) freelance service platforms like Upwork, Fiverr, and Freelancer, among others. Typically, these platforms generate net revenue through commissions. Profits are determined by subtracting platform costs from net revenue.

For these platforms, both the *pricing policy* (whether static or dynamic) and the *service delay information disclosure policy* (whether visible or invisible) play critical roles in attracting users. These factors significantly influence the platform's key performance metrics, including net revenue, profit, and throughput (Akşin et al. 2017; Lee et al. 2023; H. Wang and Yang 2019). The combination of the adopted pricing policy and service delay information disclosure policy results in four primary strategies: *static-pricing-and-visible-information* ($S\&V$), *static-pricing-and-invisible-information* ($S\&I$), *dynamic-pricing-and-visible-information* ($D\&V$), and *dynamic-pricing-and-invisible -information* ($D\&I$). These strategies are not fully understood, partly due to the computational complexity of finding optimal solutions for dynamic pricing, as highlighted by J. Kim and Randhawa (2018) and Varma et al. (2023). Obviously, platform profit and throughput are also influenced by factors beyond pricing and information, including user interface or customer service, which makes empirical studies challenging. Mertikopoulos et al. (2020) highlight that a clearing schedule achieving both rapid service speed and an optimal price proves challenging in a two-sided market. Our analytical model analyzes the interplay between pricing and information as key strategic platform decisions.

In practice, service delay information is often conveyed through real-time queue length data (Batt and Terwiesch 2015; Hassin and Roet-Green 2020). Recent research conducted by Zhu et al. (2023) (the main reference for Chapter 3), Guo et al. (2022), and Lingenbrink and Iyer (2019) has delved into disclosure policies regarding queue-length information disclosure within the queueing systems of two-sided marketplaces. Their findings indicate that improving the visibility of information in larger markets leads to increased revenue. These studies concentrated on the implications of information disclosure only, examining markets that implement static pricing. In static pricing, prices remain fixed irrespective of the service queue's length. We study the impact of information policies when dynamic pricing is implemented, a policy that sets state-dependent prices to balance supply and demand. In contrast to Banerjee et al. (2015), we examine a fully dynamic pricing policy, rather than a two-price dynamic pricing policy. In the two-price dynamic pricing policy, prices were set as either high or low from a two-element set based on a queue length threshold. Dynamic pricing also comes at a cost for platform providers. Apart from implementation costs, it has negative consequences for user perception (Bharath 2022). The same holds for excessively long queues (Bimpikis and Mantegazza 2023; R. Zhang et al. 2023). In our model, we consider such costs explicitly. Overall, our analysis investigates the combined effects of pricing and information policies on a given platform. Specifically, we focus on the optimal prices derived to maximize the platform's expected profit under different information policies.

Research questions and methodology We establish an analytical model to examine the effects of both pricing and information policies, giving priority to maximizing the platform's expected profit under a specific information policy. Our model addresses two questions:

1. **Preferred strategy**: What is the preferred strategy to maximize expected profit?
2. **Efficiency**: How do different pricing and information policies impact both profit and throughput?

We use a $M/M/1$ queueing system to capture the dynamics and features of a market. Customers and suppliers dynamically enter the platform. Customers can either join a queue or balk, while suppliers always serve customers. Within a specific market segment, the platform adopts a first-in-first-out (FIFO) principle to match homogeneous customers and suppliers. The price may fluctuate based on the current queue length, depending on the pricing policy implemented. Solving the underlying semi-Markov decision process (SMDP) for each pricing policy under the proposed information policy can be challenging, because it requires solving a nonconvex quadratically constrained quadratic program (NQCQP). We derive the optimality equations for this SMDP by uniformization, as detailed in Bertsekas (2012). This approach transforms the original NQCQP into a system of quadratic equations, as demonstrated by Ata and Shneorson (2006) and Vulcano (2008). Subsequently, we obtain optimal prices within our proposed information policy frameworks and compare the results.

4.1.1. Literature review

Our study focuses on the examination of pricing and service delay information disclosure policies within the context of on-demand service platforms. These platforms typically adopt a queueing model as their fundamental business structure, encompassing a wide range of double-sided queueing models, double-sided queueing systems, queueing networks, and more. Our literature review primarily focuses on the queueing literature related to a specific market segment. This allows us to gain insights into the effects of pricing and information disclosure while establishing connections between our research and relevant papers. Table 4.2 offers a summary of the relevant literature.

Our study considers both static and fully dynamic pricing policies, alongside an exploration of the consequences of displaying or concealing queue-length information. This distinguishes our paper from others in the field. We do not review the broader literature on on-demand service platforms, as it encompasses studies that go beyond the scope of pricing and service delay disclosure policies, which are not directly relevant to our study. See, for example, H. Wang and Yang (2019), for a more extensive review of papers on online ride-hailing platforms.

Static and dynamic pricing policies The literature on optimal static pricing policies for queues is considerably more extensive than that on dynamic pricing policies. Naor (1969) studied optimal static pricing for revenue maximization in queues with visible queue-length information. However, addressing optimal dynamic pricing poses greater challenges. As highlighted by J. Kim and Randhawa (2018), calculating an optimal dynamic pricing solution is intricate and comes with concerns related to model complexity, computational costs, and practical implementation. One approach to designing dynamic

Table 4.2.: Summary of literature review.

Paper	Objective function	Pricing policy				Information policy		Methodology
			Dynamic					
		Static	Two-price	Categorized price	Fully	Visible	Invisible	
Afèche and Ata (2013)	Rev.		✓			✓		Queue game
Ata and Shneorson (2006)	Rev.				✓	✓		MDP, DP
Akşin et al. (2013)							✓	Empirical
Banerjee et al. (2015)	Rev.	✓	✓			✓		Queue game
Batt and Terwiesch (2015)						✓		Empirical
J. C. Castillo (2022)		✓	✓	✓	✓			Empirical
J. Castillo et al. (2022)		✓			✓			Empirical
Çil et al. (2011)	Rev.	✓			✓			MDP
Chen and Frank (2001)	SW				✓	✓		Queue game
Feng et al. (2021)	WT				✓			Stylized model
Guo et al. (2022)	Rev., SW	✓				✓	✓	Queue game
Hassin and Roet-Green (2020)	Utility					✓	✓	Queue game
Haviv and Randhawa (2014)	Rev., SW	✓			✓		✓	Queue game
F. Huang et al. (2019)	Rev.	✓	✓			✓	✓	Queue game
J. Huang et al. (2022)	Profit				✓			Game theory
Ke et al. (2020)	Profit, SW	✓						Equilibrium anal.
J. Kim and Randhawa (2018)	Rev.	✓	✓		✓	✓		DP
Lin et al. (2023)	Rev., SW				✓	✓		Queue game
Lingenbrink and Iyer (2019)	Utility	✓				✓	✓	Queue game
Lu et al. (2013)						✓		Empirical
Maglaras (2006)	Rev.			✓				Fluid model
Mendelson and Whang (1990)	Rev.			✓				Queue game
Naor (1969)	Rev.	✓					✓	Queue game
Paschalidis and Tsitsiklis (2000)	Rev., SW			✓				DP
Veeraraghavan and Debo (2009)	Utility						✓	Queue game
Zhu et al. (2023)	Rev.	✓				✓	✓	Markov chain
Our paper	Profit	✓			✓	✓	✓	MDP

Note. Rev., revenue; SW, social welfare; WT, waiting time; MDP, Markov decision process; DP, dynamic programming.

pricing policies involves classifying user into different classes, with each assigned a corresponding price (Mendelson and Whang 1990; Paschalidis and Tsitsiklis 2000). Within this framework, studies like Maglaras (2006) and Çil et al. (2011) have investigated sequential rules for large-scale queueing systems.

Dynamic pricing incorporating both price and service delay sensitivities was explored in studies such as those by Chen and Frank (2001) and Ata and Shneorson (2006). These studies considered the impact of visible queue-length information on customers' balking behavior and formulated optimality equations for pricing. In particular, Chen and Frank (2001) analyzed revenue maximization, while Ata and Shneorson (2006) analyzed social welfare maximization. Haviv and Randhawa (2014) and Lin et al. (2023) studied a fully dynamic pricing policy in a queue while concealing queue-length information. Haviv and Randhawa (2014) compared static and dynamic pricing policies and discovered that when customers' waiting costs are high, a static pricing policy is not only nearly optimal for revenue maximization but also highly effective in maximizing social welfare. On the other hand, Lin et al. (2023) found that a high waiting cost for a long queue results in a non-monotonic optimal dynamic pricing function that depends on the queue length. Afèche and Ata (2013) examined a queue that accommodates both patient and impatient customers. While these customers had access to queue-length information, the suppliers were unaware of the proportions of each customer type. They developed an optimal Bayesian pricing policy as a function of queue length, involving a two-price policy. Banerjee et al. (2015) examined a two-price policy implemented in a queueing system with visible queue-length information for revenue maximization. They found that this pricing policy is asymptotically optimal for sufficiently large markets. J. Kim and Randhawa (2018) observed that the variability of queue lengths resulting from a pricing policy negatively affects revenue maximization, with dynamic pricing leading to lower variability compared to static pricing. The reduction of this variability by a two-price policy explained why it achieves nearly maximal revenue in large-scale queueing systems. F. Huang et al. (2019) examined a two-price cyclic policy in a queue that accommodated both well-informed service-quality customers and naive customers. They found that a simple two-price policy did not achieve near-optimality in their model.

In this literature, dynamic pricing offers both advantages and disadvantages compared to static pricing. On the positive side, dynamic pricing increases the revenue and profit of platforms. It regulates market supply and demand through price adjustments, as evidenced by the widespread adoption of dynamic pricing policies, also known as surging price, within online ride-hailing platforms (Phillips 2021). For instance, J. C. Castillo (2022) analyzed data from Uber in Houston and revealed a 3.53% increase in gross revenue as a result of implementing dynamic pricing. In ride-hailing platforms, drivers often engage in a “wild goose chase” (WGC) phenomenon, constantly relocating to different regions in the city in pursuit of higher-priced orders during periods of sudden demand surges. This phenomenon can ultimately lead to a decrease in the overall efficiency of the platform. Both Ke et al. (2020) and J. Castillo et al. (2022) highlighted that dynamic pricing can effectively mitigate this WGC phenomenon. However, dynamic pricing can also be controversial concerning user experience. For example, discriminatory pricing based on the time and location of accessing the service system can lead to decreased user loyalty and potentially tarnish the platform’s reputation, as discussed by Caillaud and De Nijs (2014), Z. Wang (2016), and J. Huang et al. (2022). And Feng et al. (2021) found that the implementation of a dynamic pricing policy in online ride-hailing platforms could result in increased average waiting times for passengers compared to traditional street-hailing systems, with the outcome dependent on market parameters. Based on data from Uber in Houston, J. C. Castillo (2022) observed that the advantages of implementing a dynamic pricing policy primarily benefit customers, engendering fairness concerns among suppliers.

Our paper examines a fully dynamic pricing policy, building upon the optimality equations presented in Chen and Frank (2001) and Ata and Shneorson (2006). Optimal pricing are determined under different queue-length information disclosure policies. To compare static and dynamic pricing, we incorporate an extra cost associated with implementing dynamic pricing when calculating the platform’s profit based on net revenue. While several papers have explored static and dynamic pricing, primarily concentrating on revenue maximization and identifying conditions under which static pricing is near-optimal, our paper extends these findings by taking fully dynamic pricing and information policy into account.

Queue-length information disclosure policy Both empirical studies have demonstrated the significant impact of queue-length information display on user behavior. For instance, Lu et al. (2013) and Batt and Terwiesch (2015) analyzed balking behavior using data from a hospital emergency department and a retail store. In these settings, people queued while also having the ability to observe queue length. These studies revealed that when users can see queue-length information, they tend to balk at joining the queue if the estimated wait time exceeds their expectations. Naor (1969) and Banerjee et al. (2015) examined this in an $M/M/1$ queueing model, where balking decisions were based on a self-determined admission level. Zhu et al. (2023) (the main reference for Chapter 3) considered that users observe the queue length, and if it appears too long, they balk, resulting in a truncated queue. Their study investigated the endogeneity of this truncation size on queue length concerning the queue's service rate. These studies argue that for homogeneous users within a market segment, the queue does not increase beyond a certain threshold due to the truncated balking behavior exhibited by users. As a result, revenue is influenced by the level of user patience.

Concealing queue-length information has been shown to result in lower arrival rates since some customers may balk at joining the queue due to the uncertainty about waiting times. However, this concealment may lead to longer queues, as observed by Veeraraghavan and Debo (2009). Hassin and Roet-Green (2020) studied customer behavior regarding queue joining using a parking model as an illustrative example. Their findings indicate that concealing queue-length information leads to higher throughput when the system congestion is low. Customers waiting in the queue without knowing the service rate and delays can incur costs on the platform. These costs include managing long queues (Kostami and Ward 2009), the loss of impatient customers through reneging (Akşin et al. 2013), and reduced customer loyalty (Allon et al. 2011). These factors can ultimately drive customers to choose competing platforms.

Our study focuses on understanding the joint effect of pricing and information disclosure policies. We primarily consider different user behaviors influenced by the certainty of waiting times, driven by the visibility of queue-length information. We do not examine the many different user behaviors resulting from the display of queue-length information. For a more extensive review of papers on this topic, we refer the reader to literature such as Hassin and Roet-Green (2020) and Zhu et al. (2023) (the main reference for Chapter 3). In essence, we are comparing the consequences of truncated balking behavior when queue length is visible with the effects of reduced arrival rates resulting from invisible queue length.

4.1.2. Results and contributions

Dynamic pricing increases platform profit, but it decreases efficiency. Key results are summarized in Table 4.3. We analyze different strategies of pricing and information policies, aiming to maximize the platform's expected profit. Our results reveal the

Table 4.3.: Influence of different strategies on platform performance.

	Performance of different platform strategies	Reference
Profit	$D\&V > D\&I$	Result 26
Throughput	For a low commission rate, $D\&V < D\&I$ For a high commission rate, $D\&V > D\&I$	Result 27

complementary and substitute ways in which pricing and information policies interact: Dynamic pricing and visible information policies increase expected profit, while static pricing and invisible information policies increase throughput. Dynamic pricing achieves higher profits by increasing the average transaction price and, consequently, commissions. Under the visible queue-length information policy, the queue truncates as customers balk at joining, perceiving it as too long. At this truncation point, although no additional customers join, the platform still attracts suppliers to provide services and clear the queue, causing the corresponding net revenue function to be negative. Therefore, for dynamic pricing, the price is set low at this truncation point, decreasing supplier payouts to increase profits. Consequently, this increases the likelihood of the queue being at the truncation point, resulting in the dynamic-pricing-and-visible-information ($D\&V$) strategy attracting fewer customers and suppliers, i.e., lower throughput. By concealing queue-length information, customers do not balk based on queue length but probabilistically based on the uncertainty in the waiting time. This nullifies the queue truncation, resulting in an increase in throughput. However, an invisible information policy also leads to lower arrival rates for both customers and suppliers, ultimately resulting in a decrease in expected profit. Furthermore, we find that when the commission rate is high, concealing queue-length information does not effectively increase throughput. This is due to the decreased influence of truncated balking behavior on throughput under a visible information policy. In such cases, the negative effect of concealing queue-length information on both arrival rates and throughput becomes more pronounced.

We identify unique thresholds that determine the preferred pricing and information policies. Dynamic pricing generates higher net revenue than static pricing, but it may result in user dissatisfaction and extra costs for the platform during profit calculation. Our preferred pricing policy takes into account the extra cost of implementing dynamic pricing compared to static pricing. When this cost is low, dynamic pricing is preferred; otherwise, static pricing is preferred. Regarding the information policy, we use an indifference curve to identify the preferred one based on customer patience. If customers are insensitive to queue-length information, leading to similar expected profits regardless of the information policy, the platform is indifferent to its choice. However, if customers are sensitive to this information, the indifference curve partitions markets into four different regions based on customer patience parameters, indicating the preferred information policy for each setting regarding platform profit. Within each region, a specific strategy is preferred.

4.2. Model formulations and optimality equations

4.2.1. Model and notation

We use an $M/M/1$ queuing system to model a segmented market, where homogeneous customers on the demand side either join or balk a queue, while homogeneous suppliers on the supply side, serve. A "first-in-first-out" principle is applied to match customers with suppliers. Customers and suppliers independently arrive at the queue and server sides, respectively, following Poisson processes with rates λ_d and λ_s, where the *service rate* is defined as λ_s. Both arrival rates, λ_d and λ_s, are determined by the linear price response functions:

$$\lambda_d := \alpha - \beta_d p \quad \text{and} \quad \lambda_s := \beta_s((1-\epsilon)p - \nu). \tag{4.1}$$

The parameters α, β_d, β_s and ν represent the *market potential*, the *price sensitivity* for customers and suppliers, and the *minimum wage* for suppliers. The arrival rates of customers and suppliers are lower than the market potential, indicating that $p \in \mathbb{P} := \left(0, \min\left\{\frac{\alpha}{\beta_d}, \frac{\alpha}{\beta_s(1-\epsilon)} + \frac{\nu}{1-\epsilon}\right\}\right)$. We denote the *price sensitivity ratio* of customers to suppliers as $\beta := \beta_d/\beta_s$. The minimum wage sets a price floor for supplier compensation since suppliers are unwilling to offer services for a payout below ν. For the platform, the *commission* is ϵp, where ϵ represents the commission rate. The platform's *net revenue* (NR) is obtained by subtracting the *supplier payout* (SP) of $(1-\epsilon)p$ from the *gross revenue* (GR), which is collected from customer payments at price p. For customers waiting in the queue, the service time is an independent and identically distributed exponential random variable with a mean of $1/\lambda_s$.

The platform implements a *dynamic pricing policy* when the price is state-dependent, adjusting according to the current queue length in the system. In contrast, a *static* pricing policy is implemented if the price remains constant, regardless of the queue length. Despite its potential for increased net revenue, a dynamic pricing policy may raise concerns about user satisfaction, particularly in terms of price discrimination within specific market segments. The fluctuation in prices for identical services, depending on the system's state, may lead to user dissatisfaction and extra implementation costs for dynamic pricing. This is observed from empirical studies and reports (see e.g., Fisher et al. 2018, Gibbs et al. 2018 and Bharath 2022), as well as insights modeled in analytical papers (see, e.g., Zhao and Zhang 2019). To account for this, we introduce an *extra cost*, denoted as C_d, associated with implementing a dynamic pricing policy in comparison to a static one. We convert this extra cost to a fixed relative value in the subsequent derivation, specifically as a percentage of net revenue relative to a static pricing policy. This approach helps establish the threshold for determining the preferred pricing policy in the following analysis. In the following, we use $\chi \in \{stat, dyn\}$ to represent the corresponding pricing policy.

The platform's *information policy* determines whether the queue-length information is disclosed to customers. We consider two types of information policies: *visible* and *invisible*. Under a visible information policy, customers balk at joining the queue if the queue length reaches a *truncation size* of k. This queueing model is an observable $M/M/1/K$ queue, called *vi* model. Under an invisible information policy, customers hesitate and may balk at joining the queue based on a probability denoted as the *balking probability* δ, leading to a reduced demand arrival rate of $(1-\delta)\lambda_d$. This queuing model is an unobservable $M/M/1$ queuing model with a reduced arrival rate, called *in* model. A fundamental difference in customer behavior lies in truncated balking in the former and progressive balking in the latter, influenced by the customer's ability to estimate the expected waiting time. The parameters k and δ represent *customer patience*; thus, a larger k or a smaller δ implies that customers exhibit greater patience. In the following, we use $\ell \in \{in, vi\}$ to represent the information policy.

However, a long queue is never in the interests of the platform. A long waiting time experience can lead to customer disloyalty, prompting users to seek alternative platforms for their future service needs (see, e.g., Bimpikis and Mantegazza 2023 and Zhang et. al. 2023). Our models take into account that the platform incurs a *customer attrition cost* for a lengthy queue. When the queue exceeds the length of k, the customer attrition cost

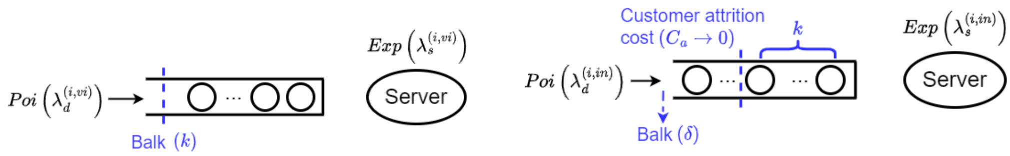

(a) (b)

Figure 4.1.: The flow diagram of the queueing models. Left: *vi* model. Right: *in* model.

is incurred at a rate of C_a per waiting customer. For example, if a customer is waiting in a queue at a position $i > k$, then the customer attrition cost is $(i - k)C_a$. We assume the effect of customer attrition cost on the platform's profit is negligible, implying that $C_a \to 0$. However, the presence of this customer attrition cost prevents the queue length from becoming infinitely long.

Figure 4.1 illustrates a flow diagram of both queuing models. The arrival rates $\lambda_d^{(i,\ell)}$ and $\lambda_s^{(i,\ell)}$ depend on the price $p_{(i,\ell)}$ at queue length i under a dynamic pricing policy. The *system load* is defined as $\rho_{(i,vi)} := \lambda_d^{(i-1,vi)} \big/ \lambda_s^{(i,vi)}$ and $\rho_{(i,in)} := (1-\delta)\lambda_d^{(i-1,in)} \big/ \lambda_s^{(i,in)}$. For a static pricing policy, we simplify the symbols of the arrival rates to λ_d^ℓ and λ_s^ℓ, which depend on the state-independent price p_ℓ. The corresponding system load is simplified as

$$\rho_{vi} := \lambda_d^{vi} \big/ \lambda_s^{vi} \quad \text{and} \quad \rho_{in} := (1-\delta)\lambda_d^{in} \big/ \lambda_s^{in}.$$

The platform selects a *strategy* that combines both pricing and information policies, consisting of four options: static-pricing-and-visible-information ($S\&V$), static-pricing-and-invisible-information ($S\&I$), dynamic-pricing-and-visible-information ($D\&V$), and dynamic-pricing-and-invisible-information ($D\&I$). The platform maximizes its expected *profit* across the four strategies, which is defined as the net revenue minus the extra cost associated with implementing a dynamic pricing policy if applied, given by

$$Pro_\ell^\chi := \begin{cases} NR_\ell^{stat} & \chi = stat \\ (1 - C_d)NR_\ell^{dyn} & \chi = dyn. \end{cases} \tag{4.2}$$

for each $\ell \in \{vi, in\}$. This implies that for a constant C_d, the optimal price under a specific pricing policy for maximizing profit is the same as that for maximizing net revenue.

4.2.2. Semi-Markov decision process

The optimal prices under different information policies can be determined by solving the corresponding semi-Markov decision processes. The state space of the vi model includes all non-negative integers up to the truncation size k, denoted as $S_{vi} = \{0, 1, \ldots, k\}$. The state space of the in model is represented by the set of all non-negative integers, as there is no truncation imposed. It is denoted as $S_{in} = \mathbb{N}_0$. The transition rates for the vi and in models are:

$$r_{ij}^{vi} = \begin{cases} \lambda_d^{(i,vi)} & \text{if } \; j = i+1 \\ \lambda_s^{(i,vi)} & \text{if } \; j = i-1 \\ 0 & \textit{otherwise} \end{cases} \quad \text{and} \quad r_{ij}^{in} = \begin{cases} (1-\delta)\lambda_d^{(i,in)} & \text{if } \; j = i+1 \\ \lambda_s^{(i,in)} & \text{if } \; j = i-1 \\ 0 & \textit{otherwise.} \end{cases}$$

The action space for the price is $p_{(i,\ell)} \in \mathbb{P}$ for every $i \in S_\ell$.

The gross revenue rate function, denoted as $GR_\ell(\cdot)$, is defined as the product of the payment collected from customers and their arrival rate at queue length i:

$$GR_{vi}(p_{(i,vi)}) := \begin{cases} \lambda_d^{(i,vi)} p_{(i,vi)} & \text{if } \; i < k \\ 0 & \text{if } \; i = k \end{cases}$$

and

$$GR_{in}(p_{(i,in)}) := (1-\delta)\lambda_d^{(i,in)} p_{(i,in)}.$$

The supplier payout rate function, denoted as $SP_\ell(\cdot)$, is defined as the product of the payout paid to suppliers and their arrival rate at queue length i:

$$SP_{vi}(p_{(i,vi)}) := \begin{cases} 0 & \text{if } \; i = 0 \\ (1-\epsilon) p_{(i,vi)} \lambda_s^{(i,vi)} & \text{if } \; 1 \le i \le k \end{cases} \tag{4.3}$$

and

$$SP_{in}(p_{(i,in)}) := \begin{cases} 0 & \text{if } \ i = 0 \\ (1-\epsilon)p_{(i,in)}\lambda_s^{(i,in)} & \text{if } \ 1 \leq i \leq k \\ (1-\epsilon)p_{(i,in)}\lambda_s^{(i,in)} + (i-k)C_a & \text{if } \ k < i. \end{cases} \tag{4.4}$$

On the server side, the platform provides payouts to suppliers when the queue is not empty. The expected net revenue function is calculated by subtracting the total supplier payout from the expected gross revenue for each queue length i. This is denoted by:

$$NR_\ell := \sum_{i \in S_\ell - \{k\}} \pi_i^\ell GR_\ell(p_{(i,\ell)}) - \sum_{i \in S_\ell - \{0\}} \pi_i^\ell SP_\ell(p_{(i,\ell)}) \tag{4.5}$$

for each $\ell \in \{vi, in\}$, where π_i^ℓ denotes the steady-state probability of queue length i under an information policy ℓ. The optimal expected net revenue is denoted by $NR_\ell^{\chi *} := \max_{p_{(i,\ell)}, \forall i \in S_\ell} \{NR_\ell^\chi\}$ for each pricing policy $\chi \in \{stat, dyn\}$ and information policy $\ell \in \{in, vi\}$. The expected profit function, as defined in (4.2), depends on the expected net revenue function for a constant C_d. The corresponding optimal expected profit is denoted by $Pro_\ell^{\chi *} := \max_{p_{(i,\ell)}, \forall i \in S_\ell} \{Pro_\ell^\chi\}$.

4.2.3. Optimal static pricing

For implementing a static pricing policy, we can simplify (4.5) to:

$$NR_{vi}^{stat} = (1-\pi_k^{vi})\lambda_d^{vi} p_{vi} - (1-\pi_0^{vi})(1-\epsilon)p_{vi}\lambda_s^{vi} \tag{4.6}$$

$$NR_{in}^{stat} = (1-\delta)\lambda_d^{in} p_{in} - (1-\pi_0^{in})(1-\epsilon)p_{in}\lambda_s^{in} - \sum_{i=k+1}^{\infty}(i-k)C_a\pi_i^{in}. \tag{4.7}$$

Under a visible information policy, the expected net revenue function NR_{vi}^{stat} is calculated as the sum of the expected customer payments collected at each queue length, excluding the truncation, since no additional customers are attracted to join. This sum is then subtracted by the total expected payout to suppliers across each queue length. Under an invisible information policy, the expected net revenue function NR_{in}^{stat} is calculated as the sum of the expected customer payments collected across each queue length with a lower arrival rate, minus the total expected payout to suppliers across each queue length, and further minus the total expected customer attrition cost across each queue length over the truncation size defined in the vi model. The optimal price is denoted as $p_\ell^* := \underset{p_\ell}{\operatorname{argmax}} NR_\ell^{stat}$, and the corresponding optimal system load are $\rho_{vi}^* := \frac{\alpha-\beta_d p_{vi}^*}{\beta_s\left((1-\epsilon)p_{vi}^*-\nu\right)}$ and $\rho_{in}^* := \frac{(1-\delta)\left(\alpha-\beta_d p_{in}^*\right)}{\beta_s\left((1-\epsilon)p_{in}^*-\nu\right)}$.

Proposition 23. *The optimal system load under an invisible information policy ρ_{in}^* is lower than 1, implying that $p_{in}^* \geq \frac{\alpha+\beta_s\nu}{\beta_d+\beta_s(1-\epsilon)}$. The expected net revenue functions* (4.6) *and* (4.7) *are quasi-concave with respect to the price $p_{vi} \in \left(0, \frac{\alpha}{\beta_d}\right)$ and $p_{in} \in \left(\frac{\alpha+\beta_s\nu}{\beta_d+\beta_s(1-\epsilon)}, \frac{\alpha}{\beta_d}\right)$.*

Proof. For an invisible information policy, a system load exceeding 1 could trigger an infinite increase in the queue length, leading to near-infinite customer attrition cost. Therefore, the optimal system load in this case is lower than 1.

Next, we demonstrate the quasi-concavity of (4.6) and (4.7) by reformulating them into equations that solely depend on the system load variable. Through analyzing the first-order and second-order derivatives of these reformulated equations, we establish that the net revenue functions exhibit quasi-concavity in the system load. Consequently, this implies quasi-concavity in price.

The vi model. We reformulate (4.6) into the equation depending on the system load:

$$NR_{vi}^{stat} = \nu\epsilon\left(\frac{\alpha}{1-\epsilon} - \frac{\beta_d\nu}{(1-\epsilon)^2}\right) \cdot \frac{\frac{\alpha}{\beta_s\nu} + \rho_{vi}}{\left(\frac{\beta_d}{\beta_s(1-\epsilon)} + \rho_{vi}\right)^2}\left(1 - \frac{\rho_{vi}-1}{{\rho_{vi}}^{k+1}-1}\right), \tag{4.8}$$

which can further be reformulated as

$$(4.8) = \nu\epsilon\left(\frac{\alpha}{1-\epsilon} - \frac{\beta_d\nu}{(1-\epsilon)^2}\right) \cdot \frac{\frac{\alpha}{\beta_s\nu} + \rho_{vi}}{\left(\frac{\beta_d}{\beta_s(1-\epsilon)} + \rho_{vi}\right)^2}\left(1 - \frac{1}{\sum\limits_{i=0}^{k} {\rho_{vi}}^i}\right). \tag{4.9}$$

The first-order derivative of Pro_{vi}^{stat} is

$$\frac{d(4.9)}{d\rho_{vi}} = \frac{\nu\epsilon\left(\frac{\alpha}{1-\epsilon} - \frac{\beta_d\nu}{(1-\epsilon)^2}\right)}{\left(\frac{\beta_d}{\beta_s(1-\epsilon)} + \rho_{vi}\right)^3} \cdot \left(\frac{\left(\frac{\alpha}{\beta_s\nu} + \rho_{vi}\right)\left(\frac{\beta_d}{\beta_s(1-\epsilon)} + \rho_{vi}\right)\sum\limits_{i=1}^{k} i{\rho_{vi}}^{i-1}}{\left(\sum\limits_{i=0}^{k} {\rho_{vi}}^i\right)^2}\right.$$

$$-\left(\frac{2\alpha}{\beta_s\nu}-\frac{\beta_d}{\beta_s(1-\epsilon)}+\rho_{vi}\right)\left(1-\frac{1}{\sum\limits_{i=0}^{k}{\rho_{vi}}^{i}}\right)\Bigg)=\frac{\nu\epsilon\left(\frac{\alpha}{1-\epsilon}-\frac{\beta_d\nu}{(1-\epsilon)^2}\right)}{\left(\frac{\beta_d}{\beta_s(1-\epsilon)}+\rho_{vi}\right)^3}\cdot(h_1-h_2) \tag{4.10}$$

where $h_1 := \frac{\left(\frac{\alpha}{\beta_s\nu}+\rho_{vi}\right)\left(\frac{\beta_d}{\beta_s(1-\epsilon)}+\rho_{vi}\right)\sum_{i=1}^{k} i{\rho_{vi}}^{i-1}}{\left(\sum_{i=0}^{k}{\rho_{vi}}^{i}\right)^2}$ and $h_2 := \left(\frac{2\alpha}{\beta_s\nu}-\frac{\beta_d}{\beta_s(1-\epsilon)}+\rho_{vi}\right)\left(1-\frac{1}{\sum_{i=0}^{k}{\rho_{vi}}^{i}}\right)$.
For h_2, it holds that

$$\frac{dh_2}{d\rho_{vi}}=1+\frac{\left(\frac{2\alpha}{\beta_s\nu}-\frac{\beta_d}{\beta_s(1-\epsilon)}+\rho_{vi}\right)\sum\limits_{i=1}^{k} i{\rho_{vi}}^{i-1}-\sum\limits_{i=0}^{k}{\rho_{vi}}^{i}}{\left(\sum\limits_{i=0}^{k}{\rho_{vi}}^{i}\right)^2}\geq 1. \tag{4.11}$$

For h_1, it is increasing and then decreasing with ρ_{vi} and $h_1>0$. Since $\frac{dh_1}{d\rho_{vi}}\overset{\rho_{vi}=0}{>}0$, $\frac{d^2h_2}{d{\rho_{vi}}^2}<0$ and (4.11), these indicate that $\frac{d(h_1-h_2)}{d\rho_{vi}}$ follows one of: i) it is increasing the decreasing with ρ_{vi}; ii) it is decreasing with ρ_{vi}. Since $h_1-h_2\overset{\rho_{vi}=0}{>}0$ and $\lim\limits_{\rho_{vi}\to\infty}(h_1-h_2)<0$, these indicates that h_1-h_2 is positive for ρ_{vi} is small and it decreases to a negative term with ρ_{vi}. This indicates that (4.9) is increasing and then decreasing with ρ_{vi}.

The *in* model. We reformulate (4.7) into the equation depending on the system load:

$$\begin{aligned}NR_{in}^{stat}=&\nu\epsilon\left(\frac{(1-\delta)\alpha}{1-\epsilon}-\frac{(1-\delta)\beta_d\nu}{(1-\epsilon)^2}\right)\cdot\frac{\frac{(1-\delta)\alpha}{\beta_s\nu}+\rho_{in}}{\left(\frac{(1-\delta)\beta_d}{\beta_s(1-\epsilon)}+\rho_{in}\right)^2}\cdot\rho_{in}\\&-\frac{{\rho_{in}}^{k+1}(-k\rho_{in}+k+1)}{1-\rho_{in}}\cdot C_a.\end{aligned} \tag{4.12}$$

The first-order derivative of Pro_{in}^{stat} is

$$\begin{aligned}\frac{d(4.12)}{d\rho_{in}}=&\frac{\nu\epsilon\left(\frac{(1-\delta)\alpha}{1-\epsilon}-\frac{(1-\delta)\beta_d\nu}{(1-\epsilon)^2}\right)}{\left(\frac{(1-\delta)\beta_d}{\beta_s(1-\epsilon)}+\rho_{in}\right)^3}\cdot\left(\frac{(1-\delta)\alpha}{\beta_s\nu}\left(\frac{(1-\delta)\beta_d}{\beta_s(1-\epsilon)}-\rho_{in}\right)+\frac{2(1-\delta)\beta_d\rho_{in}}{\beta_s(1-\epsilon)}\right)\\&-C_a\cdot\frac{{\rho_{in}}^k\left(k^2(\rho_{in}-1)^2+k({\rho_{in}}^2-3\rho_{in}+2)+1\right)}{(\rho_{in}-1)^2}.\end{aligned} \tag{4.13}$$

When $\rho_{in} = 0$, it holds that

$$(4.13) \overset{\rho_{in}=0}{=} \frac{\nu\epsilon\left(\frac{(1-\delta)\alpha}{1-\epsilon} - \frac{(1-\delta)\beta_d\nu}{(1-\epsilon)^2}\right)}{\left(\frac{(1-\delta)\beta_d}{\beta_s(1-\epsilon)}\right)^3} \left(\frac{(1-\delta)\alpha}{\beta_s\nu}\frac{(1-\delta)\beta_d}{\beta_s(1-\epsilon)}\right) > 0. \tag{4.14}$$

When $\rho_{in} \to 1$, it holds that

$$\lim_{\rho_{in}\to 1}(4.13) = \frac{\nu\epsilon\left(\frac{(1-\delta)\alpha}{1-\epsilon} - \frac{(1-\delta)\beta_d\nu}{(1-\epsilon)^2}\right)}{\left(\frac{(1-\delta)\beta_d}{\beta_s(1-\epsilon)}+1\right)^3} \cdot \left(\frac{(1-\delta)\alpha}{\beta_s\nu}\left(\frac{(1-\delta)\beta_d}{\beta_s(1-\epsilon)}-1\right) + \frac{2(1-\delta)\beta_d}{\beta_s(1-\epsilon)}\right) - \infty < 0. \tag{4.15}$$

The second-order derivative of (4.12) is

$$\frac{d^2(4.12)}{d{\rho_{in}}^2} = \frac{2\nu\epsilon\left(\frac{(1-\delta)\alpha}{1-\epsilon} - \frac{(1-\delta)\beta_d\nu}{(1-\epsilon)^2}\right)}{\left(\frac{(1-\delta)\beta_d}{\beta_s(1-\epsilon)}+\rho_{in}\right)^4} \cdot \left(\frac{(1-\delta)\alpha}{\beta_s\nu}\left(\rho_{in} - \frac{2(1-\delta)\beta_d}{\beta_s(1-\epsilon)}\right) + \left(\frac{(1-\delta)\beta_d}{\beta_s(1-\epsilon)}\right)\left(\frac{(1-\delta)\beta_d}{\beta_s(1-\epsilon)} - 2\rho_{in}\right)\right) + C_a \cdot \frac{(k(\rho_{in}-1)-1)\,{\rho_{in}}^{k-1}\left(k^2(\rho_{in}-1)^2 + k(\rho_{in}-1)^2 + 2\rho_{in}\right)}{(\rho_{in}-1)^3}. \tag{4.16}$$

Since $C_a \cdot \frac{(k(\rho_{in}-1)-1){\rho_{in}}^{k-1}\left(k^2(\rho_{in}-1)^2+k(\rho_{in}-1)^2+2\rho_{in}\right)}{(\rho_{in}-1)^3}$ is decreasing with $\rho_{in} \in (0,1)$, these indicate that

$$(4.16) < \frac{2\nu\epsilon\left(\frac{(1-\delta)\alpha}{1-\epsilon} - \frac{(1-\delta)\beta_d\nu}{(1-\epsilon)^2}\right)}{\left(\frac{(1-\delta)\beta_d}{\beta_s(1-\epsilon)}\right)^4} \cdot \left(\frac{(1-\delta)\alpha}{\beta_s\nu} + \left(\frac{(1-\delta)\beta_d}{\beta_s(1-\epsilon)}\right)^2 - \frac{2(1-\delta)\beta_d}{\beta_s(1-\epsilon)} - \frac{2(1-\delta)^2\alpha\beta_d}{{\beta_s}^2(1-\epsilon)\nu}\right) < 0. \tag{4.17}$$

Hence, (4.14), (4.15) and (4.17) indicate that (4.12) is increasing then decreasing with ρ_{in}. ■

Under an invisible information policy, if the system load ρ_{in} exceeds 1, it results in an infinitely long queue and a high customer attrition cost, which is not an optimal solution. Since Proposition 23 states that the revenue functions for both visible and invisible information policies are quasi-concave in price, this indicates the existence of a unique optimal price that maximizes the expected profit. Economically, this implies the existence of an optimal equilibrium among gross revenue, supplier payout, and platform profit, leading to a peak point in net revenue generation for the platform.

4.2.4. Optimal dynamic pricing

By applying uniformization to the underlying SMDP, we transform it into a discrete-time MDP. This transformation allows us to utilize Bellman's equation to derive the optimality equations (Bertsekas 2012) (pp. 288). We outline the steps to uniformize SMDPs for both visible and invisible information policies, and the corresponding optimal price solutions in the following.

Uniformization for visible information policy

Step 1: Uniformize Markov chain of SMDP for vi model For each transition associated with a specific state of the SMDP, we divide their transition probabilities within the same range by a specific value, converting the SMDP into a discrete-time MDP. For the states 0 and k, we can uniformize the Markov chain by dividing transition probabilities by a factor of α. For other states $0 < i < k$, we can uniformize the Markov chain by dividing transition probabilities by a factor of 2α. The transition probabilities of the Markov chain and the corresponding uniformized version are depicted in Figure 4.2. In the uniformized version of the corresponding Markov chain, the transition probability from each state to another state lies within the same range $(0, 1)$. Hence, it can be viewed as a discrete-time MDP as the sojourn time of each state being uniformized.

Step 2: Derive optimality equations

Let v_i denote the relative value function corresponding to a queue length of i. We apply Bellman's equation to derive the corresponding optimality equations:

$$v_0 = \max_{p_{(0,vi)}} \left\{ \frac{GR_{vi}\left(p_{(0,vi)}\right) - \gamma}{\alpha} + \frac{\lambda_d^{(0,vi)}}{\alpha} v_1 + \frac{\alpha - \lambda_d^{(0,vi)}}{\alpha} v_0 \right\} \tag{4.18}$$

$$\underset{i=1,..,k-1}{v_i} = \max_{p_{(i,vi)}} \left\{ \frac{GR_{vi}(p_{(i,vi)}) - SP_{vi}(p_{(i,vi)}) - \gamma}{2\alpha} + \frac{\lambda_d^{(i,vi)}}{2\alpha} v_{i+1} \right.$$

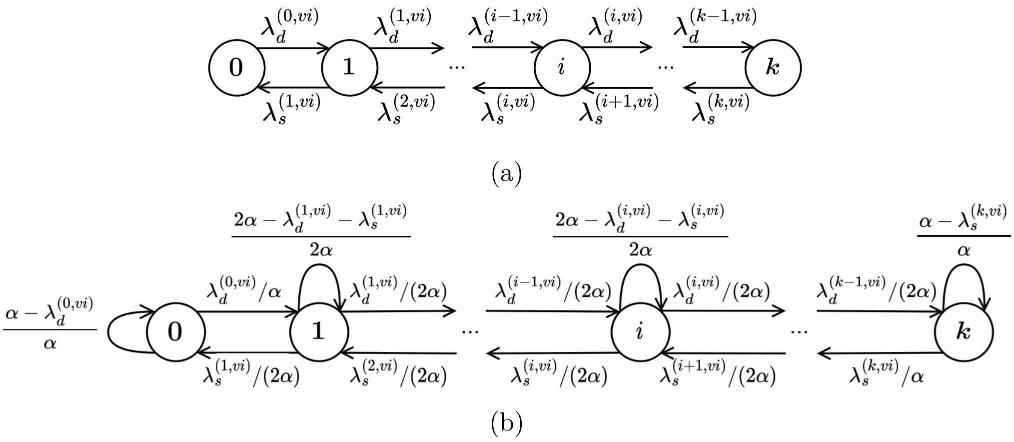

Figure 4.2.: Markov chain and its uniformized version of vi model. Left: Markov chain of SMDP. Right: Uniformized version of a discrete-time MDP.

$$+\frac{\lambda_s^{(i,vi)}}{2\alpha}v_{i-1}+\frac{2\alpha-\lambda_d^{(i,vi)}-\lambda_s^{(i,vi)}}{2\alpha}v_i\Bigg\} \tag{4.19}$$

$$v_k=\max_{p_{(k,vi)}}\left\{\frac{-SP_{vi}(p_{(k,vi)})-\gamma}{\alpha}+\frac{\lambda_s^{(k,vi)}}{\alpha}v_{k-1}+\frac{\alpha-\lambda_s^{(k,vi)}}{\alpha}v_k\right\} \tag{4.20}$$

Here, γ is a guess at the maximum average value. This implies that there are unique values for γ and v_i for $i \in S_{vi}$ that satisfy equations (4.18)-(4.20), which is proven by Ata and Shneorson (2006). These unique values correspond to the optimal prices for maximizing the expected net revenue.

Step 3: Determine optimal prices

By maximizing the right-hand side (RHS) of equations (4.18)-(4.20) and introducing an intermediate variable $y_i := v_{i-1} - v_i$ for each $i = 1, 2, .., k$, we can reformulate these equations as follows:

$$\gamma=\frac{(\alpha+\beta_d y_1)^2}{4\beta_d}-\alpha y_1 \tag{4.21}$$

$$\gamma=\frac{(\alpha+\beta_s(1-\epsilon)(\nu+y_i)+\beta_d y_{i+1})^2}{4\left(\beta_d+\beta_s(1-\epsilon)^2\right)}-\alpha y_{i+1}-\beta_s\nu y_i \quad \text{for each} \quad i=1,..,k-1 \tag{4.22}$$

$$\gamma=\frac{\beta_s\left(\nu+y_k\right)^2}{4}-\beta_s\nu y_k. \tag{4.23}$$

The corresponding values of optimal prices are

$$p^*_{(i,vi)} = \begin{cases} \dfrac{\alpha + \beta_d y_1}{2\beta_d} & \text{if } \ i = 0 \\ \dfrac{\alpha + \beta_s(1-\epsilon)(\nu + y_i) + \beta_d y_{i+1}}{2\left(\beta_d + \beta_s(1-\epsilon)^2\right)} & \text{if } \ 0 < i < k \\ \dfrac{\nu + y_k}{2(1-\epsilon)} & \text{if } \ i = k. \end{cases} \tag{4.24}$$

Here, (4.21)-(4.23) constitute a system of multivariate quadratic equations, and a unique solution exists for γ, y_1, y_2, ..., y_k. After solving the equation system (4.21)-(4.23) to obtain the value of y_i for each $i = 1, 2, .., k$, we integrate these y_i values into (4.24) to get optimal prices.

Uniformization for Invisible Information Policy

We follow the same steps outlined in the visible information policy case above to transform the SMDP model into a Discrete-Time MDP.

Step 1: Uniformize Markov chain of SMDP for in model

In the in model, when considering a lower arrival rate $(1-\delta)\lambda_d$, we have $(1-\delta)\lambda_d \in (0, (1-\delta)\alpha)$ and $\lambda_s \in (0, \alpha)$. Hence, for the first state 0, we can uniformize the Markov chain by using $(1-\delta)\alpha$. For a state $0 < i < N$, we can uniformize the Markov chain by using $(2-\delta)\alpha$. For the last state N, we can uniformize the Markov chain by using α. The transition probabilities of the Markov chain and the corresponding uniformized version are depicted in Figure 4.3. In the uniformized version of the corresponding Markov chain, the transition probability from each state to another state lies within the interval $(0, 1)$. Hence, it can be viewed as a discrete-time MDP as the sojourn time of each state being uniformized. Specifically, in the in model, the value of N is set to a large number because the queue reaching lengths beyond this point has a negligible impact on the expected revenue. This is due to the queue avoiding such long lengths to prevent incurring infinite customer attrition costs.

Step 2: Derive optimality equations

Recall v_i denote the relative value function corresponding to a queue length of i. We apply Bellman's equation and derive the corresponding optimality equations:

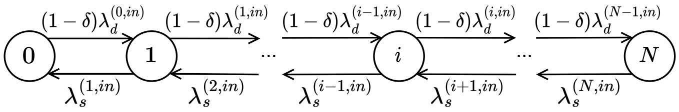

(a)

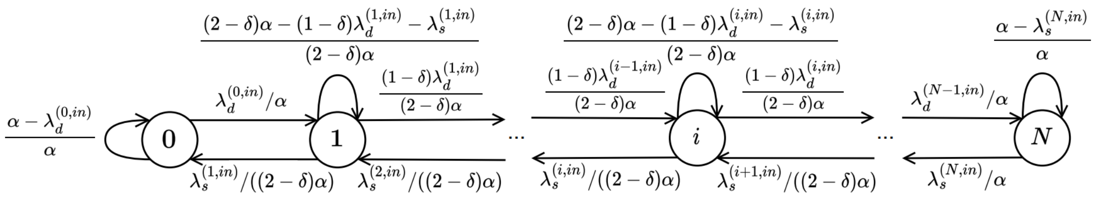

(b)

Figure 4.3.: Markov chain and its uniformized version of *in* model. Left: Markov chain of SMDP. Right: Uniformized version of a discrete-time MDP.

$$v_0 = \max_{p_{(0,in)}} \left\{ \frac{GR_{in}\left(p_{(0,in)}\right) - \gamma}{(1-\delta)\alpha} + \frac{\lambda_d^{(0,in)}}{\alpha} v_1 + \frac{\alpha - \lambda_d^{(0,in)}}{\alpha} v_0 \right\} \tag{4.25}$$

$$\underset{i=1,..,N-1}{v_i} = \max_{p_{(i,in)}} \left\{ \frac{GR_{in}(p_{(i,in)}) - SP_{in}(p_{(i,in)}) - \gamma}{(2-\delta)\alpha} + \frac{(1-\delta)\lambda_d^{(i,in)}}{(2-\delta)\alpha} v_{i+1} + \frac{\lambda_s^{(i,in)}}{(2-\delta)\alpha} v_{i-1} \right.$$
$$\left. + \frac{(2-\delta)\alpha - (1-\delta)\lambda_d^{(i,in)} - \lambda_s^{(i,in)}}{(2-\delta)\alpha} v_i \right\} \tag{4.26}$$

$$v_N = \max_{p_{(N,in)}} \left\{ \frac{-SP_{in}(p_{(N,in)}) - \gamma}{\alpha} + \frac{\lambda_s^{(N,in)}}{\alpha} v_{N-1} + \frac{\alpha - \lambda_s^{(N,in)}}{\alpha} v_N \right\} \tag{4.27}$$

Here, γ is a guess of the maximum average value. This implies that there exists a unique value for γ that satisfies equations (4.25)-(4.27), and the solutions to these equations, as proven by Ata and Shneorson (2006), correspond to the optimal prices for maximizing the expected revenue.

Step 3: Determine optimal prices

By maximizing the RHS of equations (4.25)-(4.27) and introducing an intermediate variable $y_i := v_{i-1} - v_i$ for each $i = 1, 2, .., N$, we can reformulate these equations as follows:

$$\gamma = \frac{(1-\delta)\left(\alpha + \beta_d y_1\right)^2}{4\beta_d} - (1-\delta)\alpha y_1 \tag{4.28}$$

$$\gamma = \frac{\left((1-\delta)\alpha + \beta_s(1-\epsilon)(\nu + y_i) + (1-\delta)\beta_d y_{i+1}\right)^2}{4\left(\beta_d(1-\delta) + \beta_s(1-\epsilon)^2\right)} - (1-\delta)\alpha y_{i+1} - \beta_s \nu y_i \qquad i = 1, .., k \tag{4.29}$$

$$\gamma = \frac{\left((1-\delta)\alpha + \beta_s(1-\epsilon)(\nu + y_i) + (1-\delta)\beta_d y_{i+1}\right)^2}{4\left(\beta_d(1-\delta) + \beta_s(1-\epsilon)^2\right)} - (i-k)C_a - (1-\delta)\alpha y_{i+1} - \beta_s \nu y_i \qquad i = k+1, .., N-1 \tag{4.30}$$

$$\gamma = \frac{\beta_s\left(\nu + y_k\right)^2}{4} - NC_a - \beta_s \nu y_k. \tag{4.31}$$

The corresponding values of optimal prices are

$$p^*_{(i,in)} = \begin{cases} \dfrac{\alpha + \beta_d y_1}{2\beta_d} & \text{if } \ i = 0 \\ \dfrac{(1-\delta)\alpha + \beta_s(1-\epsilon)(\nu + y_i) + (1-\delta)\beta_d y_{i+1}}{2\left(\beta_d(1-\delta) + \beta_s(1-\epsilon)^2\right)} & \text{if } \ 0 < i < k \\ \dfrac{\nu + y_k}{2(1-\epsilon)} & \text{if } \ i = k \end{cases} \tag{4.32}$$

Here, (4.28)-(4.31) form a system of multivariate quadratic equations, and there exists a unique solution for γ, y_1, y_2, ..., y_k. After solving the equation system (4.28)-(4.31) to obtain the value of y_i for each $i = 1, 2, .., N$, we integrate these y_i values into (4.32) to get optimal prices.

Figure 4.4 provides an example illustrating the optimal prices for both static and dynamic pricing policies.

Proposition 24. *When implementing a dynamic pricing policy under a visible information policy, the optimal price decreases with the queue length. Specifically, $p^*_{(i,vi)} > p^*_{(i+1,vi)}$ holds for any $i < k$. Under an invisible information policy, the optimal price decreases when the queue transitions from empty to non-empty, and then increases with the queue length. Specifically, $p^*_{(0,in)} > p^*_{(1,in)}$ and $p^*_{(i,in)} < p^*_{(i+1,in)}$ for any $i \geq 1$.*

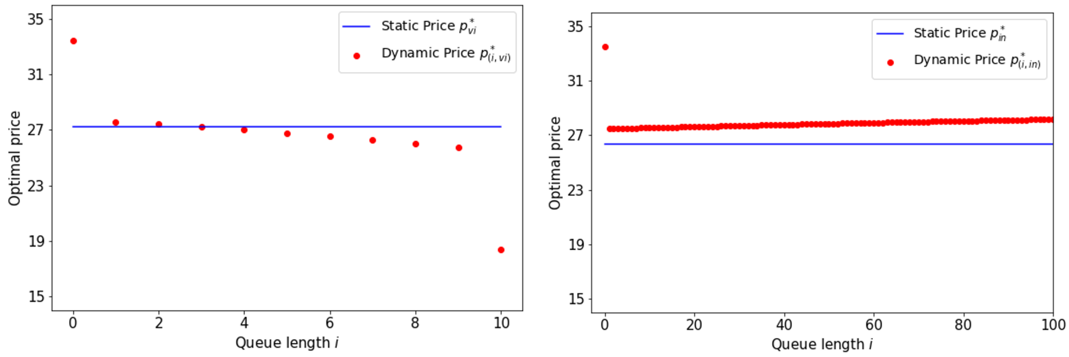

(a) (b)

Figure 4.4.: Optimal prices of static and dynamic pricing policies for a market with $\alpha = 40$, $\beta_d = \beta_s = 1$, $\nu = 10$ and $\epsilon = 10\%$: Setting truncation size and balking probability as $k = 10$ and $\delta = 0.067$ to satisfy $Pro^{stat*}_{vi} = Pro^{stat*}_{in}$. Left: Visible information policy. Right: Invisible information policy.

Proof. We prove the monotonicity of the optimal price and queue length under a visible information policy. We show that $p^*_{(i,vi)} > p^*_{(i+1,vi)}$ holds for any $i < k$.

The vi model. For the results calculated in (4.21)-(4.23), we show that $y_i > y_{i+1}$ for $i < k$. We first show that $y_1 > y_k$. By calculating (4.21) and (4.23), it holds $y_1 = \frac{\alpha}{\beta_d} - \sqrt{\frac{4\gamma}{\beta_d}}$ and $y_k = \nu + \sqrt{\frac{4\gamma}{\beta_d}}$, which indicating $y_1 > y_k$ since $\alpha \gg \beta_d \nu$. By the first-order derivation of the RHS of (4.22), it holds

$$\frac{d\text{RHS of (4.22)}}{dy_i} = \frac{\left(\alpha + \beta_s(1-\epsilon)(\nu + y_i) + \beta_d y_{i+1}\right)\left(\beta_s(1-\epsilon)\right)}{2\left(\beta_d + \beta_s(1-\epsilon)\right)} - \beta_s \nu > 0 \tag{4.33}$$

$$\frac{d\text{RHS of (4.22)}}{dy_{i+1}} = \frac{\left(\alpha + \beta_s(1-\epsilon)(\nu + y_i) + \beta_d y_{i+1}\right)\beta_d}{2\left(\beta_d + \beta_s(1-\epsilon)\right)} - \alpha < 0. \tag{4.34}$$

Since the RHS of (4.21)-(4.23) are equal, this indicates that $y_i \in (y_{i-1}, y_{i+1})$. We illustrate by (4.22) with $k = 1$ and $k = 2$, it holds

$$\gamma = \frac{\left(\alpha + \beta_s(1-\epsilon)(\nu + y_1) + \beta_d y_2\right)^2}{4\left(\beta_d + \beta_s(1-\epsilon)^2\right)} - \alpha y_2 - \beta_s \nu y_1 \tag{4.35}$$

$$\gamma = \frac{\left(\alpha + \beta_s(1-\epsilon)(\nu + y_2) + \beta_d y_3\right)^2}{4\left(\beta_d + \beta_s(1-\epsilon)^2\right)} - \alpha y_3 - \beta_s \nu y_2. \tag{4.36}$$

Given that $y_1 > y_3$, and considering (4.33) and (4.34), if $y_2 > y_1$ or $y_2 < y_3$, then the RHS of (4.35) cannot equal to the RHS of (4.36). Hence, it indicates that $y_1 > y_2 > y_3$.

To compare $p^*_{(0,vi)}$ and $p^*_{(1,vi)}$. Joint equations (4.21) and (4.22), it holds

$$\begin{aligned}\frac{(\alpha+\beta_d y_1)^2}{4\beta_d} =& \frac{(\alpha+\beta_s(1-\epsilon)(\nu+y_1)+\beta_d y_2)^2}{4\left(\beta_d+\beta_s(1-\epsilon)^2\right)} + (\alpha-\beta_s\nu)y_1 - \alpha y_2 \\ &> \frac{(\alpha+\beta_s(1-\epsilon)(\nu+y_1)+\beta_d y_2)^2}{4\left(\beta_d+\beta_s(1-\epsilon)^2\right)}.\end{aligned}$$

This indicates that

$$\frac{(\alpha+\beta_d y_1)^2}{(\alpha+\beta_s(1-\epsilon)(\nu+y_1)+\beta_d y_2)^2} > \frac{\beta_d}{\beta_d+\beta_s(1-\epsilon)^2} > \left(\frac{\beta_d}{\beta_d+\beta_s(1-\epsilon)^2}\right)^2$$

which implies that

$$\frac{(\alpha+\beta_d y_1)^2}{4{\beta_d}^2} > \frac{(\alpha+\beta_s(1-\epsilon)(\nu+y_1)+\beta_d y_2)^2}{4\left(\beta_d+\beta_s(1-\epsilon)^2\right)^2}.$$

By (4.24), it indicates $p^*_{(0,vi)} > p^*_{(1,vi)}$.

To compare $p^*_{(i,vi)}$ and $p^*_{(i+1,vi)}$ for $0<i<k$. By the first-order derivation of the RHS of (4.24), it holds

$$\frac{d\text{RHS of (4.24)}}{dy_i} = \frac{\beta_s(1-\epsilon)}{2\left(\beta_d+\beta_s(1-\epsilon)^2\right)} > 0$$

and

$$\frac{d\text{RHS of (4.24)}}{dy_{i+1}} = \frac{\beta_d}{2\left(\beta_d+\beta_s(1-\epsilon)^2\right)} > 0.$$

This indicates that $p^*_{(i,vi)} > p^*_{(i+1,vi)}$ since, for the RHS of (4.24) with $k=i+1$, the values of y_i and y_{i+1} in the RHS of (4.24) with $k=i$ are substituted by y_{i+1} and y_{i+2}, and $y_i > y_{i+1} > y_{i+2}$.

To compare $p^*_{(k-1,vi)}$ and $p^*_{(k,vi)}$. For (4.24) with $i=k-1$, it holds

$$p^*_{k-1} = \frac{\alpha+\beta_s(1-\epsilon)(\nu+y_{k-1})+\beta_d y_k}{2\left(\beta_d+\beta_s(1-\epsilon)^2\right)} \overset{y_{k-1}>y_k=0}{>} \frac{\alpha+\beta_s(1-\epsilon)(\nu+y_k)+\beta_d y_k}{2\left(\beta_d+\beta_s(1-\epsilon)^2\right)}. \tag{4.37}$$

It holds that

$$p^*_{(k-1,vi)} - p^*_{(k,vi)} > (4.37) - p^*_{(k,vi)} = \frac{\alpha+\beta_s(1-\epsilon)(\nu+y_k)+\beta_d y_k}{2\left(\beta_d+\beta_s(1-\epsilon)^2\right)} - \frac{\nu+y_k}{2(1-\epsilon)}$$

$$= \frac{(1-\epsilon)\alpha + (1-\epsilon)\beta_d y_k - \nu\beta_d - \beta_d y_k}{2\left(\beta_d + \beta_s(1-\epsilon)^2\right)(1-\epsilon)} > 0.$$

Next, we prove the monotonicity of the optimal price and queue length under an invisible information policy. We show that $p^*_{(0,in)} > p^*_{(1,in)}$ and $p^*_{(i,in)} < p^*_{(i+1,in)}$ holds for any $i \geq 1$.

The *in* model. For the results calculated in (4.21)-(4.23), we show that $y_i < y_{i+1}$ for $i \in S_{in}$. We first show that $y_1 < y_N$ where N is a large number. By calculating (4.28) and (4.31), it holds $y_1 = \frac{\alpha}{\beta_d} - \sqrt{\frac{4\gamma}{\beta_d(1-\delta)}}$ and $y_k = \nu + \sqrt{\frac{4(\gamma+NC_a)}{\beta_d}}$, which indicating $y_1 < y_N$ for a large number N. By the first-order derivation of the RHS of (4.29) and (4.30), it holds $\frac{d(4.29)}{dy_i} > 0$, $\frac{d(4.29)}{dy_{i+1}} < 0$, $\frac{d(4.30)}{dy_i} > 0$ and $\frac{d(4.30)}{dy_{i+1}} > 0$. Since the RHS of (4.21)-(4.23) are equal, this indicates that $y_i \in (y_{i+1}, y_{i-1})$. Specifically, it holds $y_{i+1} < y_i < y_{i-1}$. By (4.32), it implies that $p^*_{(i,in)} < p^*_{(i+1,in)}$ for any $i \geq 1$. We note that, given N is a large number and y_1 and y_N are fixed, the difference $|y_i - y_{i+1}|$ is very small. This indicates that $|y_0 - y_1|$ is very small. Hence, it holds

$$\begin{aligned}
&\lim_{|y_0-y_1|\to 0} p^*_{(0,in)} - p^*_{(1,in)} \\
&= \lim_{|y_0-y_1|\to 0} \frac{\alpha + \beta_d y_1}{2\beta_d} - \frac{(1-\delta)\alpha + \beta_s(1-\epsilon)(\nu + y_1) + (1-\delta)\beta_d y_2}{2\left(\beta_d(1-\delta) + \beta_s(1-\epsilon)^2\right)} \\
&= \lim_{|y_0-y_1|\to 0} \Big(\alpha\beta_s(1-\epsilon)^2 + {\beta_d}^2 y_1(1-\delta) + \beta_d\beta_s y_1(1-\epsilon)^2 - \beta_d\beta_s(1-\epsilon)\nu - \beta_d\beta_s(1-\epsilon)y_1 \\
&\quad - {\beta_d}^2(1-\delta)y_2\Big) \\
&= \frac{\alpha\beta_s(1-\epsilon)^2 - \beta_d\beta_s(1-\epsilon)\nu - \epsilon\beta_d\beta_s(1-\epsilon)y_1}{2\beta_d\left(\beta_d(1-\delta) + \beta_s(1-\epsilon)^2\right)} > 0.
\end{aligned}$$

■

Under the visible information policy, as observed in Figure 4.4 (a), the price decreases with the queue length. When the queue length reaches the truncation size, no additional customers are attracted to join the queue, yet the platform continues to pay to attract suppliers for service. Consequently, this situation results in negative net revenue for the queue at the truncation. The decrease in price with the queue length is for minimizing the probability of the queue reaching the truncated size, thereby maximizing expected profit. We note that, when the queue transitions from empty to non-empty, i.e., comparing

$p^*_{(0,vi)}$ and $p^*_{(1,vi)}$, the decrease in price is relatively large. This is because in our model, when the queue is empty, the platform sets a price to attract customers but does not payout to suppliers since there is no customer in the queue to serve. Therefore, when the queue is empty, the gross revenue is equal to the net revenue, so the platform increases the price to maximize the expected profit. When the queue length is at the truncation size, the price decreases relatively largely, i.e., comparing $p^*_{(k-1,vi)}$ and $p^*_{(k,vi)}$, responding to customer balking behavior. The platform decreases the price at the truncation point to reduce the negative net revenue for maximizing the expected profit.

Under the invisible information policy, as observed in Figure 4.4 (b), the price decreases when the queue transitions from empty to non-empty, and then it increases with the queue length. The reason why the price decreases when the queue transitions from empty to non-empty is similar to that under the visible information policy. The platform increases the price to increase both gross revenue and corresponding net revenue, ultimately maximizing expected profits. As more customers join the queue, the price increases, on the one hand, to attract more suppliers to serve, ultimately clearing the queue and resulting in a higher expected profit. On the other hand, the platform increases the price to decrease the system load, avoiding the queue being too long and incurring high user attrition costs.

4.3. Determining preferred pricing and information policy

In this section, we identify the unique thresholds that determine the preferred pricing and information policies, respectively. By combining these thresholds, we provide strategies that are preferred for the platform. We then conduct a sensitivity analysis of these thresholds on main market parameters.

4.3.1. Threshold to determine pricing policy

A dynamic pricing policy results in higher net revenue than a static pricing policy. However, the complexity of how incremental net revenues vary with main market parameters and user patience makes it challenging to generalize the thresholds that determine the preferred pricing policy. We define the parameter $\eta_\ell := \frac{NR_\ell^{dyn*}}{NR_\ell^{stat*}} - 1$ as the *incremental net revenue ratio* for each information policy $\ell \in \{in, vi\}$. This metric η_ℓ quantifies the percentage increase in the expected net revenue from using a dynamic pricing policy

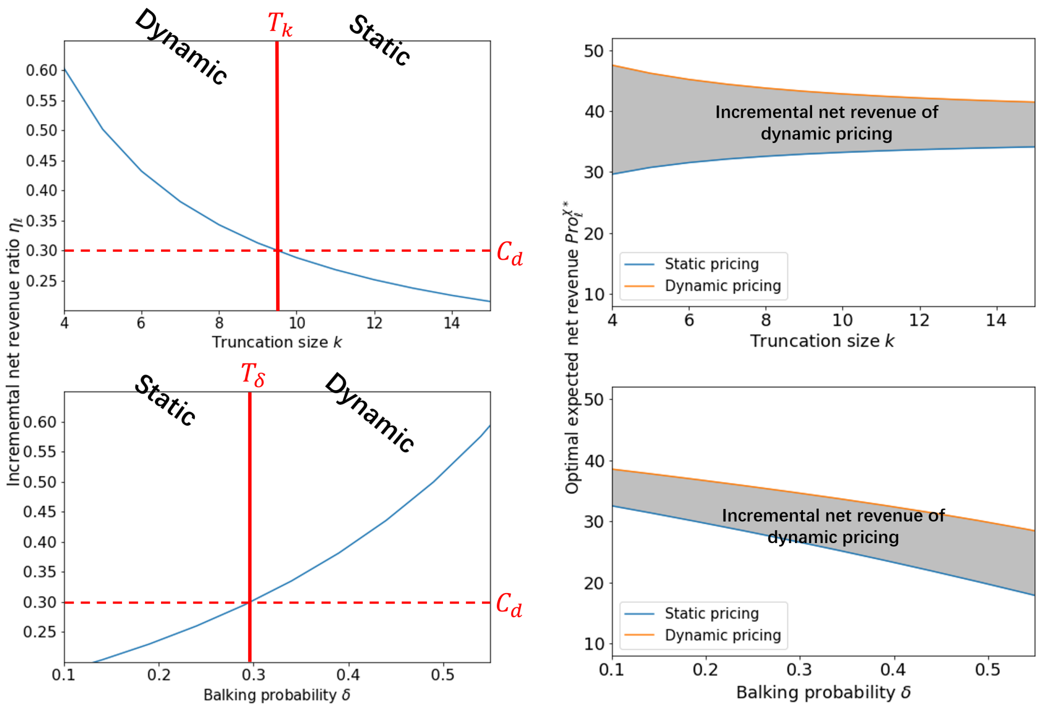

(a) (b)

Figure 4.5.: Incremental net revenue ratio η_ℓ in a market with $\alpha = 40$, $\beta_d = \beta_s = 1$, $\nu = 10$, $\epsilon = 10\%$, $C_d = 0.3$, $k \in [4, 20]$ and $\delta \in [0.04, 0.82]$. Left: Incremental net revenue ratio η_ℓ. Right: Optimal expected profit $Pro_\ell^{\chi*}$.

compared to a static pricing policy. The extra cost of implementing dynamic pricing is a defined measure, expressed as a percentage of net revenue relative to static pricing. Therefore, by comparing this metric η_ℓ with the extra cost C_d associated with using a dynamic pricing policy, we determine the preferred pricing policy for maximizing expected profit.

Proposition 25. *Given that the incremental net revenue ratio decreases as customer patience increases (i.e.,* $\frac{d\eta_{vi}}{dk} < 0$ *and* $\frac{d\eta_{in}}{d\delta} > 0$*),*

1. *Under a visible information policy, if the truncation size k is below a unique threshold T_k, then a dynamic pricing policy is preferred over a static pricing policy, and vice versa. The threshold T_k is the truncation size at which the incremental net revenue ratio η_{vi} equals the extra cost C_d, and it monotonically decreases with the extra cost C_d.*

2. *Under an invisible information policy, if the balking probability δ is below a unique threshold T_δ, then a static pricing policy is preferred over a dynamic pricing policy, and vice versa. The threshold T_δ is the balking probability at which the incremental net revenue ratio η_{in} equals the extra cost C_d, and it monotonically increases with the extra cost C_d.*

Proof. As $\lim_{k\to\infty} Pro_{vi}^{stat*} = \lim_{k\to\infty} Pro_{vi}^{dyn*}$ and $\lim_{\delta\to 0} Pro_{in}^{stat*} = \lim_{\delta\to 0} Pro_{in}^{dyn*}$, this implies that $\lim_{k\to\infty} NR_{vi}^{stat*} = \lim_{k\to\infty} NR_{vi}^{dyn*}$ and $\lim_{\delta\to 0} NR_{in}^{stat*} = \lim_{\delta\to 0} NR_{in}^{dyn*}$. Therefore, for the incremental net revenue ratio η_ℓ, it is evident that $\lim_{k\to\infty} \eta_{vi} = 0$ and $\lim_{\delta\to 0} \eta_{in} = 0$. Given our assumption of monotonicity in the truncation size k and balking probability δ for η_ℓ, unique thresholds T_k and T_δ exist to determine the optimal pricing policy. ■

Figure 4.5 illustrates an example of the relative net revenue ratio when determining the preferred pricing policy. If customers are impatient (e.g., $k < T_k$ and $\delta > T_\delta$ in Figure 4.5 (a)), the incremental net revenue ratio of using a dynamic pricing policy is high, indicating the significant advantages of using a dynamic pricing policy. As the level of customer patience is higher, this advantage is lower. When customers are patient (e.g., $k > T_k$ and $\delta < T_\delta$ in Figure 4.5 (a)), the incremental net revenue ratio of using a dynamic pricing policy is low, indicating the significant advantages of using a static pricing policy. This result is due to the scale effect associated with customer patience. Figure 4.5 (b) implies that the incremental net revenue of using a dynamic pricing policy over a static one remains relatively constant across different levels of customer patience, whether it is represented by k or δ. As customer patience is higher, both the net revenues of static and dynamic pricing policies are higher, resulting in a lower incremental net revenue ratio. This monotonicity implies the uniqueness of thresholds T_k and T_δ for determining the preferred pricing policy.

4.3.2. Threshold to determine information policy

The higher the patience of customers, the higher the expected net revenue for the platform. With higher patience, customers are less likely to balk at joining the queue under both visible and invisible information policies at a given price, resulting in higher expected net revenue. For a fixed extra cost C_d, this demonstrates the monotonic impact of customer patience on expected profit. We define an *indifference curve* to determine the preferred information policy. The function is defined as

$$\begin{aligned} f_{C_d} :=& \max\left\{Pro_{vi}^{stat*}, Pro_{vi}^{dyn*}\right\} - \max\left\{Pro_{in}^{stat*}, Pro_{in}^{dyn*}\right\} \\ =& \max\left\{NR_{vi}^{stat*}, (1-C_d)NR_{vi}^{dyn*}\right\} - \max\left\{NR_{in}^{stat*}, (1-C_d)NR_{in}^{dyn*}\right\} \triangleq 0 \end{aligned}$$

This function compares the maximum profit from implementing static and dynamic pricing policies under a visible information policy with that under an invisible information policy. If the market parameters satisfy this function and it equals zero, it implies that the platform is indifferent to which information policy is implemented because the expected profits are the same. If the market parameters lead to $f_{C_d} > 0$, then a visible information policy is preferred, and vice versa.

4.3.3. Preferred strategy to maximize profit

Based on the thresholds T_k and T_δ for determining the preferred pricing policy and the indifference curve for determining the preferred information policy, we can provide recommendations on the preferred strategy for the platform to maximize its expected profit. Specifically, for a market

1. If $\delta < T_\delta$ and $f_{C_d}(k, \delta) < 0$, then $S\&I$ is preferred.
2. If $\delta > T_\delta$ and $f_{C_d}(k, \delta) < 0$, then $D\&I$ is preferred.
3. If $k < T_k$ and $f_{C_d}(k, \delta) > 0$, then $D\&V$ is preferred.
4. If $k > T_k$ and $f_{C_d}(k, \delta) > 0$, then $S\&V$ is preferred.

Figure 4.6 graphically illustrates the preferred strategy as outlined, based on the customer patience. Specifically, it determines the preferred strategy based on the truncation size k under the visible information policy and the balking probability δ under the invisible information policy. A higher truncation size k indicates that customers are more patient under a visible information policy, while a lower balking probability δ indicates the same under an invisible information policy. When customers are patient, a static pricing policy is preferred regardless of the information policy, while a dynamic pricing policy is preferred when customers are impatient. It reveals that the preferred strategy depends on the sensitivity to the displayed queue-length information. If customers are not sensitive to the displayed queue-length information, meaning that they are patient

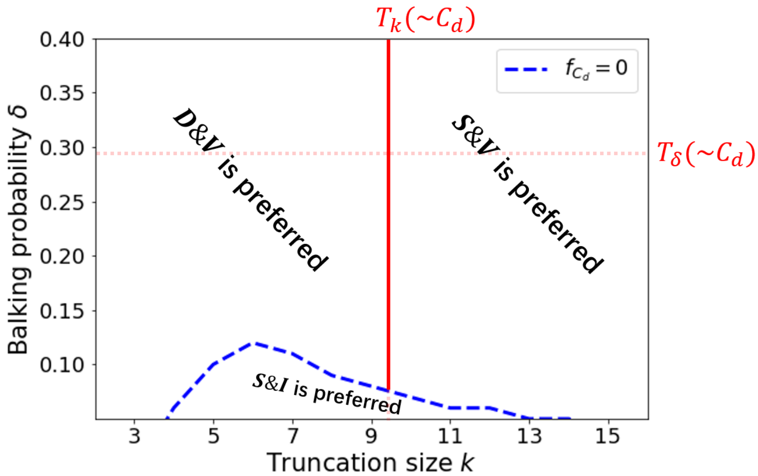

Figure 4.6.: The preferred strategy of pricing and information policies for $\alpha = 40$, $\beta_d = \beta_s = 1$, $\epsilon = 10\%$, $\nu = 10$, $C_d = 0.3$, $k \in [2, 16]$ and $\delta \in [0.05, 0.4]$.

under both visible and invisible information policies, or impatient under both, then the indifference curve determines the preferred strategy. If customers are sensitive to the displayed information, there are two cases: (i) customers are patient under a visible information policy, while they are impatient under an invisible information policy; and (ii) customers are impatient under a visible information policy, while they are patient under an invisible information policy. In both cases, the preferred information policy is the one where customers are more patient. This corresponds to a high truncation size under the visible information policy or a low balking probability under the invisible information policy. In either case, the static pricing policy is preferred.

4.3.4. Sensitivity analysis of market parameters

We analyze the impact of main parameters on the thresholds of pricing and information policies numerically. Table 4.4 summarizes the parameter ranges changed for sensitivity for $C_d = 10\%$ and $C_a = 0.05$. With an extra cost of $C_d = 10\%$, a dynamic pricing policy is preferred only if the incremental net revenue ratio surpasses 10%. The user attrition cost prevents the queue length from increasing infinitely but has a negligible impact on platform profits. In our numerical experiments, we set $C_a = 0.05$ to ensure it remains relatively small compared to market potential α, specifically $\frac{C_a}{\alpha} < 1\%$. We systematically vary main market parameters within the base case (i.e., α, β_s, β_d, ν and ϵ), sampling points in the range for numerical experiments to observe sensitivity.

Table 4.4.: Parameter ranges changed for sensitivity for $C_d = 10\%$ and $C_a = 0.05$.

	Pricing policy		Information policy	
Base case	Range of parameter changed for sensitivity	Numerical result	Range of parameter changed for sensitivity	Numerical result
$\alpha = 40$	[35, 45]	Figure 4.7 (a) and (c)	[35, 45]	Figure 4.8 (a) and (c)
$\beta_d = 1$	[0.8, 1.2]	Figure 4.7 (e)	[0.8, 1.2]	Figure 4.8 (e)
$\beta_s = 1$	[0.8, 1.2]	Figure 4.7 (f)	[0.8, 1.2]	Figure 4.8 (f)
$\nu = 10$	[8, 15]	Figure 4.7 (b)	[8, 15]	Figure 4.8 (b)
$\epsilon = 10\%$	[10%, 40%]	Figure 4.7 (d)	[7.5%, 12.5%]	Figure 4.8 (d)

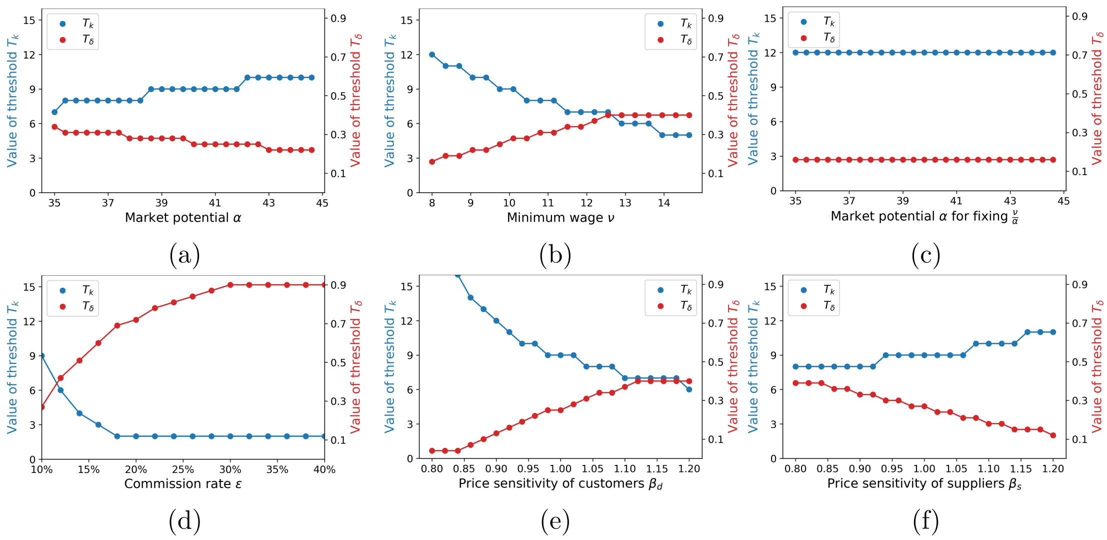

Figure 4.7.: Change of thresholds T_k and T_δ in accordance with market parameters α, β_d, β_s, ν and ϵ. (a): Market potential α; (b): Minimum wage ν; (c): For fixing $\frac{\nu}{\alpha} = 0.2$; (d): Commission ratio ϵ; (e): Price sensitivity of customers β_d; (f): Price sensitivity of suppliers β_s.

To standardize sensitivity comparisons and ensure consistent ranges for variations in thresholds T_k, T_δ , and δ_k when varying different market parameters, we set different parameter change ranges for sensitivity analysis under pricing and information policies, as outlined in Table 4.4.

Pricing policy threshold (T_k and T_δ)

We examine the impact of main market parameters α, β_d, β_s, ν and ϵ, on the two thresholds T_k and T_δ, as shown in Figure 4.7. We summarize the observations that (i) A higher market potential α, a lower minimum wage ν, or a lower commission rate ϵ make a dynamic pricing policy more preferable under both visible and invisible information policies. (ii) A higher supplier price sensitivity β_s, and conversely, a lower customer price sensitivity β_d make a dynamic pricing policy more preferable under both visible and invisible information policies.

Market potential α, minimum wage ν and commission rate ϵ A higher market potential α, a lower minimum wage ν, or a lower commission rate ϵ leads to increased arrival rates of both customers and suppliers, as indicated by (4.1) (a)-(d). This results

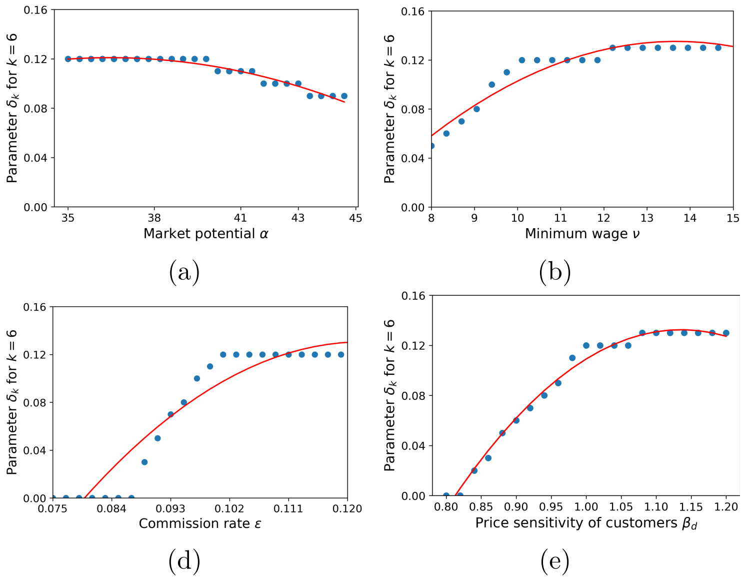

Figure 4.8.: Change of parameter δ_k (a sample point for the indifference curve $f_\delta = 0$ at $k = 6$) in accordance with market parameters α, β_d, β_s, ν and ϵ. (a): Market potential α; (b): Minimum wage ν; (c): For fixing $\frac{\nu}{\alpha} = 0.2$; (d): Commission ratio ϵ; (e): Price sensitivity of customers β_d; (f): Price sensitivity of suppliers β_s.

in a higher incremental net revenue for implementing a dynamic pricing policy, consequently leading to a higher incremental net revenue ratio. Therefore, this implies a higher threshold T_k under the visible information policy and a lower threshold T_δ under the invisible information policy. Given that the effects of increasing market potential α and decreasing minimum wage ν on thresholds T_k and T_δ are opposite, we maintain a fixed ratio of α and ν in Figure 4.7 (c) while increasing the market potential α. It is observed that when both factors change simultaneously, their effects on the thresholds can be counterbalanced.

Price sensitivities of customers β_d and suppliers β_s The effects of price sensitivities of customers and suppliers are opposite. A higher price sensitivity of customers β_d or a lower price sensitivity of suppliers β_s leads to lower arrival rates of both customers and suppliers. This results in a lower incremental net revenue for implementing a dynamic pricing policy, consequently leading to a lower incremental net revenue ratio. Therefore, this implies a lower threshold T_k under the visible information policy and a higher threshold T_δ under the invisible information policy.

Information policy threshold ($f_{C_d} = 0$)

Define δ_k as the value of δ that satisfies the indifference curve $f_{C_d} = 0$ for a given value of k. The parameter δ_k indicates the position of the indifference curve $f_{C_d} = 0$. An increase in δ_k signifies an upward shift of the indifference curve on the graph, implying that the invisible information policy is more preferred, and vice versa. We examine the impact of main market parameters α, β_d, β_s, ν and ϵ on δ_k to indicate their effects on the indifference curve f_{C_a}, as shown in Figure 4.8.

Market potential α, minimum wage ν and commission rate ϵ. A higher market potential α, a lower minimum wage ν, or a lower commission rate ϵ results in higher arrival rates for both customers and suppliers, as indicated by (4.1). This leads to a longer corresponding queue length, causing more customers to balk when the queue is at the truncation size under the visible information policy. Since, under the visible information policy, customers balk at joining the queue based on a balking probability, more customers are attracted to join the queue compared to that under the invisible information policy. Hence, the invisible information policy is more preferable.

Price sensitivity of customers β_d and suppliers β_s. The effects of price sensitivities of customers and suppliers are opposite. A higher price sensitivity of customers β_d or a lower price sensitivity of suppliers β_s leads to lower arrival rates of both customers and suppliers. Consequently, the queue length becomes shorter, resulting in fewer customers balk when the queue is at the truncation size under the visible information policy. Hence, the visible information policy is more preferable.

4.4. Profit, throughput and price

The *throughput* represents the expected matching rate of the platform, i.e., the rate at which customers arrive at the market without balking and enter the queue, waiting for a match. The throughput metric serves as an indicator of the social welfare of customers and suppliers, reflecting the change in the number of successful matches between them. It is denoted by

$$\varsigma_\ell^\chi := \begin{cases} \lambda_d^{vi}\left(1-\pi_k^{vi}\right) & \text{if} \quad \chi = stat \quad \text{and} \quad \ell = vi \\ \sum\limits_{i\in S_{vi}-\{k\}} \lambda_d^{(i,vi)}\pi_i^{vi} & \text{if} \quad \chi = dyn \quad \text{and} \quad \ell = vi \\ (1-\delta)\lambda_d^{in} & \text{if} \quad \chi = stat \quad \text{and} \quad \ell = in \\ \sum\limits_{i\in S_{in}} (1-\delta)\lambda_d^{(i,in)}\pi_i^{in} & \text{if} \quad \chi = dyn \quad \text{and} \quad \ell = in. \end{cases}$$

We first analyze the influence of strategies on expected profit and throughput.

4.4.1. An illustrative market example

User patience is measured differently for markets under different information policies, specifically the truncation size k for a visible information policy and the balking probability δ for an invisible information policy. Standardizing user patience under different information policies is crucial for comparing the impacts of different strategies. To achieve this, we examine an illustrative market where, with the same main market parameters, truncation size k and balking probability δ are set to result in the same expected net revenue under different information policies, satisfying $Pro_{vi}^{stat*} = Pro_{in}^{stat*}$ for static pricing. This is to ensure the consistency of market measurement under different information policies, meaning that the market is indifferent to the choice of information policy when implementing a static pricing policy. In doing so, we can address the following equations: (i) How does price change for different strategies? (ii) Which information policy increases profit when using a dynamic pricing policy? (iii) What impact does the information policy have on throughput?

4.4.2. Profit analysis

When comparing the expected profits of the *D&V* and *D&I* strategies in Figures 4.9 (a)-(d), we observe the following

Result 26. *Implementing a dynamic pricing policy under a visible information policy results in higher expected profit. Specifically, if* $Pro_{vi}^{stat*} = Pro_{in}^{stat*}$*, then* $Pro_{vi}^{dyn*} > Pro_{in}^{dyn*}$.

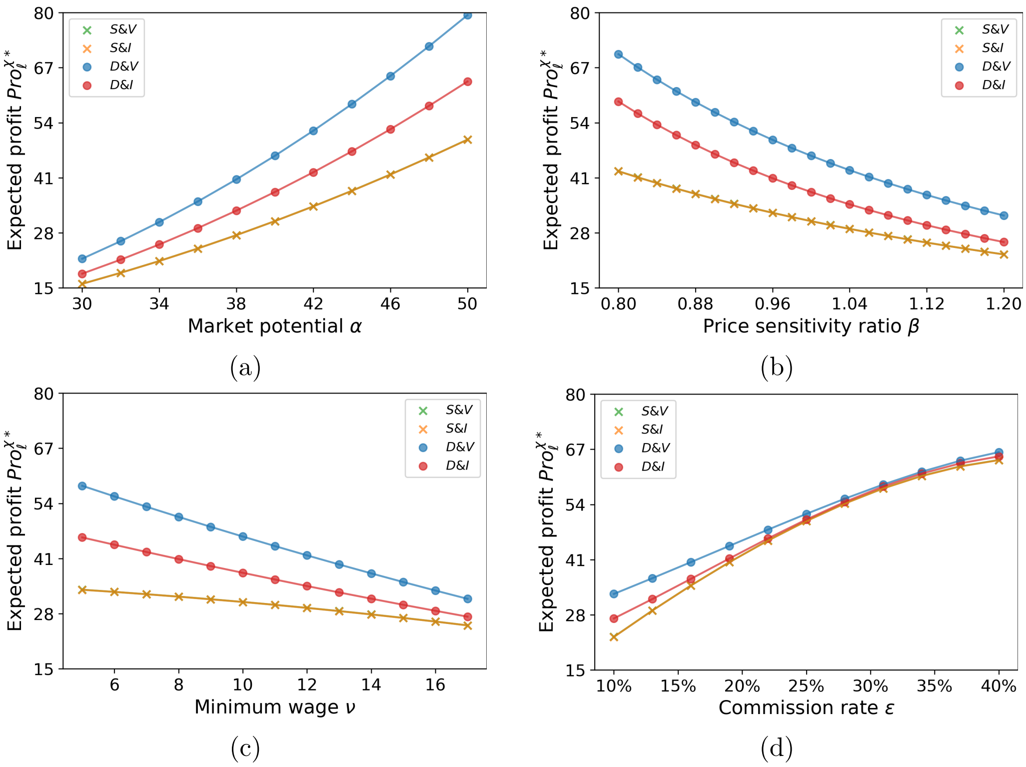

Figure 4.9.: Expected profit with market parameters α, β, ν and ϵ. The base case uses parameter values outlined in Table 4.4. (a): Market potential α; (b): Price sensitivity ratio β; (c): Minimum wage ν; (d): Commission rate ϵ.

This is due to the fact that under the invisible information policy, the invisibility of queue-length information directly leads to a proportional decrease in the arrival rates of both customers and suppliers. When comparing a dynamic pricing policy to a static pricing one, the dynamic pricing policy results in a proportional increase in the expected profit based on the arrival rates of customers and suppliers. However, due to the lower arrival rates under the invisible information policy compared to the visible one, the incremental net revenue for using a dynamic pricing policy is lower. Consequently, the expected profit is higher under a visible information policy.

4.4.3. Throughput analysis

When comparing the throughput of the *D&V* and *D&I* strategies in Figures 4.10 (a)-(d), we observe the following

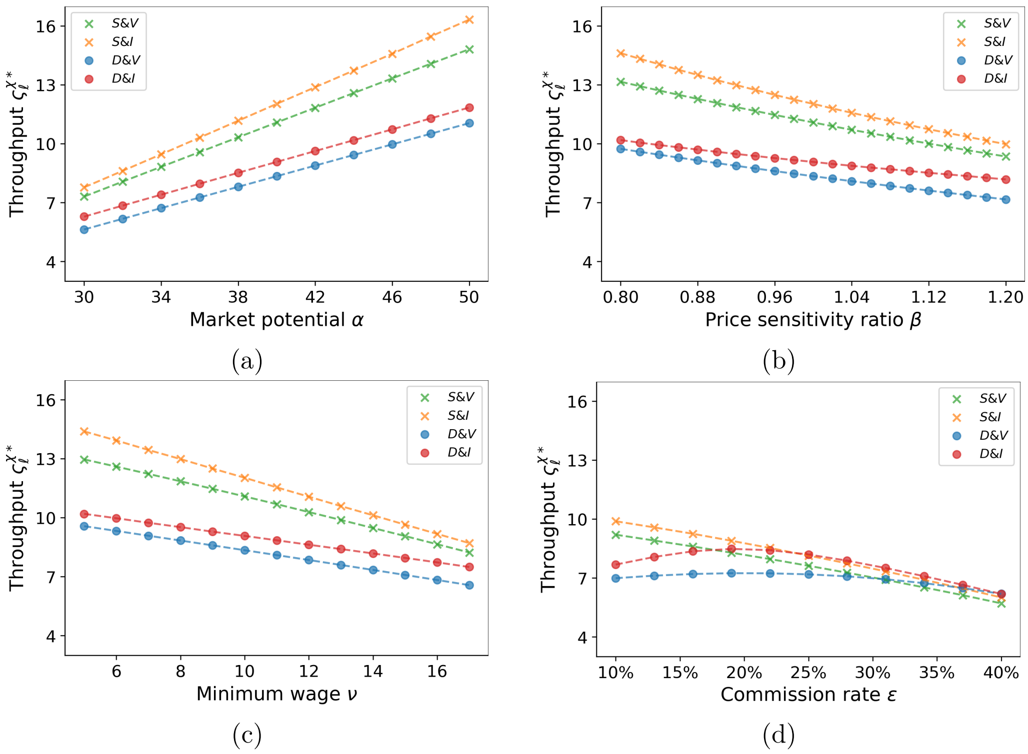

Figure 4.10.: Expected profit with market parameters α, β, ν and ϵ. The base case uses parameter values outlined in Table 4.4. (a): Market potential α; (b): Price sensitivity ratio β; (c): Minimum wage ν; (d): Commission rate ϵ.

Result 27. *Implementing a static or dynamic pricing policy under a invisible information policy results in higher throughput, especially for a low commission rate. Specifically, if* $Pro_{vi}^{stat*} = Pro_{in}^{stat*}$, *then* $\varsigma_{vi}^{\chi*} < \varsigma_{in}^{\chi*}$ *for each* $\chi \in \{stat, dyn\}$.

By comparing Result 27 and Result 26, we observe a trade-off regarding the visibility of queue-length information under a dynamic pricing policy. For a dynamic pricing policy, displaying the queue-length information results in a higher expected profit, while concealing it leads to a higher throughput for markets with a low commission rate. However, as shown in Figure 4.10 (d), in markets with a high commission rate, displaying the queue-length information results in both a higher expected profit and throughput. The difference in how dynamic pricing policies affect throughput is due to different customer balking behaviors under different information policies. In particular, these different balking behaviors result in different stationary distributions of the market under

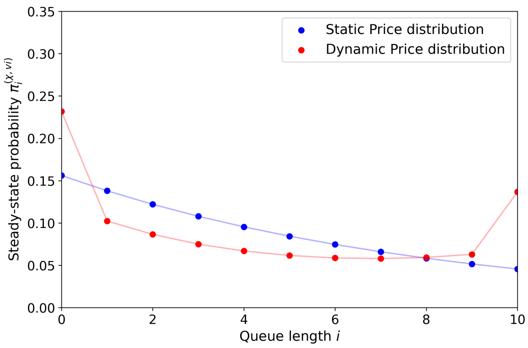

(a)

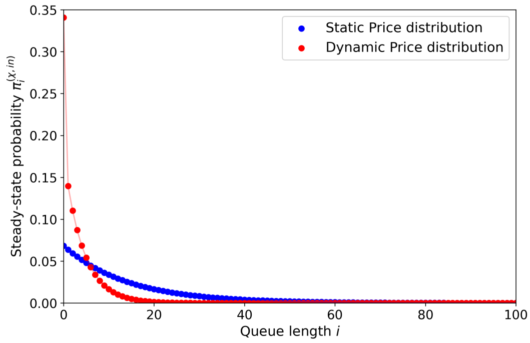

(b)

Figure 4.11.: Stationary distribution under different information policies with $Pro_{vi}^{stat*} = Pro_{in}^{stat*}$ in a market with $\alpha = 40$, $\beta_d = \beta_s = 1$, $\nu = 10$, $k = 10$, $\delta = 0.1$ and $\epsilon = 10\%$. Left: Visible information policy. Right: Invisible information policy.

different pricing policies, consequently affecting throughput. We analyze this in cases including low and high commission rates.

When the commission rate is low As illustrated in Figure 4.10 (a)-(d), the concealment of queue-length information results in a higher throughput $\varsigma_{in}^{\chi *} > \varsigma_{vi}^{\chi *}$ for each $\chi \in \{stat, dyn\}$. Figure 4.11 shows the corresponding stationary distribution of the case $\epsilon = 10\%$ under both visible and invisible information policies. As shown in Figure 4.11 (a), under a visible information policy,the steady-state probability of reaching the truncation (i.e., a queue length where $i = k$) is higher when implementing a dynamic pricing policy compared to implementing a static pricing policy. As indicated by (4.1), when the commission rate is relatively low, the arrival rates for both customers and suppliers are high. This, in turn, implies that the arrival rate of suppliers at the truncation point is also relatively high. Previously, we pointed out that the platform's net revenue is negative at the point of truncation. Although lowering the price at queue truncation may decrease the supplier arrival rate, the consequential significant decrease in negative net revenue (4.3) ultimately works to increase the platform's expected profit. In contrast, Figure 4.4 (b) shows that under an invisible information policy, a dynamic pricing policy, as compared to a static pricing policy, progressively increases the price to avoid excessively long queues and the corresponding high customer attrition costs. As a result, the steady-state distribution is more concentrated on shorter queue lengths, as shown in Figure 4.11 (b). This suggests that a larger proportion of customers tend to join queues

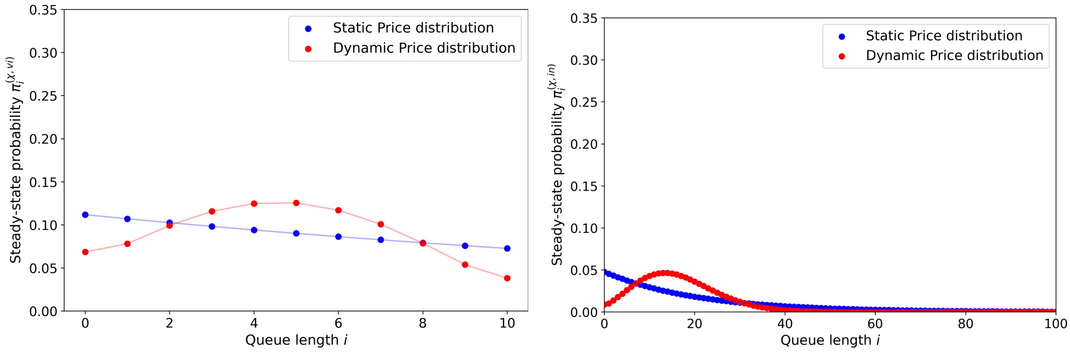

(a) (b)

Figure 4.12.: Optimal price and stationary distribution of different pricing policies under a visible information policy in a market with $\alpha = 40$, $\beta_d = \beta_s = 1$, $\nu = 10$, $k = 10$ and $\epsilon = 35\%$. Left: Optimal price. Right: Stationary distribution.

of shorter lengths and receive service, while no truncation occurs for a very long queue, collectively contributing to a higher throughput.

When the commission rate is high As illustrated in Figure 4.9 (d), the concealment of queue-length information results in a lower throughput $\varsigma_{in}^{dyn*} < \varsigma_{vi}^{dyn*}$ when the commission rate is high. Figure 4.12 shows the optimal price and stationary distribution of the case $\epsilon = 35\%$, encompassing both static and dynamic pricing policies under a visible information policy. As shown in Figure 4.12 (b), when implementing a dynamic pricing policy in a market with a relatively high commission rate, the stationary distribution concentrates on shorter queue lengths. This contrasts with Figure 4.11 (a), where the stationary distribution concentrates on the truncation size and an empty queue length. Consequently, the steady-state probability of reaching the truncation size is lower for a dynamic pricing policy because, as shown by (4.3), when the commission rate is relatively high, the net revenue function is minimized at the point of queue truncation. The corresponding negative net revenue at the queue truncation point has a relatively smaller impact on the expected profit compared to a market with a low commission rate. As a result, reducing the price at the queue truncation point is not as advantageous in increasing the platform's expected profit. This dynamic can also be observed in Figure 4.12 (a), where despite a decrease in the price at queue truncation $p^*_{(k,vi)}$ compared to the preceding queue length $p^*_{(k-1,vi)}$, this reduction in price is less pronounced when compared to Figure 4.11 (a), where the commission rate is lower. Since the steady-state probability of the queue being at truncation is low under a visible information policy, this contributes to a higher throughput when using a dynamic pricing policy under a visible information policy.

4.4.4. Impact of queue-length display on price

We define the *average transaction price* for customers and suppliers as

$$\varrho_d^\ell := \left(\sum_{i \in S_\ell} \pi_i^\ell GR_\ell(p_{(i,\ell)}) \right) \Big/ \varsigma_\ell^{dyn}$$

and

$$\varrho_s^\ell := \left(\sum_{i \in S_\ell} \pi_i^\ell SP_\ell(p_{(i,\ell)}) \right) \Big/ \varsigma_\ell^{dyn},$$

calculated as the ratio of the gross revenue and supplier payout to the throughput for each information policy $\ell \in \{in, vi\}$. We define the *volatility* of a dynamic pricing policy as

$$\sigma_\ell := \sqrt{\frac{1}{|S_\ell| - 1} \sum_{i=0}^{|S_\ell|} \pi_\ell^\ell \left(p^*_{(i,\ell)} - \varrho_s^\ell \right)^2}$$

for each information policy $\ell \in \{in, vi\}$. The metric σ_ℓ is estimated based on the standard deviation, providing insights into the level of price discrimination. In this section, we examine the optimal price, average transaction price, and price volatility as shown in Figure 4.13, shedding light on their impacts on the interests of both the platform and its users. Our results indicate that concealing the queue-length information results in a higher price when implementing a static pricing policy, as shown in Figure 4.13 (a)-(d).

Proposition 28. *In a market implementing a static pricing policy the optimal price is higher under a visible information policy. Specifically, if $Pro_{vi}^{stat*} = Pro_{in}^{stat*}$, then $p^*_{vi} > p^*_{in}$.*

Proof. For the optimal static price, the invisible information policy differs from the visible policy in two ways. First, there is no truncation size k of the queue under the invisible information policy. Second, when the queue is too long, our model takes into

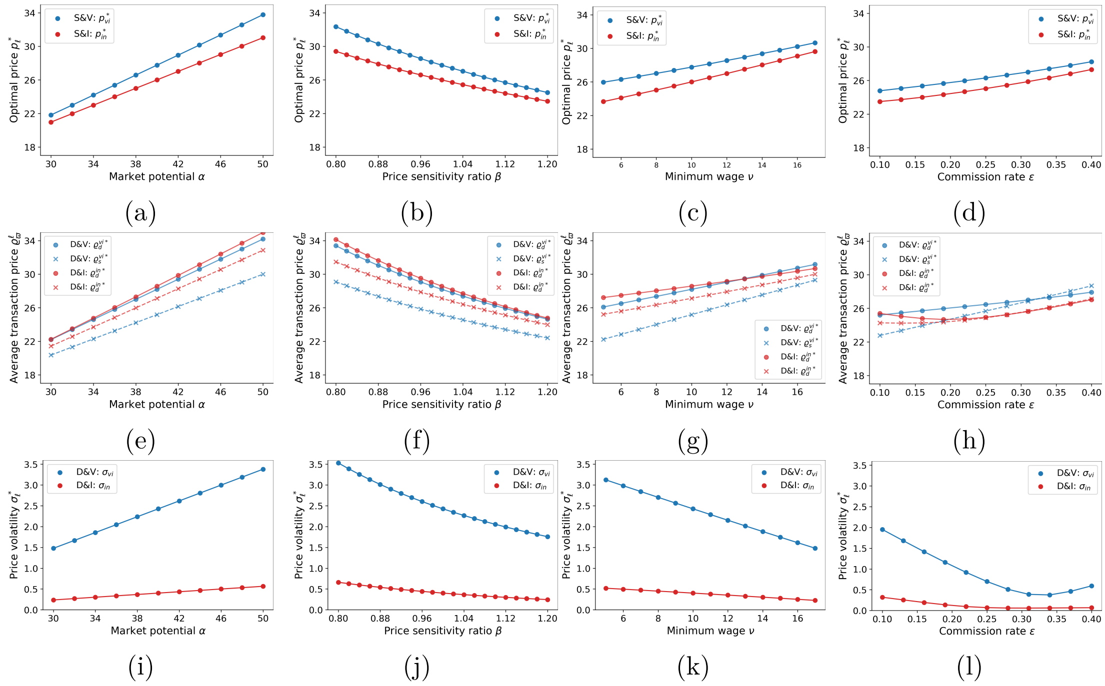

Figure 4.13.: Optimal price, average transaction price and price volatility with market parameters α, β, ν and ϵ. Parameter ranges for sensitivity follow Table 4.13. (a): Static pricing with α; (b): Static pricing with β; (c): Static pricing with ν; (d): Static pricing with ϵ; (e): Dynamic pricing with α; (f): Dynamic pricing with β; (g): Dynamic pricing with ν; (h): Dynamic pricing with ϵ; (i): Price volatility with α; (j): Price volatility with β; (k): Price volatility with ν; (l): Price volatility with ϵ.

account the user attrition cost C_a. Observe from (4.12) that not considering this user attrition cost under the invisible information policy, i.e., $C_a \to 0$, leads only to an increase in price. Therefore, we consider that if the price is higher under the visible information policy when $C_a \to 0$, then we can complete the proof. In the following, we show that the optimal static price under the visible information policy decreases with the queue length. Therefore, the price under the visible information policy with a truncation size should be lower than that of the invisible information policy.

From (4.10), it holds that the optimal static price satisfies

$$\frac{\left(\frac{\alpha}{\beta_s\nu}+\rho_{vi}^*\right)\left(\frac{\beta_d}{\beta_s(1-\epsilon)}+\rho_{vi}^*\right)\sum\limits_{i=1}^{k} i{\rho_{vi}^*}^{i-1}}{\left(\sum\limits_{i=0}^{k}{\rho_{vi}^*}^{i}\right)^2}-\left(\frac{2\alpha}{\beta_s\nu}-\frac{\beta_d}{\beta_s(1-\epsilon)}+\rho_{vi}^*\right)\left(1-\frac{1}{\sum\limits_{i=0}^{k}{\rho_{vi}^*}^{i}}\right)=0 \tag{4.38}$$

where $\left(\frac{\alpha}{\beta_s\nu}+\rho_{vi}^*\right)\left(\frac{\beta_d}{\beta_s(1-\epsilon)}+\rho_{vi}^*\right)\overset{\alpha\gg\beta_s\nu}{<}\frac{2\alpha}{\beta_s\nu}-\frac{\beta_d}{\beta_s(1-\epsilon)}+\rho_{vi}$. It holds

$$\begin{aligned}
&\left(\frac{\sum\limits_{i=1}^{k} i{\rho_{vi}^*}^{i-1}+(k+1){\rho_{vi}^*}^{k}}{\left(\sum\limits_{i=0}^{k}{\rho_{vi}^*}^{i}+{\rho_{vi}^*}^{k+1}\right)^2}-\frac{\sum\limits_{i=1}^{k} i{\rho_{vi}^*}^{i-1}}{\sum\limits_{i=0}^{k}{\rho_{vi}^*}^{i}}\right)-\left(\frac{\sum\limits_{i=1}^{k}{\rho_{vi}^*}^{i}+{\rho_{vi}^*}^{k+1}-1}{\sum\limits_{i=0}^{k}{\rho_{vi}^*}^{i}+{\rho_{vi}^*}^{k+1}}-\frac{\sum\limits_{i=0}^{k}{\rho_{vi}^*}^{i}-1}{\sum\limits_{i=0}^{k}{\rho_{vi}^*}^{i}}\right)\\
&=\left(\frac{\sum\limits_{i=1}^{k} i{\rho_{vi}^*}^{i-1}+(k+1){\rho_{vi}^*}^{k}}{\sum\limits_{i=0}^{k}{\rho_{vi}^*}^{i}+{\rho_{vi}^*}^{k+1}}\cdot\frac{1}{\sum\limits_{i=0}^{k}{\rho_{vi}^*}^{i}+{\rho_{vi}^*}^{k+1}}-\frac{\sum\limits_{i=1}^{k}{\rho_{vi}^*}^{i}+{\rho_{vi}^*}^{k+1}-1}{\sum\limits_{i=0}^{k}{\rho_{vi}^*}^{i}+{\rho_{vi}^*}^{k+1}}\right)\\
&\quad+\left(\frac{\sum\limits_{i=0}^{k}{\rho_{vi}^*}^{i}-1}{\sum\limits_{i=0}^{k}{\rho_{vi}^*}^{i}}-\frac{\sum\limits_{i=1}^{k} i{\rho_{vi}^*}^{i-1}}{\sum\limits_{i=0}^{k}{\rho_{vi}^*}^{i}}\right)\overset{\rho_{vi}^*<1}{<}0.
\end{aligned} \tag{4.39}$$

For (4.39), it indicates that the LHS of (4.38) <0 if k increases by 1 while the price remains constant for a given k. We show in Proposition 23 that the net revenue function (4.8) is quasi-concave with respect to the system load $\rho_v i$. Therefore, this implies that the optimal static price for a given $k+1$ is lower than that for a given k. ■

Under the visible information policy, the price set by the platform when the queue is empty attracts customers to pay to join the queue, while suppliers are compensated since there are no customers in the current queue for them to provide their services. When the queue length reaches the truncation size, the net revenue equation is negative because there are no more customers joining the queue. Therefore, the platform increases the price. On one hand, this makes it more likely that the queue is empty at the steady-state distribution, thereby increasing the platform's gross revenue when the queue is empty. On the other hand, it decreases the likelihood that the queue length will reach the truncated size. Under an invisible information policy, the platform can increase net revenue when the queue is long by lowering the price. This is evident in our throughput analysis, where the platform increases throughput and, consequently, expected profits by decreasing the price.

As shown in Figure 4.13 (e)-(h), under the visible information policy, the average transaction price for the customer ϱ_d^{vi} increases, while the average transaction price for the supplier ϱ_s^{vi} decreases compared to the optimal price p_{vi}^* for a static pricing strategy in a dynamic pricing strategy. These changes are due to balking behavior at the truncation of the queueing system. When the queue length is long enough to reach the truncation size, no new customers enter the queue, resulting a higher average transaction price per customer. However, the platform will continue to attract suppliers, leading to a lower average transaction price per supplier. Under the invisible information policy, the average transaction prices for both customers ϱ_d^{in} and suppliers ϱ_s^{in} are approximately the same as the optimal price p_{in}^* for a static pricing strategy. These observations illustrate that under a dynamic pricing strategy, displaying queue-length information leads to a decrease in benefits for both customers and suppliers, consequently increasing the platform's profit. Conversely, concealing queue-length information can increase the benefits for both customers and suppliers.

As shown in Figure 4.13 (i)-(l), price volatility is lower when implementing a dynamic pricing policy under the invisible information policy compared to the visible information policy. When comparing optimal prices for different information policies, as illustrated in Figure 4.4 (a) and (b), we see that the queue increases considerably under the invisible information policy compared to the visible information policy. Under the visible information policy, the queue exhibits a truncation size due to the truncated balking behavior of customers. At this truncation point, the optimal price decreases compared to when the queue length is shorter, as analyzed in Section 4.4.3. Consequently, the combination of a long queue and a more gradual price change under the invisible information policy leads to a lower price volatility, reflecting a lower level of price discrimination. While a visible information policy is effective in increasing the platform's profit, considering the extra cost associated with implementing dynamic pricing, the platform can opt to mitigate price discrimination by concealing queue-length information, thus increasing benefits for users.

4.5. Conclusions

Pricing and the disclosure of queue-length information are two key factors in platform design, but their joint effects on profit are still not well understood. We address this gap by using a $M/M/1$ queueing model to capture a market segment in an on-demand service platform. In our model, customers' balking behavior is influenced by the uncertainty surrounding waiting times resulting from the disclosure of current queue-length information. We derive optimal prices that maximize expected profit under the proposed information policy for both static and dynamic pricing, solving the underlying Markov decision process using the uniformization method. Our model encompasses different strategies for both pricing and information policies. We compare the resulting solutions and investigate their influence on the platform.

We find that pricing and information policies are complementary: Both dynamic pricing and visible information policies result in higher expected profit, whereas static pricing and invisible information policies result in higher throughput. Dynamic pricing, when the current queue-length information is visible, triggers more customers to balk. It is designed to increase the platform's profit by increasing the average price per transaction, achieving higher commissions, albeit at the cost of reduced throughput. Under the visible information policy, the service queue is truncated at a certain length, as customers perceive it as lengthy and balk at joining. Concealing queue-length information nullifies this queue truncation, attracting more customers and improving throughput, thus benefiting both customers and suppliers. However, an invisible information policy may lead to lower profits, as customer prices decrease while supplier prices increase (resulting in lower arrival rates) compared to the average transaction prices observed under the visible information policy.

This study focuses on a single market segment. Our model simplifies the scenario by considering homogeneous customers and suppliers, employing a "first-in-first-out" matching principle. It can be regarded as a benchmark model for the development of queuing networks. For example, taxi drivers on ride-hailing platforms often move to different regions to pick up orders when their current location is idle. Consequently, an upsurge in orders within one region can influence neighboring regions. Future research could focus on developing a queueing network that accommodates heterogeneous demand and supply, considering the interplay between different market segments.

5. Summary and Outlook

In this thesis, we investigate two important factors in platform design: information disclosure policy and pricing policy. In Chapter 3, we analyze the impact of different queue-length information disclosure policies on platform revenues, taking into account the different balking and reneging behaviors exhibited by customers and suppliers. The preferred information policy is identified under different market parameters, highlighting its significance in platform design. Additionally, we emphasize the importance of information design in the context of multiple platforms, where the impact of information policy on service quality can have long-term implications for the platform's expected revenue. In Chapter 4, we investigate the joint effect of pricing policy and information policy. We identify unique thresholds for pricing and information policies. We reveal that pricing and information policies are complementary. Specifically, both dynamic pricing and visible information policies increase expected profit, while static pricing and invisible information policies increase throughput.

The business models studied in this paper operate within a market segment characterized by homogeneous customers and suppliers on both the demand and supply sides. We separate and examine the disclosure and pricing policies, allowing us to single out multiple market factors. This approach helps us to concentrate on the design factor of interest. However, it simultaneously overlooks the endogenous influence of certain other aspects. For instance, Chapter 3 uncovers that the revenue effect of information policies increases in a multi-platform model when there are endogenous effects on service quality and user arrival rates, compared to a single-platform model. Similarly, Chapter 4 reveals that the information policy can influence the platform's pricing policy and, consequently, its performance metrics such as throughput. Therefore, it is worthwhile to consider developing a model that is both realistic and technically tractable. This model should be able to account for the impact of various elements on design factor within a complex market environment.

Beyond information and pricing policies, there are numerous other elements of platform design that warrant exploration based on our models. These include, but are not limited to: i), Service matching and scheduling aims to efficiently match heterogeneous customers and suppliers, such as drivers or carriers in freight exchange, with customers based on factors like location, availability, and preferences. This process optimizes resource allocation and minimizes waiting times to enhance overall operational efficiency. ii), Management involves the development of effective strategies to handle sudden surges in demand and prevent system overload, thereby ensuring a smooth user experience during peak periods. iii), Developing robust mechanisms to establish and maintain trust between customers and suppliers, such as implementing rating systems, reviews, and efficient dispute resolution processes. iv), Service quality assurance: Establishing effective mechanisms to monitor and uphold service quality standards, encompassing customer feedback, performance metrics, and rigorous quality control processes. The queuing theory model presented in this thesis establishes a foundational framework for addressing these compelling problems. We eagerly anticipate future research that expands these models to encompass an even greater array of intriguing issues.

References

Afèche, P. and Ata, B. (2013). Bayesian dynamic pricing in queueing systems with unknown delay cost characteristics. In: *Manufacturing & Service Operations Management* 15.2, pp. 292–304.

Aksin, O. Z., Gencer, B., and Gunes, E. D. (2019). How observed queue length and service times drive queue behavior in the lab. In: *Available at SSRN 3387077*.

Akşin, Z., Ata, B., Emadi, S. M., and Su, C.-L. (2017). Impact of delay announcements in call centers: An empirical approach. In: *Operations Research* 65.1, pp. 242–265.

Akşin, Z., Ata, B., Emadi, S. M., and Su, C.-L. (2013). Structural estimation of callers' delay sensitivity in call centers. In: *Management Science* 59.12, pp. 2727–2746.

Allon, G., Drakopoulos, K., and Manshadi, V. (2019). Information inundation on platforms and implications. In: *Proceedings of the 2019 ACM Conference on Economics and Computation*, pp. 555–556.

Allon, G., Federgruen, A., and Pierson, M. (2011). How much is a reduction of your customers' wait worth? An empirical study of the fast-food drive-thru industry based on structural estimation methods. In: *Manufacturing & Service Operations Management* 13.4, pp. 489–507.

Anunrojwong, J., Iyer, K., and Manshadi, V. (2022). Information design for congested social services: Optimal need-based persuasion. In: *Management Science*. DOI: `10.1287/mnsc.2022.4548`.

Armony, M., Plambeck, E., and Seshadri, S. (2009). Sensitivity of optimal capacity to customer impatience in an unobservable M/M/S queue (Why you shouldn't shout at the DMV). In: *Manufacturing & Service Operations Management* 11.1, pp. 19–32.

Ata, B. and Shneorson, S. (2006). Dynamic control of an M/M/1 service system with adjustable arrival and service rates. In: *Management Science* 52.11, pp. 1778–1791.

Bai, J., So, K. C., Tang, C. S., Chen, X., and Wang, H. (2019). Coordinating supply and demand on an on-demand service platform with impatient customers. In: *Manufacturing & Service Operations Management* 21.3, pp. 556–570.

Banerjee, S., Riquelme, C., and Johari, R. (2015). Pricing in ride-share platforms: A queueing-theoretic approach. In: *Available at SSRN 2568258*.

Batt, R. and Terwiesch, C. (2015). Waiting patiently: An empirical study of queue abandonment in an emergency department. In: *Management Science* 61.1, pp. 39–59.

Bergemann, D. and Morris, S. (2019). Information design: A unified perspective. In: *Journal of Economic Literature* 57.1, pp. 44–95.

Bernstein, F., DeCroix, G. A., and Keskin, N. B. (2021). Competition between two-sided platforms under demand and supply congestion effects. In: *Manufacturing & Service Operations Management* 23.5, pp. 1043–1061.

Bertsekas, D. (2012). Dynamic programming and optimal control. Vol. 2. Athena scientific.

Bharath, S. (2022). Dynamic pricing – definition, advantages, disadvantages & examples. Accessed November 25, 2022. In: URL: `https://www.feedough.com/dynamic-pricing-definition-examples/`.

Bimpikis, K. and Mantegazza, G. (2023). Strategic release of information in platforms: Entry, competition, and welfare. In: *Operations Research* 71.5, pp. 1619–1635.

Bimpikis, K., Papanastasiou, Y., and Zhang, W. (2020). Information provision in two-sided platforms: Optimizing for supply. In: *Available at SSRN 3617351*.

Bisiere, C., Décamps, J.-P., and Lovo, S. (2015). Risk attitude, beliefs updating, and the information content of trades: an experiment. In: *Management Science* 61.6, pp. 1378–1397.

Caillaud, B. and De Nijs, R. (2014). Strategic loyalty reward in dynamic price discrimination. In: *Marketing Science* 33.5, pp. 725–742.

Castillo, J., Knoepfle, D., and Weyl, E. (2022). Matching in ride hailing: Wild goose chases and how to solve them. In: *Available at SSRN 2890666*.

Castillo, J. C. (2022). Who benefits from surge pricing? In: *Available at SSRN 3245533*.

Chen, H. and Frank, M. Z. (2001). State dependent pricing with a queue. In: *Iie Transactions* 33.10, pp. 847–860.

Çil, E. B., Karaesmen, F., and Örmeci, E. L. (2011). Dynamic pricing and scheduling in a multi-class single-server queueing system. In: *Queueing Systems* 67, pp. 305–331.

Cui, S., Veeraraghavan, S. K., Wang, J., and Zhang, Y. (2022). Observational reneging. In: *Available at SSRN 3290868*.

Feng, G., Kong, G., and Wang, Z. (2021). We are on the way: Analysis of on-demand ride-hailing systems. In: *Manufacturing & Service Operations Management* 23.5, pp. 1237–1256.

Fisher, M., Gallino, S., and Li, J. (2018). Competition-based dynamic pricing in online retailing: A methodology validated with field experiments. In: *Management Science* 64.6, pp. 2496–2514.

Gibbs, C., Guttentag, D., Gretzel, U., Yao, L., and Morton, J. (2018). Use of dynamic pricing strategies by Airbnb hosts. In: *International Journal of Contemporary Hospitality Management* 30.1, pp. 2–20.

Guo, P., Haviv, M., Luo, Z., and Wang, Y. (2022). Optimal queue length information disclosure when service quality is uncertain. In: *Production and Operations Management* 31.5, pp. 1912–1927.

Gur, Y., Macnamara, G., Morgenstern, I., and Saban, D. (2023). Information disclosure and promotion policy design for platforms. In: *Management Science*. DOI: `10.1287/mnsc.2023.4677`.

Hänel, G. (2021). Top 10 online freight exchanges 2021 in Europe. Accessed February 22, 2022. In: URL: `https://impargo.de/en/blog/top-10-freight-exchanges`.

Hassin, R. (2016). Rational queueing. CRC press.

Hassin, R. and Koshman, A. (2017). Profit maximization in the M/M/1 queue. In: *Operations Research Letters* 45.5, pp. 436–441.

Hassin, R. and Roet-Green, R. (2020). On queue-length information when customers travel to a queue. In: *Manufacturing & Service Operations Management* 23.4, pp. 989–1004.

Haviv, M. and Randhawa, R. S. (2014). Pricing in queues without demand information. In: *Manufacturing & Service Operations Management* 16.3, pp. 401–411.

Huang, F., Guo, P., and Wang, Y. (2019). Cyclic pricing when customers queue with rating information. In: *Production and Operations Management* 28.10, pp. 2471–2485.

Huang, J., Mani, A., and Wang, Z. (2022). The value of price discrimination in large social networks. In: *Management Science* 68.6, pp. 4454–4477.

Jeitschko, T. D. and Tremblay, M. J. (2020). Platform competition with endogenous homing. In: *International Economic Review* 61.3, pp. 1281–1305.

Jian, L. and Sami, R. (2010). Aggregation and manipulation in prediction markets: effects of trading mechanism and information distribution. In: *Proceedings of the 11th ACM Conference on Electronic Commerce*, pp. 207–208.

Ke, J., Yang, H., Li, X., Wang, H., and Ye, J. (2020). Pricing and equilibrium in on-demand ride-pooling markets. In: *Transportation Research Part B: Methodological* 139, pp. 411–431.

Kendall, D. G. (1951). Some problems in the theory of queues. In: *Journal of the Royal Statistical Society: Series B (Methodological)* 13.2, pp. 151–173.

Kim, B. and Kim, J. (2017). Optimal information disclosure policies in a strategic queueing model. In: *Operations Research Letters* 45.2, pp. 181–186.

Kim, J. and Randhawa, R. S. (2018). The value of dynamic pricing in large queueing systems. In: *Operations Research* 66.2, pp. 409–425.

Kostami, V. and Ward, A. (2009). Managing service systems with an offline waiting option and customer abandonment. In: *Manufacturing & Service Operations Management* 11.4, pp. 644–656.

Kritikos, K., Pernici, B., Plebani, P., Cappiello, C., Comuzzi, M., Benrernou, S., Brandic, I., Kertész, A., Parkin, M., and Carro, M. (2013). A survey on service quality description. In: *ACM Computing Surveys (CSUR)* 46.1, pp. 1–58.

Lee, K., Bellamy, M. A., and Joglekar, N. R. (2023). Distributed service with proximal capacity and pricing on a two-sided sharing economy platform. In: *Journal of Operations Management* 69.5, pp. 742–763.

Ligon, H. (2021). Trust and Transparency: How Uber Freight forges customer relationships through tech. Accessed February 22, 2022. In: URL: `https://www.supplychain247.com/article/trust_and_transparency_how_uber_freight_forges_customer_relationships_throu/Freight_Transportation`.

Lin, C.-A., Shang, K., and Sun, P. (2023). Wait time–based pricing for queues with customer-chosen service times. In: *Management Science* 69.4, pp. 2127–2146.

Lingenbrink, D. and Iyer, K. (2019). Optimal signaling mechanisms in unobservable queues. In: *Operations Research* 67.5, pp. 1397–1416.

Lu, Y., Musalem, A., Olivares, M., and Schilkrut, A. (2013). Measuring the effect of queues on customer purchases. In: *Management Science* 59.8, pp. 1743–1763.

Maglaras, C. (2006). Revenue management for a multiclass single-server queue via a fluid model analysis. In: *Operations Research* 54.5, pp. 914–932.

Maglaras, C., Yao, J., and Zeevi, A. (2014). Observational learning and abandonment in congested systems. Tech. rep. Columbia University.

Martin, G. E. and Pankoff, L. D. (1982). Reneging in queues revisited. In: *Decision Sciences* 13.2, pp. 340–347.

Mendelson, H. and Whang, S. (1990). Optimal incentive-compatible priority pricing for the M/M/1 queue. In: *Operations Research* 38.5, pp. 870–883.

Mertikopoulos, P., Nax, H. H., and Pradelski, B. S. (2020). Quick or cheap? Breaking points in dynamic markets. In: *Proceedings of the 21st ACM Conference on Economics and Computation*, pp. 877–878.

Naor, P. (1969). The regulation of queue size by levying tolls. In: *Econometrica* 37(1), pp. 15–24.

Norris, J. R. (1998). Markov chains. Cambridge university press.

Parkan, C. and Warren Jr, E. (1978). Optimal reneging decisions in a G/M/1 queue. In: *Decision Sciences* 9.1, pp. 107–119.

Parker, G. G., Van Alstyne, M. W., and Choudary, S. P. (2016). Platform revolution: How networked markets are transforming the economy and how to make them work for you. WW Norton & Company.

Paschalidis, I. C. and Tsitsiklis, J. N. (2000). Congestion-dependent pricing of network services. In: *IEEE/ACM Transactions on Networking* 8.2, pp. 171–184.

Pazgal, A. I. and Radas, S. (2008). Comparison of customer balking and reneging behavior to queueing theory predictions: An experimental study. In: *Computers & Operations Research* 35.8, pp. 2537–2548.

Phillips, R. (2021). Pricing and revenue optimization. Stanford university press.

Simhon, E., Hayel, Y., Starobinski, D., and Zhu, Q. (2016). Optimal information disclosure policies in strategic queueing games. In: *Operations Research Letters* 44.1, pp. 109–113.

Sivakumar, K., Li, M., and Dong, B. (2014). Service quality: The impact of frequency, timing, proximity, and sequence of failures and delights. In: *Journal of Marketing* 78.1, pp. 41–58.

Taylor, T. A. (2018). On-demand service platforms. In: *Manufacturing & Service Operations Management* 20.4, pp. 704–720.

Varma, S. M., Bumpensanti, P., Maguluri, S. T., and Wang, H. (2023). Dynamic pricing and matching for two-sided queues. In: *Operations Research* 71.1, pp. 83–100.

Veeraraghavan, S. and Debo, L. (2009). Joining longer queues: Information externalities in queue choice. In: *Manufacturing & Service Operations Management* 11.4, pp. 543–562.

Vulcano, G. (2008). Dynamic pricing for an M/M/1 make-to-stock system with controllable backlog. In: *Available at SSRN 1301942*.

Wang, H. and Yang, H. (2019). Ridesourcing systems: A framework and review. In: *Transportation Research Part B: Methodological* 129, pp. 122–155.

Wang, Z. (2016). Intertemporal price discrimination via reference price effects. In: *Operations Research* 64.2, pp. 290–296.

Winston, W. L. (2022). Operations research: applications and algorithms. Cengage Learning.

Zhang, R., Han, X., Wang, R., Zhang, J., and Zhang, Y. (2023). Please don't make me wait! Influence of customers' waiting preference and no-show behavior on appointment systems. In: *Production and Operations Management*. DOI: 10.1111/poms.13928.

Zhao, C. and Zhang, Y. (2019). Dynamic quality and pricing decisions in customer-intensive service systems with online reviews. In: *International Journal of Production Research* 57.18, pp. 5725–5748.

Zhu, D., Minner, S., and Bichler, M. (2023). Information Design for On-Demand Service Platforms: A Queueing-Theoretic Approach. *Available at SSRN 4480537*.

A. Table of Notations in Chapter 3

Notation	Description
ϖ	demand side with customers ($\varpi = d$) and supply side with suppliers ($\varpi = s$)
Λ_ϖ	potential arrival rate of side $\varpi \in \{d, s\}$
λ_ϖ	effective arrival rate of side $\varpi \in \{d, s\}$
ξ_ϖ	matching probability of side $\varpi \in \{d, s\}$
n	endogenous arrival rate model
ρ	system load in an exogenous model
ρ_n	system load in an endogenous model
k	truncation size in a single-sided model
k_ϖ	truncation size of side $\varpi \in \{d, s\}$ in a double-sided model
t	truncation time in a single-sided model
t_ϖ	truncation time of side $\varpi \in \{d, s\}$ in a double-sided model
δ	reneging rate in a single-sided model
δ_ϖ	reneging rate of side $\varpi \in \{d, s\}$ in a dboule-sided model
M	defined as $M := \{BV, DV, SV, BI\}$
S	state space
r_{ij}	transition rate
π_i	steady-state probability
$f_x^{(A,B)}$	indifference curve function for policies A and B in an exogenous model
$f_n^{(A,B)}$	indifference curve function for policies A and B in an endogenous model
T_ρ	threshold used in Proposition 4 and Theorem 5
T_d	threshold used in Theorem 5
T_f	threshold used in Theorem 5
$\overline{T_\rho}$	threshold used in Proposition 7
$\underline{T_\rho}$	threshold used in Proposition 7
T_l	threshold used in Proposition 7 and Theorem 8

T_u	threshold used in Theorem 8
T_b	threshold used in Theorem 8
Rev	expected revenue
Rev_{ϖ}	expected revenue for queueing on the side $\varpi \in \{d, s\}$ in a single-sided model
v	relative revenue difference between information policies
a	maximum revenue among all four information policies
b	minimum revenue among all four information policies
ϕ_d^ℓ	auxiliary variables defined by $\phi_d^{BV} = \phi_d^{DV} := \frac{\rho - \rho^{k_d+1}}{1-\rho}$
ϕ_s^ℓ	auxiliary variables defined by $\phi_s^{BV} = \phi_s^{SV} := \frac{\rho^{k_s}-1}{\rho^{k_s+1}-\rho^{k_s}}$
ζ	auxiliary variable defined by $\zeta := \sum_{i=1}^{\infty} \prod_{j=1}^{i} \frac{\rho}{1+j\delta/\Lambda_s}$
ζ_d^ℓ	auxiliary variables defined by $\zeta_d^{BI} = \zeta_d^{SV} := \sum_{i=1}^{\infty} \prod_{j=1}^{i} \frac{\rho}{1+j(\delta_d/\Lambda_s)}$
ζ_s^ℓ	auxiliary variables defined by $\zeta_s^{BI} = \zeta_s^{DV} := \sum_{i=1}^{\infty} \prod_{j=1}^{i} \frac{1}{\rho+j(\delta_s/\Lambda_s)}$
α	patience coefficient defined by $\alpha := \frac{t_d}{t_s} = \frac{\delta_s}{\delta_d}$
h_p	auxiliary function defined in the proof of Lemma 11
f_p	auxiliary function defined in the proof of Lemma 12
$\xi_{\varpi}^{(\ell,n)}$	matching probability of side $\varpi \in \{d, s\}$ under information policy ℓ in an endogenous model
y	auxiliary variable defined by $y := \delta/(\Lambda_s \xi_s^{(R,n)})$ in the proof of Lemma 12
λ_{ϖ}^ℓ	endogenous arrival rate of side $\varpi \in \{d, s\}$ under information policy ℓ
ζ_n	auxiliary variable defined by $\zeta_n := \sum_{i=1}^{\infty} \prod_{j=1}^{i} \left(\frac{\rho_n}{1+j\delta/\lambda_s^R}\right)$
k_n	truncation size in an endogenous single-sided model defined by $k_n := \lceil t\lambda_d^K \rceil$
k^s	truncation size in an exogenous model for a supply market
k_n^s	truncation size in an endogenous model for a supply market
ζ^s	auxiliary variable defined by $\zeta^s := \sum_{i=1}^{\infty} \prod_{j=1}^{i} \left(\frac{1}{\rho+j\delta/\Lambda_s}\right)$
ζ_n^s	auxiliary variable defined by $\zeta_n^s := \sum_{i=1}^{\infty} \prod_{j=1}^{i} \left(\frac{1}{\rho_n+j\delta/\lambda_s^R}\right)$
z	auxiliary variable defined by $z := \delta/\Lambda_s$
f_r	auxiliary function defined in the proof of Proposition 3
f_v	auxiliary function defined in the proof of Proposition 3
g_v	auxiliary function defined in the proof of Proposition 3

$\lambda_s^{(R,qs)}$ endogenous arrival rate of suppliers in a supply market with $\ell = R$

υ variable used in the proof of Proposition 3

ε variable used in the proof of Proposition 3

f_r^n auxiliary functions defined in the proof of Proposition 14

$sgn(\cdot)$ sign function

ϵ variable used in the proof of Proposition 4 and Proposition 7

$\phi_d^{(\ell,n)}$ auxiliary variable defined by $\phi_d^{(\ell,n)} := \frac{\rho_n - \rho_n^{k_d^{(\ell,n)}+1}}{1-\rho_n}$ for each $\ell \in \{DV, BV\}$

$\phi_s^{(\ell,n)}$ auxiliary variable defined by $\phi_s^{(\ell,n))} := \frac{\rho_n^{k_s^{(\ell,n)}} - 1}{\rho_n^{k_s^{(\ell,n)}+1} - \rho_n^{k_s^{(\ell,n)}}}$ for each $\ell \in \{SV, BV\}$

$k_d^{(\ell,n)}$ demand side's truncation size in an endogenous double-sided model

$k_s^{(\ell,n)}$ supply side's truncation size in an endogenous double-sided model

$\zeta_d^{(\ell,n)}$ auxiliary variables defined by $\zeta_d^{(\ell,n)} := \sum_{i=1}^{\infty} \prod_{j=1}^{i} \frac{\rho_n}{1+j(\delta_d/\lambda_s^\ell)}$ for each $\ell \in \{SV, BI\}$

$\zeta_s^{(\ell,n)}$ auxiliary variables defined by $\zeta_s^{(\ell,n)} := \sum_{i=1}^{\infty} \prod_{j=1}^{i} \frac{1}{\rho_n+j(\delta_s/\lambda_s^\ell)}$ for each $\ell \in \{DV, BI\}$

t_b symmetric truncation time defined by $t_b := t_d = t_s$

δ_b symmetric truncation size defined by $\delta_b := \delta_d = \delta_s$

h auxiliary function defined in the proof of Theorem 8

$\phi_d^{(\ell,n)}$ auxiliary variable defined by $\phi_d^{(\ell,n)} := \frac{\rho_n - \rho_n^{k_d^{(\ell,n)}+1}}{1-\rho_n}$ for each $\ell \in \{DV, BV\}$

$\phi_s^{(\ell,n)}$ auxiliary variable defined by $\phi_s^{(\ell,n))} := \frac{\rho_n^{k_s^{(\ell,n)}} - 1}{\rho_n^{k_s^{(\ell,n)}+1} - \rho_n^{k_s^{(\ell,n)}}}$ for each $\ell \in \{SV, BV\}$

$k_d^{(\ell,n)}$ demand side's truncation size in an endogenous double-sided model

$k_s^{(\ell,n)}$ supply side's truncation size in an endogenous double-sided model

$\zeta_d^{(\ell,n)}$ auxiliary variables defined by $\zeta_d^{(\ell,n)} := \sum_{i=1}^{\infty} \prod_{j=1}^{i} \frac{\rho_n}{1+j(\delta_d/\lambda_s^\ell)}$ for each $\ell \in \{SV, BI\}$

$\zeta_s^{(\ell,n)}$ auxiliary variables defined by $\zeta_s^{(\ell,n)} := \sum_{i=1}^{\infty} \prod_{j=1}^{i} \frac{1}{\rho_n+j(\delta_s/\lambda_s^\ell)}$ for each $\ell \in \{DV, BI\}$

t_b symmetric truncation time defined by $t_b := t_d = t_s$

δ_b symmetric truncation size defined by $\delta_b := \delta_d = \delta_s$

h	auxiliary function defined in the proof of Theorem 8

B. Table of Notations in Chapter 4

Notation	Description
ϖ	demand side with customers ($\varpi = d$) and supply side with suppliers ($\varpi = s$)
ℓ	visible information policy ($\ell = vi$) and invisible information policy ($\ell = in$)
χ	static pricing policy ($\chi = stat$) and dynamic pricing policy ($\chi = dyn$)
$S\&V$	static-pricing-and-visible-information combination decision
$D\&V$	dynamic-pricing-and-visible-information combination decision
$S\&I$	static-pricing-and-invisible-information combination decision
$D\&I$	dynamic-pricing-and-invisible-information combination decision
λ_{ϖ}^{ℓ}	arrival rate of side ϖ under a static pricing policy and for an information policy ℓ
ρ_{ℓ}	system load under a static pricing policy for an information policy ℓ defined by $\rho_{\ell} := \frac{\lambda_d^{\ell}}{\lambda_s^{\ell}}$
$\lambda_{\varpi}^{(i,\ell)}$	arrival rate of side ϖ at queue length i for an information policy ℓ under a dynamic pricing policy
α	market potential
β_{ϖ}	price sensitivity of customers ($\varpi = d$) or suppliers ($\varpi = s$)
β	ratio of price sensitivities defined by $\beta := \frac{\beta_d}{\beta_s}$
ϵ	commission rate
ν	minimum wage for suppliers
p_{ℓ}	the price under a static pricing policy for an information policy ℓ
$p_{(i,\ell)}$	the price at queue length i under a dynamic pricing policy for an information policy ℓ
k	truncation size under a visible information policy
δ	balking probability
C_a	customer attrition cost per customer for a long queue

C_d	extra cost of implementing a dynamic pricing policy compared with a static one
S	state space
r_{ij}	transition rate
π_i	steady-state probability
$\rho_{(i,\ell)}$	system load under a dynamic pricing policy defined by $\rho_{(i,\ell)} := \frac{\lambda_d^{(i-1,\ell)}}{\lambda_s^{(i,\ell)}}$ for each $i \in S_\ell \backslash \{0\}$
$GR_\ell(\cdot)$	gross revenue rate function for an information policy ℓ
$SP_\ell(\cdot)$	supplier payout function for an information policy ℓ
$NR_\ell(\cdot)$	expected net revenue function for an information policy ℓ
Pro_ℓ^χ	expected profit function for a pricing policy χ and an information policy ℓ
$*$	as the superscript denotes the optimal
v_i	relative value function corresponding to a queue length of i
γ	guess of the maximum average value
y_i	intermediate variable defined by $y_i := v_{i-1} - v_i$ for $i = 1, .., k$
$f_{C_d} \triangleq 0$	indifference curve for extra cost C_d of implementing a dynamic pricing policy
ς_ℓ^χ	throughput under a pricing policy χ and for an information policy ℓ
δ_k	the value of δ that satisfies the indifference curve $f_{\delta_d} = 0$ for a given value of k
σ_ℓ	price volatility of a dynamic pricing policy under an information policy ℓ
ϱ_ϖ^ℓ	average transaction price of side ϖ for an information policy ℓ
η_ℓ	incremental net revenue ratio of using a dynamic pricing policy over a static one for an information policy ℓ
T_k	unique threshold to determine the preferred pricing policy for a visible information policy
T_δ	unique threshold to determine the preferred pricing policy for an invisible information policy